Effect of inoculum on bioelectricity yield and the use of factorial experiments for assessing microbial fuel cells

Jamie Hinks

A thesis submitted for the Degree of Doctor of Philosophy in the faculty of Science Agriculture and Engineering at Newcastle University

School of Civil Engineering and Geosciences

Newcastle University

Newcastle upon Tyne

NE1 7RU

June 2011

ABSTRACT

The study aim was to understand the effect of inoculum on bioelectricity production and the interactions that occur between organic load, external resistance and fuel type during the operation of a Microbial Fuel Cell (MFC).

The first experiment explored the effect of four different environmental inocula (freshwater sediment, two types of return activated sludge (RAS) and anaerobic sludge) on microbial fuel cell performance. The number of bacteria in each of the inocula were standardised prior to experiments to achieve an inoculum density of 1.29 x 10^7cells ml^{-1} so that the comparison between treatments could be carried out fairly. For almost every metric (voltage, current and coulombic efficiency) the RAS inoculum outperformed freshwater sediment and anaerobic sludge inoculum. The treatment efficiency was high in all instances (>79%) with the exception of anaerobic sludge (33%). Microbial community analysis showed that anodes from MFCs exhibited a more complex microbial community profile than anodes from MFCs inoculated with anaerobic sludge.

Two experiments were performed to investigate the relationship between fuel type, organic load and external resistance and their effects on MFC performance using an iterative Design of Experiments (DoE) approach. In the first experiment, a half factorial design was used as a screening study to investigate the main effects of fuel type (glucose vs acetate), organic load and external resistance. The study found that acetate performed poorly compared with glucose and that the experimental settings for external resistance should be modified for future experiments. The second experiment used a full factorial design and showed that only organic load exerted a statistically significant effect on cell potential, current and coulombic efficiency and that a statistically significant interaction effect between organic load and external resistance is exerted on cell potential and coulombic efficiency. The dominant effect of organic load was also apparent in DGGE community fingerprint profiles, which clustered according to organic load, of the anode community samples taken from MFCS in this study.

In conclusion, the experiments yielded useful insights into inoculum effects and the interactions between basic operational parameters in an MFC that will be useful for

selecting the operational parameters of MFCs depending on the field conditions and process requirements. The novelty of the techniques deployed in this study – standardisation the inoculum and exploring MFCs within a Design of Experiments framework – are noted along with the advances to our understanding of MFCs and the fact they have provided new tools with which to study MFCs systems. The wider implications of the performance characteristics of the MFCs used in this study and the findings presented within are discussed.

DECLARATION

I hereby certify that this work is my own, except where otherwise acknowledged, and that it has not been submitted for fulfilment of a degree at this or any other university.

Jamie Hinks

ACKNOWLEDGEMENTS

My heartfelt thanks go to the following:

My supervisors, Professor Ian Head, Professor Tom Curtis and Professor Keith Scott for giving me the opportunity to study MFCs. It has been a challenge that I have enjoyed grappling with and your guidance and comments have been invaluable.

Krishna Katuri who allowed me to join him on his first explorations into MFCs and who shared his knowledge generously. You were instrumental in shaping my understanding of this technology and I have a debt of gratitude that I hope you will recall one day.

All the people that provided technical support from the schools of Civil Engineering & Geosciences and Chemical Engineering & Advanced Materials: Donna Swan, Fiona Read, Kate Osbourne, Keith Tweddle, Ian Harrison, Paul Donohoe, Jimmy Banks, Simon Daley, Rob Dixon, Paul Sterling and Paul strong. Trevor booth who operated the CSLM and Graham Patterson for being the quickest IT guy in the world. Thanks to you all for you help in answering my endless questions and attending to things I have no clue about. Ange, if I mention you then the list will get out of control but thanks anyway.

On a personal level, I run the risk of leaving out some names so I will say only this: you know who you are and it has been a joy knowing you and sharing intellectual (or otherwise) banter over a pint, a coffee, in corridors and lifts, over poker, a glass of wine, out fishing or camping, at conferences, overseas, over dinner, in the labs and late at night or weekends when one can hear the buildings breathing. CEG is a great place to work and thanks to everyone for making it like that. It would have been a grim affair without you so I urge you to keep up the good work

Eui Jo, Sarang Hae, thanks for being a great wife and a good mother to Archie. I have took the scenic route in places (and I always will) but thanks for sticking by me when I got lost from time to time. Archie, you have taught me a new kind of love and I promise I will spend more time with you and your little brother (Milo?) when he arrives now that this thesis is finished. Mum, Aron & Danny – a fine mother and the greatest brothers – cheers. Nan, get prepared to be royally thrashed at Scrabble®.

CONTENTS

FIGURES & TABLES

FIGURES

TABLES

1 INTRODUCTION

1.1 CLIMATE CHANGE – POLITICAL AND ECONOMIC CONSIDERATIONS

Modern *scientific* concerns about our climate date back to at least the 1970s (Gribbin, 1978) and were compounded by a series of scientific observations in the 1980s. Farman, Gardiner & Shanklin (1985) of the British Antarctic survey reported the thinning of the ozone layer over Antarctica. Two years later a Franco-Russian team were the first to make a link between historical climatic anomalies and atmospheric greenhouse gas (carbon dioxide and methane) concentrations using data obtained from sections of Antarctic ice cores (Crutzen, 1993; Jouzel *et al.*, 1987). By 1988 a survey showed consensus amongst leading scientists that climate change was a significant threat that warranted action to implement controls on greenhouse gas emissions (Oreskes, 2004).

Later that year international political concern was demonstrated by the formation Intergovernmental Panel on Climate Change (IPCC) in Toronto (Drake, 2000). Climate change quickly became the subject of intense political focus globally and two major events were instrumental in ensuring climate change remained high on the political agenda: the Second World Climate Conference in Geneva in 1990 followed by the United Nations Conference on Environment and Development (UNECD) in Rio de Janeiro in 1992. The second of these was the largest and most internationally representative conference ever organised with over 25,000 delegates from across the world in attendance – accordingly it is often referred to informally as the Earth Summit (Houghton, 2004). The framework for tackling climate change was laid down at the Earth Summit but despite further meetings in 1995, and 1996 it was not until 1997 that emissions targets were agreed in Kyoto, Japan.

Throughout much of the 1990s the IPCC was responsible for providing assessments of climate change and by 2006 had produced four reports. And whilst the concept of climate change has caused widespread public concern, little apparent political progress had emerged from the rhetoric until the publication of the now infamous Stern Review in 2006. Stern's findings were the first to render climate change in the hard light of economics and the message was simple: by taking action now to mitigate climate change

we can limit the economic cost to 1% of worldwide annual GDP. The cost of inaction is likely to be 5%-20% of GDP per annum now and forever (Stern, 2007).

Currently, climate change is accepted by all but the most stalwart polemics. Most authorities recognise its link to industrialisation, in particular the burning of fossil fuels for energy, and that the agents of concern are a suite of green house or Kyoto gasses: carbon dioxide (CO_2), methane (CH_4), nitrous oxide (N_2O), perfluorocarbons (PFCs), hydrofluorocarbons (HFCs), and Sulphur Hexafluoride (SF_6) (Stern, 2007; Parry, 2007).

Climate modellers concede that a doubling of atmospheric CO_2 concentrations on pre industrial levels will lead to a 2-5°C rise in mean global temperatures. Pre industrial levels are estimated at around 280 ppm and current atmospheric CO_2 concentration is about 390ppm with the total radiative forcing of all six greenhouse gases being equivalent to 440ppm of carbon dioxide (CO_2e) (Stern, 2007; www.co2now.org, 2012). If current emissions are not curbed, atmospheric CO_2 concentrations will double pre-industrial levels by 2030-2050 and treble by 2100. The latter will see global mean temperatures rise by 3-10°C (Stern, 2007). Stern concludes that stabilising atmospheric GHG concentrations in the range 450-550 ppm CO_2e will be sufficient to avert the most serious consequences of climate change.

Accordingly, through implementation of the Kyoto protocol – now ratified by 236 states globally - the EU has committed to long term greenhouse gas reductions of 80% by 2050 with an interim target of a 20% reduction by 2020 based on 1990 levels. The EU introduced the first international carbon emissions trading scheme (EUETS) in 2006 to drive these changes. This is a cap and trade scheme where national emissions quotas are set and translated into credits which are allocated to industry by auction or other means. Each credit allows the operator to emit one tonne of CO_2, they are allocated sparingly and reduced annually. Operators must either reduce their emissions to meet their allowance or purchase credits through an approved carbon trading mechanism to avoid penalty. The rationale is that carbon is commoditised which provides an economic incentive to adopt low carbon strategies. The EUETS is aimed at large polluters such as the power and

chemical industries and is in its second phase. A new scheme, the Carbon Reduction Commitment (CRC), will mandate a cap and trade scheme for around 5000 previously unregulated businesses in the UK and was scheduled to become binding in April 2010 although revisions by the coalition government (like diverting revenue raised from the purchase of carbon credits to the treasury instead of recycling it within the scheme) has stalled proceedings and the CRC is currently under review. Meeting the 2050 deadline for carbon emissions reductions of 80% on 1990 levels will require wholesale changes in *every* aspect of modern living and the EU has recognised the need to incentivise change and to introduce further statutes. Observance of the CRC is expected to cause a trickledown effect in GHG emissions as CRC participants, seeking to reduce their supply chain related GHG emissions, will demand low carbon goods and services.

1.2 WASTEWATER TREATMENT

Wastewater is essentially a community's water after it has been subject to domestic, institutional and industrial use. Many things are added to water as it is used and accordingly wastewater is a complex mixture containing, amongst other things, human and animal excreta, food wastes, detergents, toilet paper, industrial chemicals, prophylactics and a number of pathogenic organisms (Tchobanoglous, 2003; Mara, 2003).

Wastewater is usually characterised by the things it contains. A popular metric is its strength and it usually refers to the amount of organic material it contains and is described as a function of the amount of oxygen it would take to oxidise this organic material. Other metrics are concerned with the propensity of wastewater to transmit bacterial, viral and helminthic diseases to humans. Three common metrics describe the strength of wastewater: Theoretical Oxygen Demand (ThOD), Chemical Oxygen Demand and Biological Oxygen Demand (COD). COD is used throughout this project. The microbial quality of wastewater is usually described in terms of faecal coliforms or by reference to other indicator organisms.

Table 1.1 A tabular summary showing the steps in wastewater treatment. Adapted from Tchobanoglous, 2003.

Treatment Level	Purpose
Preliminary	Removal of bulk items such as rags, sticks, grit, grease and floatables that can cause subsequent equipment or process failure.
Primary	Removal of suspended solids and some organic matter. Usually by settling.
Advanced Primary	Enhanced removal of suspended solids and organic matter. Usually accomplished by filtration or addition of chemicals
Secondary	Removal of biodegradable organic matter and suspended solids. Disinfection is also included in this definition.
Secondary with Nutrient Removal	As above but removal of components such as nitrogen & phosphorous
Tertiary	Removal of residual suspended solids. Disinfection and nutrient removal can also be affected.
Advanced	Removal of dissolved and suspended solids remaining after conventional levels of treatment to satisfy particular reuse standards.

Because of public health and environmental concerns, wastewater must be treated before it is reused or discharged into the environment (Tchobanoglous, 2003). The quality standards for treated effluent wastewater are governed by statute in most countries, and

whilst requirements may vary according to the intended fate of the wastewater, they are usually concerned with reducing the strength of the wastewater and its ability to transmit disease or damage the environment by removal of the corresponding causative agents. The wastewater treatment directive (91/217/EEC) governs the quality of wastewater that can be legally discharged into UK receiving waters.

Wastewater is usually treated in steps, a common way in which these treatment steps can be categorised and the purpose of each step is summarised in table 1. (Tchobanoglous, 2003):

Wastewater treatment is costly, it accounts for 1.5% of total energy use in the US with the whole water infrastructure accounting for 4-5% US (Logan, 2009). In the UK, it is around 3% and accounts for around 1% of the UKs greenhouse gas emissions (Prescott, 2009). The water industry in the UK have voluntarily monitored their greenhouse gases for years although and the UKs economic regulator of the water industry (Ofwat) mandated annual, industry wide GHG emissions returns since 2008 (Prescott, 2009). The CRC is the second of the EUs cap and trade schemes and includes all corporate entities that settle on the half-hourly electricity market and use more than 6000 MWh of electricity annually. This will include all water companies and the scheme went live in Autumn 2010. There is, therefore, a large regulatory pressure on water companies to reduce the energy intensity of their operations. Because of regulatory pressure, current wastewater treatment practices that consume vast amounts of energy such as the activated sludge process are unsustainable and technology that can treat wastewater passively or even with a net energy gain will see widespread application in WWT over the coming years.

1.3 ROLE OF MFCS IN WASTEWATER TREATMENT

Because of concerns about climate change and a mandatory pressure for organisations to reduce carbon emissions there is a need within the water industry to not only reduce the financial and environmental costs of treating wastewater but to capitalise on its resource

potential too. Therefore, emerging clean technologies like Microbial Fuel Cells (MFCs) that can simultaneously treat wastewater whilst generating electricity directly from the organic pollutants within the wastewater are desirable as they will allow the water industry to meet its regulatory obligations to treat wastewater to the required standard whilst also adhering to its commitments under the CRC.

MFCs are a relatively underexplored discipline and despite the promise of MFCs in wastewater treatment there has been little progress towards real world manifestations of MFC technology on a scale that would be useful in industrial settings. For this reason MFCs are still the focus of intense research effort globally and they represent an opportunity for significant breakthroughs in scientific understanding.

2 MICROBIAL FUEL CELLS (MFCS)

2.1 INTRODUCTION

Microbes have forced us to reconsider our assumptions about the outer limits of life. Over the last 3.5 billion years, nature has evolved seemingly endless strategies allowing life to capitalise on almost every energetic niche on this planet; nowhere is this more apparent than in the microbial domains of life (Horneck, 2000; Abrevaya *et al.*, 2009). Almost everywhere biologists look for life on earth it either exists, or there is evidence that it existed previously. Microbes can inhabit such extremes that belief in extra-terrestrial life is no longer the preserve of fantasists but attracts serious scientific attention from exobiologists (Horneck, 2000).

A watershed in microbiology, one that is of vast importance in Microbial Fuel Cells and that has forced a radical rethink of microbial capabilities, is the discovery of dissimilatory metal reducing organisms (Loveley; 1988; Lovley, 1991; Nealson & Myers, 1992; Caccavo, 1994; Lovley, 1993). It is the extraordinary ability of microbes to reduce solid interfaces that is important in capturing the reducing power of microbes at the anode of MFCs to produce electricity. Coupling biological systems to electrical ones overcomes the thermal disadvantages of combustion and combines the catabolic diversity of microbes with the established technology of fuel cells (Bullen *et al.*, 2006; Picioreau *et al.*, 2010).

The concept of using microorganisms to perform useful tasks is not a new one. Brewing and fermentation technology are familiar to us all and the world would be a dismal place had our ancestors failed to master these processes – particularly the former. The idea of using microorganisms to directly generate electricity is sometimes met with scepticism; most likely because the conversion of sewage to valuable electricity and carbon credits, in the minds of some, has analogies with alchemy.

2.2 HISTORY

The historical indifference to microbial fuel cells is apparent from the relative obscurity of a technology that has been a bench top curiosity for almost a century (Stirling *et al.*, 1983; Shukla, *et al.*, 2004). The discovery of the electrochemical nature of some biological

phenomena is attributed to Galvani who, in 1791, discovered that severed frogs' legs twitched when an electrical current was applied to them (Piccolino 1998; Shukla *et al.*, 2004; Bullen *et al.*, 2006). In 1911, here at Newcastle, then part of Durham University, a professor of botany, Michael C. Potter, demonstrated the potentiometric intensity of chemical reactions accompanying the degradation of organic compounds during the growth of *Saccharomyces cerevisea*, *E. coli* and a *Bacillus sp.* and noted that the potentiometric properties of the microbes that he studied might be harnessed for useful work. Later at Cambridge, Cohen (1931) revived Potter's work and described the redox potential of a number of anaerobes and was the first to attempt to harness the reduction potential of microbes in a galvanic cell. The idea of bioelectricity, in a sense similar to how we consider it today in MFC research, can be attributed to Potter and later Cohen. Despite this early work, microbial fuel cell research lay dormant until the 1960s when the technology was picked up by NASA who was interested in MFCs as a waste management solution during space expeditions. Under the NASA research program, Rohrback *et al.,* (1962), reported a fuel cell where *Clostridium butyricum* was the biocatalyst responsible for generating hydrogen by glucose fermentation (Berk & Canfield 1964, Shukla *et al.*, 2004; Bullen *et al.*, 2006). Berk & Canfield (1964) demonstrated the bioelectrochemical potential of two photosynthetic organisms one acting on the cathodic side (a blue green marine alga belonging to the family *Ocillatoriaceae*) and the second on the anodic side (*Rhodospirillum rubrum*) but concluded that these types of MFCs would never yield useful energy. During this period, Davis and Yarborough looked at current generation in MFCs inoculated with *E. coli* and a *Norcadia sp* as well as in an enzymatic fuel cell with glucose oxidase (Davis & Yarborough, 1962). Biological fuel cells were commercially available in the 1960s but market conditions where tough and they were superseded by cheaper alternatives and other technological developments such as photovoltaics (Shukla *et al.*, 2004; Rabaey & Verstraete, 2005; Bullen *et al.*, 2006; Lovley, 2006). Interest in biological fuel cells increased again in the 1970s and 1980s and much research in this area was lead by Bennetto and his team (Stirling *et al.*, 1983; Bennetto and Stirling 1985; Bennetto, 1993; Shukla *et al.*, 2004, Bullen *et al.*, 2006) and a group at the Tokyo Institute of

Technology who looked at immobilized cells of *C. butyricum* and the potential of MFCs as BOD sensors (Karube *et al.*, 1977a; Karube, 1977b). The majority of the research carried out during the 1970s and 1980s required mediators to facilitate the electronic transfer between the microbe and the anode of an MFC.

A sceptic would argue that the lack of commercial progress in MFC technology over the last century is testament to the fact that it is doomed to failure but the last decade or so has witnessed a renaissance in biological fuel cell research. Most notably this was instigated by researchers at the Korean Institute of Science and Technology (KIST) under Byeong Hong Kim who described MFCs that do not require mediators (Kim *et al.*, 1999a; Kim *et al*, 1999b). The socio-economic motivation behind the renaissance in MFC research is driven by a need for an integrated system of sustainable energy generation and use influenced by the economics of peak oil and the need to mitigate serious climate change (Katz *et al.*, 2003; Prescott 2009).

2.3 BASIC PRINCIPLES

Biological fuel cells can loosely be described as fuel cells that owe at least part of their functionality to biological processes (Bullen *et al.*, 2006). This includes whole organisms or enzymes and other purified biological macromolecules. A more preferable umbrella term, which includes Microbial Electrolysis cells, is bioelectrochemical systems (BES) or, more recently proposed, MXCs (the x being sufficiently general to cover a number of candidate technologies), a subcategory of which is Microbial Fuel Cells – those which owe their functionality to the reducing powers of whole organisms. Certain types of biological fuel cells do not rely on the electrochemical activity of microbes or biological macromolecules for their function but instead utilise biological metabolites, such as hydrogen in an electrochemical process that, in theory, could be temporally and spatially separated from the metabolic process responsible for their production (Katz, 2003; Bullen *et al.*, 2006).

The underlying principal in MFC function is the direct conversion of chemical energy to electrical energy using microbial biocatalysts. This is achieved by coupling electrons produced during an organism's oxidative metabolism to an insoluble electrode rather than a more conventional, dissolved terminal electron acceptor such as oxygen, nitrate or sulphate (Rabaey & Verstraete, 2005). For an electron to be taken up by an electrode there must be steric accessibility and the electrode potential must be higher than that of other electron acceptors meaning that the anode electrode reaction must be thermodynamically feasible and favourable (Rabaey and Verstratete, 2005). Steric accessibility can be achieved by direct microbial contact with the electrode or by the reduction of intermediate, soluble electron shuttles (Bennetto *et al.*, 1985; Allen & Bennetto, 1993; Shukla *et al.*, 2004; Rabaey & Verstraete, 2005; Bullen *et al.*, 2006; Lovley, 2006). Electrons transmitted to the anode either directly or by mediator compounds pass through an external circuit under load to the cathode. Excess protons generated during the catabolism of carbohydrates migrate to the cathode where they are reduced to water in the oxygen reduction reaction (ORR). Consider Equation 2.1 proceeding under anaerobic conditions in the anode chamber of an MFC (Shukla *et al*, 2004):

$$C_6H_{12}O_6 + 6H_20 \rightarrow 6C0_2 + 24H^+ + 24e^- \ (E^o = 0.014\ V)$$

Equation 2.1

This reaction represents the catabolism of glucose although the principle is true for any carbohydrate. In the absence of oxygen or alternative electron acceptors, the electrons are transmitted by the microbe to the anode. The anode chamber is connected to the cathode chamber and electrons are transported through the outer circuit to the cathode resulting current flow. The cathode reaction is shown below for the reduction of oxygen in air cathode MFCs:

$$6O_2 + 24H^+ + 24e^- \rightarrow 12H_2 \ (E^o = 1.23\ V)$$

Equation 2.2

The anode and the cathode chamber are generally separated from one another by a mechanism that is selective to proton transport such as proton exchange membrane or a salt bridge (Min *et al.*, 2005) although membraneless types have also been investigated (Hu, 2008; Woodward *et al.*, 2009). The charge balance is completed in an MFC by transmission of the protons that were generated from the oxidation of glucose (Figure 2.2) through the anolyte to the cathode where they are reduced by atmospheric oxygen or other chemical oxidants such as ferricyanide. Recently, an unknown oxidant produced by the bacterium *Burkholderia cenocepacia* has been discovered and demonstrated to produce cell voltages 11 times greater than oxygen and 3 times that of ferricyanide (Hunter & Manter 2011).

The functional organisms in a MFC need not be anaerobic and indeed aerobic and facultative electricigens have been reported as well as anaerobic ones (Park & Zeikus, 2002; Liu *et al.*, 2005; Logan *et al.*, 2005; Gorby *et al.*, 2006; Holmes *et al.*, 2006; Rabaey & Verstraete, 2005; Khan *et al.*, 2010). It is however desirable from an energetic point of view in MFCs for the anode potential to be as low as possible (anoxic or reducing conditions) whilst at the same time maintaining a high cathode potential (oxic or oxidising conditions). This ideal situation results in a large potential difference between electrodes and therefore high cell potential. The type of electrochemical metabolism that proceeds in a given MFC depends on a number of factors but the anode potential is significant. Low anode potentials will favour fermentative and anaerobic organisms. The anode potential is influenced by a combination of anolyte composition as well as anode material and the organisms that colonise it (Logan, 2008, Christgen, 2010; Kim & Regan, 2011).

2.4 EXOCELLULAR ELECTRON TRANSFER IN MFCS

The way biological reducing power is captured in and MFC is a convenient way of classifying the devices. MFCs can be classified according to whether artificial mediators need to be added to the anolyte for the purpose of shuttling electrons to the anode. Microorganisms that require electron shuttles to mediate the redox process between the terminal part of the microbial electron transport chain and the anode include various

Pseudomonads, *Enterobacte*r, *Proteus spp*. and *E. coli* (Kim *et al.*, 2000; Park & Zeikus 2002; Ieropoulous *et al.*, 2005; Rabaey *et al.*, 2004; Rabaey & Verstraete, 2005; Kim *et al.*, 2006). Microbes that do not require electron mediators include the widely reported representatives of the *Geobacteraceae* such as *G. sulfureducens* (Bond & Lovley 2002, Holmes *et al.*, 2006), *G. metallireducens* (Bond & Lovley, 2002) and *Desulfuromonas acetoxidans* (Bond *et al.*, 2003) alongside *Shewanella* species such as *S. oneidensis* (Gorby *et al.*, 2000), *S. putrefaciens* (Kim *et al.*, 2002) and a close relative of *S. affinis* (Logan *et al.*, 2005). Other genera found to function in mediatorless MFCs include various *Clostridia*, *Rhodoferax ferrireducens* (Chaudry & Lovley, 2003), and a thermophillic fermentative bacterium *Pelotomaculum thermopropionicum* (Gorby *et al.*, 2006). In the past, it was common for investigators to use pure cultures of electrochemically active species, presumably for experimental clarity, although recently there has been a move towards using mixed, undefined cultures derived from environmental samples such as wastewater and marine sediments to inoculate MFCs (e.g. Tender *et al.*, 2002; Park & Zeikus, 2002; Phung *et al.*, 2004). In mediatorless MFCs direct bacterial contact with the anode is the primary mechanism by which electronic exchange occurs and is thought to be the case with, for example, the *Geobacteracea* (e.g. Gorby *et al.*, 2006) but some organisms produce electroactive metabolites that are thought to function as electron shuttles as well as participating in direct reduction of the anode (e.g. *Shewanella spp*).

2.5 ARTIFICIALLY MEDIATED ELECTRON TRANSFER

For the majority of organisms, including mammals, the natural respiratory terminal electron acceptor is a dissolved chemical species. Insoluble electrodes are not obvious biocompatible interfaces and may explain why redox mediators, either natural or synthetic, were often essential in coupling biological reducing power to electricity production at a solid electrode interface. This is particularly true of the organisms used in earlier investigations such as *E. coli*, *Saccharomyces spp*. and *Proteus spp.* which are predominantly mesophilic enteric organisms that have evolved efficient electron exchange mechanisms and whose environments offer a variety of dissolved terminal

electron acceptors when compared with, for instance, the more recently studied extremophiles.

Electron mediators or shuttles infiltrate the cell in their oxidised state and participate in redox couples with cellular reducing agents (e.g. cytochromes, glutathione and NADH) that function in the organism's electron transport chain (ETC). The electron shuttle in its reduced form must be able leave the cell and diffuse through the anolyte to reduce the electrode.

Bennetto *et al.* (1985) described a number of such electron shuttles and their tendency to oxidise NADH, which they assumed to be representative of biological electron exchange mechanisms. They examined phenothiazine derivatives including thionine, methylene blue and naphthoquinone; compounds that have applications as electron shuttles in modern MFCs. Bennetto and his colleagues compared the reduction rates of these phenothiazine derivatives with free NADH to the rates at which they were reduced by microorganisms. They concluded that it was the ability of electron shuttles to penetrate cell membranes that was limiting rather than redox interactions at the biological interface (Benetto *et al.*, 1985; Allen & Benetto, 1993).

Electron mediators with a potential close to but slightly higher than the potential of the terminal reductase in the microbial ETC should confer the best MFC performance. A Large difference in potential between the terminal reductase and the mediator will results in a loss that will manifest itself as low cell potential in an MFC. Biological compatibility too appears to be as important as thermodynamic considerations – this is perhaps why the coupling of biological systems to electrodes is problematic in the first place. Ieropoulos *et al.*, (2005) showed that methylene blue functioned much better than neutral red as an electron mediator in a MFC despite it having a higher potential. They reasoned, that this was owing to the inability of neutral red to interact efficiently with the cell perhaps because the potential between the principal redox couples was too low to allow efficient electronic transfer. Since different taxonomic groups occupy specific niches and the redox

potential of their terminal electron transfer components may differ accordingly, it may be the case that electron mediators are genera specific.

In summary, electron mediators must readily partake in reversible redox couples and pass through cell membranes in both the oxidised and reduced state. Ideally they should couple biological reducing power to an anode with low potential whilst being able to partake in multiple subsequent redox reactions. They must be able to overcome mass transport limitations and be non toxic.

2.6 MEDIATOR-LESS MFCS

Microbes that are able to interact directly with anodes have been reported. The most well know of these is the dissimilatory iron reducing bacteria *Geobacter sulfurreducens* first described by Caccavo *et al.*, (1994) and other dissimilatory genera such as *Shewanella, Rhodoferax* and *Desulfuromonas*. The mechanisms by which microorganisms engage with insoluble electron acceptors in natural communities, and presumably anodic electrochemical interfaces, has been studied in detail (Lovley 1993; Regura *et al.*, 2005; Gorby *et al.*, 2006; Holmes *et al.*, 2006; Nielsen *et al.*, 2010). Electron shuttling between an organism's electron transport system and insoluble metal oxides may proceed with the aid of naturally occurring soluble electron shuttling compounds such as humic substances or cell metabolites (Gorby *et al.*, 2006). Alternatively, the cell may interact directly with the anode by means of cytochromes associated with its outer membrane.

In 2005, Reguera showed that *Geobacter sulfurreducens* extrude electrically conductive pili or 'nanowires' and proposed that they were important in extracellular electron transfer. Later, Gorby *et al.* (2006) described the same phenomenon in *Shewanella onedensis*, *Pelotomaculum thermopropionicum* and a cyanobacterium, S*ynechocystis* spp. Reguera *et al.* (2006) suggested that nanowires do not exclusively function in conducting electrons but Gorby and his team at the J Craig Venter institute produced a micrograph that showed a single *Shewanella* cell which had extruded nanowires could complete a circuit between two electrical contacts thus demonstrating unequivocally the conductive

properties of nanowires (Gorby *et al.*, 2010). The function of nanowires has been controversially postulated as one of the mechanisms of electron transfer in MFCs although they have been shown to be important in biofilm formation as well – suggesting at least dual functionality (Gorby *et al.*, 2006; Holmes *et al.*, 2006; Reguera *et al.*, 2006; Reguera *et al.*, 2007; Gorby *et al.*, 2010; Picioreanu *et al.*, 2010).

Holmes *et al.* (2006) noted a correlation between increased transcript levels coding for membrane bound cytochromes during the anodic growth of G*. sulfurreducens* and increased power output in an MFC. In this study, MFC power was adversely affected when these genes were 'knocked out' in *G. sulfurreducens* but the deletion of genes coding for pilin expression had no observable effect on MFC output. Thus, whilst there must be an evolutionary benefit (motility, communication and biofilm formation) for 'nanowire' expression in a number of organisms, and their function is important in dissimilatory iron reduction, their precise role in MFC function is contentious despite their electrical properties having been unequivocally demonstrated (El-Naggar *et al.*, 2010).

2.7 MIXED CONSORTIA MFCS

Substrate degradation and thus electron transfer in MFCs is complex and is likely to occur through a series of community interactions and indirect, multi-step electron transfer to the anode. Analogies between natural systems and electron transfer in the anodic compartment are useful to understand microbial interactions in MFCs. Thermodynamically, anaerobic environments are challenging and organisms rely on complex interspecies relationships to exploit marginal energetic gains.

In classic models of anoxic carbon degradation, polymers are hydrolysed to monomers or smaller subunits and the hydrolysis products undergo fermentation to products such as acetate and butyrate. Organisms known to participate in fermentation processes and which have been isolated from the anodic compartment of MFCs include *Clostridium, Alcaligenes,* and *Enterococcus* spp. (Rabaey & Verstraete, 2005; Kim *et al.*, 2006).

Alternatively, acetogenesis yields acetate from molecular hydrogen and CO_2 (Figure 2.1). Acetate and hydrogen can (assuming the absence of sulphate or other thermodynamically more suitable electron acceptors such as oxygen) be utilised by methanogens (Stams *et al.*, 2006; Dolfing, 1998). A number of the reactions catalysed in anoxic environments are highly dependent on the concentration of hydrogen for them to remain thermodynamically favourable and the complete oxidation of organic compounds in anaerobic environments only proceeds within strictly defined limits. This state of metabolic dependency is known as syntrophy and ultimately results in methane production (Stams *et al.*, 2006; Khanal, 2009). A simplified schematic model of anaerobic carbon oxidation is presented in Figure 2.1. In an MFC, the production of either hydrogen or methane is indicative that the electrons from the catabolism of the carbohydrate electron donors are not being delivered to the anode. In MFCs, the anodic redox couple is likely to result from the metabolism of fermentation products by organisms as such as Geobacter and *Shewanella* spp. and, based on studies examining electron transfer mechanisms of these species, is much more likely to involve direct anodic contact although the role of redox shuttles cannot be ruled out (Bond *et al.,* 2002; Holmes *et al.*, 2006; Gorby *et al.*, 2006). Methanogens and electrogens are in direct competition with one another. Electrogens often outcompete slow growing methanogens, especially when the conditions in an MFC (high anode potential) favour high current flux to the anode (Jung & Regan, 2011).

Kim *et al.* (2006) studied the anodic community in depth and described how organisms inhabit either the true anodic biofilm, a 'bacterial clump' that is attached to the anode but does not constitute the biofilm, or the anolyte itself. They reasoned that the electrogens inhabited the biofilm whilst fermentative organisms inhabited the surrounding 'bacterial clump'. They also suggest that a number of redox-active metabolites might constitute a portion of the bacterial clump surrounding the anode (Kim *et al.*, 2006). This conclusion is likely as Stams *et al.* (2006) describe how, in natural systems, formate has a role as an electron mediator and the presence of nanowires may

allow electron transfer in biofilms, over distances as large as 12 mm (Reguera, 2006; Nielsen, 2010).

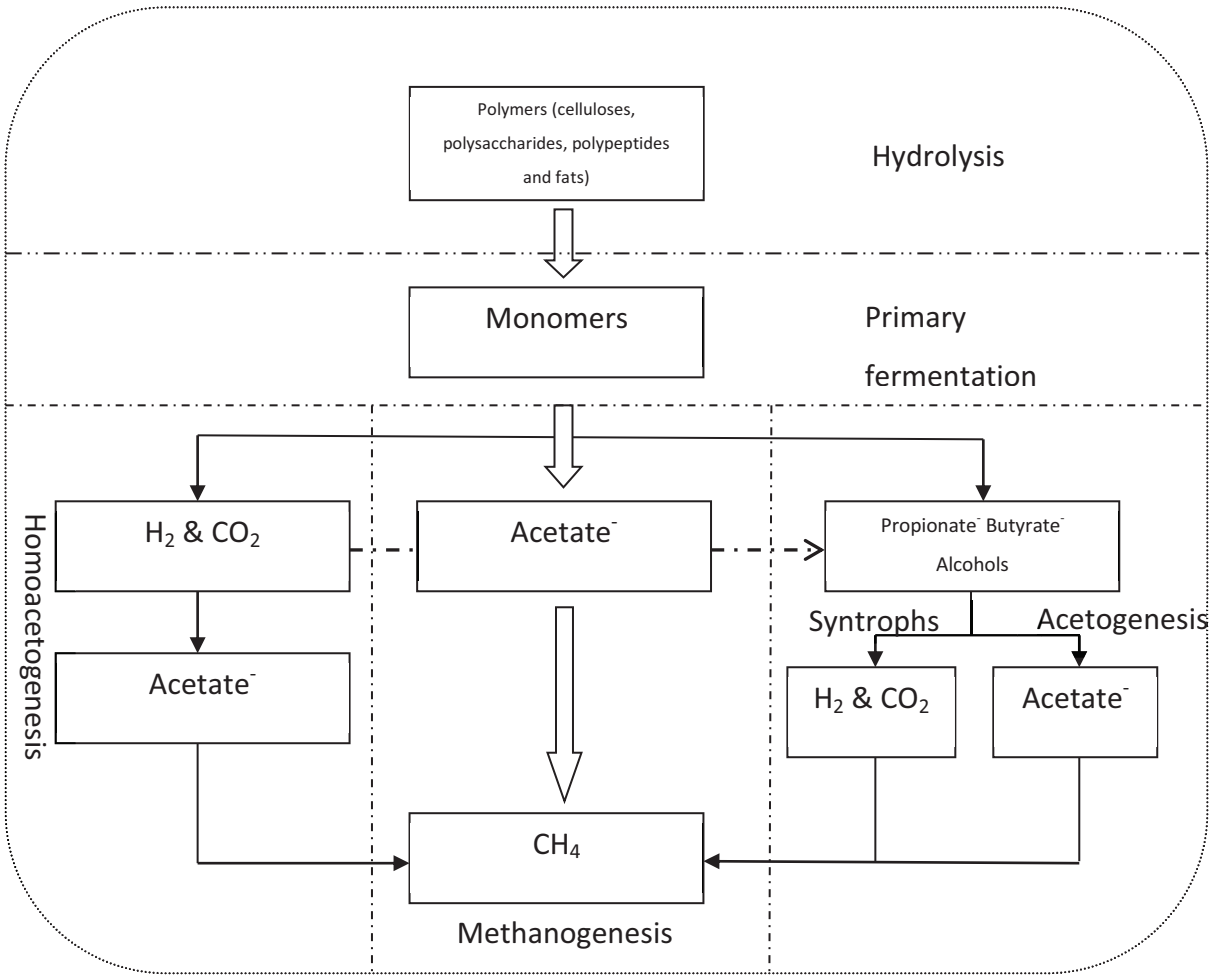

Figure 2.1 Schematic depicting anoxic carbon degradation pathways. For simplicity the steps can be broadly divided into hydrolysis, primary fermentation, secondary fermentation and obligate proton reduction by syntrophs, homoacetogenesis, and methanogeneis. It is worth noting that true homoacteogens utilise the acetyl co-A pathway (Wood Ljungdahl pathway) to synthesis acetate from CO_2 and Hydrogen although under certain conditions the acetyl-CoA pathway may result in the production of butyrate and other >C1 reduced species as indicated by the dashed arrow (Drake *et al.*, 2006). Adapted from Khanal (2009).

2.8 MFC DESIGN AND OPERATION

The current research drive behind MFCs has yielded advances in MFC design. The basic motivation behind design is optimising performance (output) and minimising cost for a given set of conditions dependent on the intended application. For example, MFCs designed for use in a wastewater treatment plant (WWTP) will have very different design specifications than for use in robotics. The former, for instance, will have to be large and stackable and have high treatment efficiency whilst not being prohibitively expensive; the latter will be less constrained by cost but will need to be, small, highly efficient and stable.

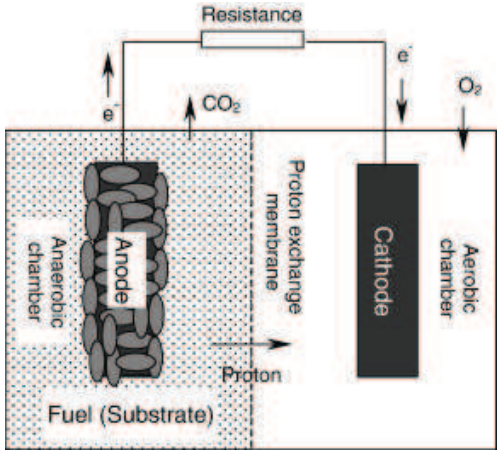

Figure 2.2 A schematic of a two chamber fuel cell taken from Du *et al.*, 2007. Note the aerobic cathode chamber can be filled with any oxidant such as ferricyanide aerated water or can be removed totally in air cathode MFCs where the cathode and proton exchange membrane are combined to make a membrane electrode assembly (MEA).

The output of an MFC is dependent upon a range of biological, chemical and physical parameters including: substrate mass transfer; electron transfer between the microbe and the anode; external resitance; microbial oxidation of substrate; proton transfer to the cathode; oxygen supply and reduction at the cathode (Picioreanu *et al.*, 2009). To favourably influence these factors, design based approaches can target, for example: internal resistance; anolyte composition; electrode surface area, geometry and

composition; MFC architecture, size and material; catalysts; and biology (Frank *et al.*, 2010).

The basic design of an MFC is very simple. At its most basic it requires an anode chamber, a cathode chamber, two electrodes (an anode and a cathode in their respective chambers), a wire to connect the electrode under load and a separator that is selectively permeable to protons and which divides the two compartments (Du *et al.*, 2007). This is known as a two chamber configuration and a schematic is shown below in Figure 2.2.

The design of MXC devices has flourished since the re-emergence of research effort in the late 1990s. Conceptually, design progress can be seen as diverging into four main directions: scale up; miniaturisation; benthic; and MECs although this classification is the author's own convenience and not based on consensus. Benthic MFCs such as that described by Tender *et al.* (2002) are distinctive from all other classes of MFC in an architectural sense and have received interest as devices which can power remote sensors in marine environments. Benthic MFCs are the understatement of the MFC world and have furthered our understanding of both bioelectrochemical systems and geochemical processes (Nielsen *et al.*, 2008; Nielsen *et al.*, 2010). MECs are likely to yield the most interesting designs in the near future and recently a sophisticated and novel reactor design was demonstrated by Cheng *et al* (2011) that could produce methane in bioelectrochemical reaction (Cheng *et al.*, 2006; Cheng *et al.*, 2011). Miniaturisation at the millilitre scale has provided the highest power density to date of 1010 mW m^3 but systems at the microlitre scale have suffered from lower power densities (Wang *et al.*, 2009). The effort to scale up MFCs has attracted the most research interest and is most relevant to this thesis and in wastewater treatment (WWT) applications. While it is conceivable that small devices will be used in WWT applications this will be in a modular form and must still be scaled up by staking them (Ieropoulous *et al.*, 2010).

Early two chamber MFCs required the addition of and oxidant in the cathode chamber – ferricyanide was a commonly used oxidant (Bullen *et al.*, 2006). Researchers quickly noted that ferricyanide was not sustainable as it would need to be chemically

regenerated (oxidised) or continuously replaced negating the energetic gains of reducing it in the first place. This is unfortunate as power densities reported with ferricyanide are generally very high up to 7200 mW m^{-2} (Oh *et al.*, 2004; Logan, 2008).

Atmospheric oxygen is a more sustainable oxidant and a single chamber MFC that did not require ferricyanide was first reported by Park & Zeikus (2002) and Liu *et al.* (2004) later described a single chamber MFC that could treat wastewater whilst reducing atmospheric O_2 to water. This innovative design, often termed an air cathode MFC, is perhaps the most important design modification to date has been a superlative research tool and subject to all manner of testing including: different separators (Li *et al.*, 2010), electrode materials (Deng *et al.* 2010), catalysts (Cheng *et al.*, 2006), sizes (Scott *et al.*, 2007), and stacking, (Ieropolus *et al.*, 2010; Aelterman *et al.*, 2006). Single chamber air-cathode MFCs have greatly increased our understanding of BES. The main barrier to their practical use is the unfortunate fact that the Pt catalyst has yet to be improved upon and MFCs that use noble metal catalysts are inherently unsustainable and prohibitively expensive (See section 2.8.1).

Outputs from MFCs scaled up to the litre sizes have proved largely in agreement with sub litre scale bench tests yet scale up beyond this remains largely understudied (Logan, 2009). A one cubic meter MFC was tested at the Foster's brewery in Yatala in Queensland by Jurg Keller and Korneel Rabaey. There are scant data from this pilot study although Jurg Keller, in a presentation (www.microbailfuelcell.org), reported that the current was 2A at 400 mV per cell (800 mW m^{-3}) and asserts that wastewater conductivity (high IR) was the main impediment to higher power densities. Recently, Jiang *et al.* (2010) reported a 20L pilot scale MFC with a power density of 325 mW $m^{-3}$with a treatment efficiency of 80%. The only other pilot study that has been conducted is with a 1 m^3 hydrogen MEC in California's Napa valley wine region by Bruce Logan and his team (Cusick *et al*, 2011). Although the MEC could produce currents of up to 7A m^{-3}, most of the anodic product was methane rather than hydrogen.

Other interesting designs of MFC have included a hybrid up-flow MFC (Katuri & Scott, 2010); an advective flow-through porous anode MFC (Cheng *et al.*, 2006); an overflow wetted wall MFC (Li *et al.*, 2009); tubular membrane cathodes (Zuo *et al.*, 2006); Graphite fibre brush anodes (Logan *et al.*, 2007); and a cassette electrode MFC (Shimoyama *et al.* 2008).

2.8.1 ELECTRODE PERFORMANCE AND DESIGN

From a purely electrochemical perspective, platinum is the ideal electrode material on account of it being corrosion resistant and having superlative catalytic properties and a higher oxygen reduction reaction (ORR) activity than any other metal (Jaouen *et al.*, 2010). Platinum is a rare precious metal with world reserves estimated at only 40,000 tonnes. The US department of energy has set a Pt utilisation target for energy generation technologies of 0.2 g kW^{-1} at 55% efficiency.

Researchers have investigated a variety of electrode materials and configurations (e.g. Park & Zeikus 2002; Schroeder *et al.*, 2003). Cathode performance is a function of either the material it is constructed from or by properties bestowed on the material from added catalysts. Various forms of carbon (cloth, graphite, vitreous, and paper) are often coated with platinum or doped with other chemicals in an attempt to improve performance (Park & Zeikus, 2002; Oh *et al*, 2004; Logan, 2009; Jaouen *et al.,* 2010). Oh *et al.* (2004) compared the effect of a platinum coated carbon cathode with a plain graphite cathode immersed in ferricyanide solution on MFC power output. They found that the plain graphite cathode immerse in ferricyanid*e* performed better, perhaps because of mass transfer efficiencies and the higher cathode potential of ferriciyanide (332 mV) compared to oxygen (268 mV). Despite the superior performance of ferricyanide, it is still considered an unsustainable approach to MFC design.

Non precious metal catalysts (NPMC) have received much attention both in MFC and conventional fuel cell research with Metal, Nitrogen Carbon (Me/N/C) catalysts derived from heat treatment with the Co and Fe precursors showing the most promise (Jaouen *et al.*, 2010). Park and Zeikus (2002) reported up to a 1000 fold increase in power output

from an MFC, which was, in part, attributable to the cathode which was doped with Fe^{3+}. Cheng *et al.* (2006) investigated refinements to cathode configuration and showed that the Pt content of the cathode can be reduced to more affordable levels or replaced completely by NPMC catalysts (cobalt in this instance) with little effect on performance.

Cathode modifications that increase its potential are favourable as is increasing cathode surface area (real or apparent) in relation to the anode. The density of active sites and the specific turnover activity of these sites are what confers the catalytic properties to a particular compound and what increase the apparent surface area, and hence ORR activity of the cathode material (Jaouen *et al.,* 2010). Whilst some solutions are effective, i.e. the use of a ferricyanide catholyte, they are unlikely to find real world applications in MFC technology as they are unsustainable and create disposal and maintenance problems (Logan *et al.*, 2006; Huang *et al*; 2011). The most promising recent advances lately are activated carbon with current collectors and biocathodes (Logan, 2009; You *et al.*, 2011). Biocathodes offer the greatest hope of sustainability in MXC technology although the mechanisms of electron transfer in electrode oxidation are as complex as electrode reduction, as are their numerous applications (Huang *et al.*, 2011).

The anode presents a complex problem as it has the dual function of electrode and biological interface. The addition of mediators to MFCs is not likely to provide a commercially successful solution to enhancing MFC performance on account of expense and toxicity (Logan, 2009). Embedding electron mediators such as Mn^{4+} or neutral red in the anode surface was shown by Park and Zeikus (2002) to be an effective way of boosting fuel cell performance. Schröder *et al.* (2003) took this one step further and showed that anodes coated with polymerised electron mediators such as polyanaline, or poly-neutral, increased cell performance. This, they reasoned, was because the polymers rendered the insoluble anode more biocompatible but also because of the redox properties of the polymer coatings. Various types of carbon have been used as anodes such as graphite, sponge, paper, cloth, felt, fibre, foam, reticulated vitreous carbon and glassy carbon (Borole *et al.*, 2009; Larrosa-Guerrero, 2010; Katuri *et al.*, 2010). Heat and

ammonia treatments have been shown to increase performance as have graphite brushes, however, the more elaborate the material or treatments that it is subjected to the greater the cost which must be kept to a minimum.

Alternative means for increasing MFC performance have been investigated. Liu *et al.*, (2005) showed that increased ionic strength in the anode chamber as well as operating temperature improved fuel cell performance. They also showed that the proximity of the anode and cathode increased MFC performance. This has been shown by other modifications in MFC design (e.g. the flat plate arrangement reported by Min & Logan (2004)) and is perhaps owing to decreased proton migration distances which will lower the internal resistance of the cell.

2.9 FUEL CELL PERFORMANCE

Essentially, the definitive measure of MFC performance is extractable power. Power (P) is generated by the cell's electromotive force (EMF) which is the potential difference between the oxidant and the fuel or reductant and is measured in volts (V) and shown the expression (Equation 2.3) below (Katz *et al.*, 2003):

$$E_{emf} = E_{ox}^{o'} - E_{red}^{o'}$$

Equation 2.3

More specifically this is the difference in potential of the catholyte and the anolyte and can be determined using standard electrodes and or thermodynamic calculations such as the Nernst equation (Bard & Faulkner 2001; Logan *et al.*, 2006):

$$E_{emf} = E^{0\prime} - \frac{\mathrm{R}T}{nF}\ln(\Pi)$$

Equation 2.4

Where emf is the electron motive force, $E^{o'}$ is emf at standard biological conditions (pH 7, 303 K) R is the gas constant (8.31447 J K^{-1} mol^{-1}; T, the temperature (K); n the number of

electrons transferred and F is Faraday's constant (96,485C mol^{-1}), Π is the reaction quotient (Logan, 2008). Equation 2.4 returns a positive result if the reaction is thermodynamically favourable (exergonic) and a negative one if it is endergonic.

Where a potential difference exists and the two half cells are connected by a circuit, a current will flow from the low potential electrode (anode) to the high potential electrode (cathode) and current will be a function of the potential across the two electrodes and the resistance of the circuit:

$$E = IR$$

Equation 2.5

The power of the cell is measured in watts (W) and is the product of the potential difference and the cell current (I) which is measured in amperes (A) both of which can be readily determined with simple equipment:

$$P_{cell} = I\ E_{cell}$$

Equation 2.6

The open circuit potential (OCP) of an MFC (the potential of an MFC when it is not under load) should, theoretically be an indication of the EMF of a cell. In reality, the open circuit potential of the cell is much less than the theoretical potential as the EMF of a cell is used to drive current not only through the load in the external circuit but also through the components of a cell. This results in irreversible losses that are known as overpotentials. They are caused by ohmic losses, which are a function of the internal resistance of the MFC; activations losses, which are caused by overcoming the activation energy required for a reaction to proceed; concentration losses, that are caused by mass transfer and concentration limitations; and turnover losses which are caused by the biocatalytic capability of the anode (analogous to the metabolic rate of the electrogens). The effect of overpotential on cell voltage is described in Equation 2.7 (Katz *et al.*, 2003):

$$E_{cell} = E_{EMF} - (\Sigma\eta_{\mathrm{An}} + \Sigma\eta_{\mathrm{Cat}} + \mathrm{IR}_{\Omega})$$

Equation 2.7

Where $\Sigma\eta_{An}$ is the anodic overpotential, $\Sigma\eta_{Cat}$ is the cathodic overpotential and IR_{Ω} is the ohmic loss proportional to the current and the internal resistance of the system.

The key to excellent MFC performance is maximising the cell potential and current. The internal resistance of the cell can be seen as the ease of which electrons and protons can flow through the system and is affected by kinetic and thermodynamic limitations, the composition of the anolyte and catholyte (including fuels used and the presence of electron shuttles), pH, temperature, microbial composition, ohmic resistance, the separator used, the particular MFC design and concentration gradients (Katz *et al.*, 2003; Ieropoulous *et al.*, 2005; Logan *et al.*, 2006).

A powerful tool for measuring MFC performance is a polarisation curve (Figure 2.3). Polarisation curves for the whole cell or each electrode can be obtained by switching out resistances across the cell and plotting the cell or electrode voltage as a function of current density. The shape of the polarisation curve can help identify MFC overpotentials.

Whilst traditional electrochemistry is undoubtedly useful for assessing fuel cell performance it is clear that the unrivalled complexity in describing microbial communities in purist electrochemical terms may be problematic. There is emerging evidence that conventional electrochemical methods may not be directly applicable to MFCs and in some cases may need modification. Watson & Logan (2010) demonstrated that polarising MFCs using Linear Sweep Voltammetery does not appropriately accommodate the response times of microbial redox apparatus and consequently may result in the overestimation of peak power outputs when used to conduct polarisation studies in MFCs. This is undoubtedly an area that will advance as MFC research develops from a nascent research area to a mature discipline.

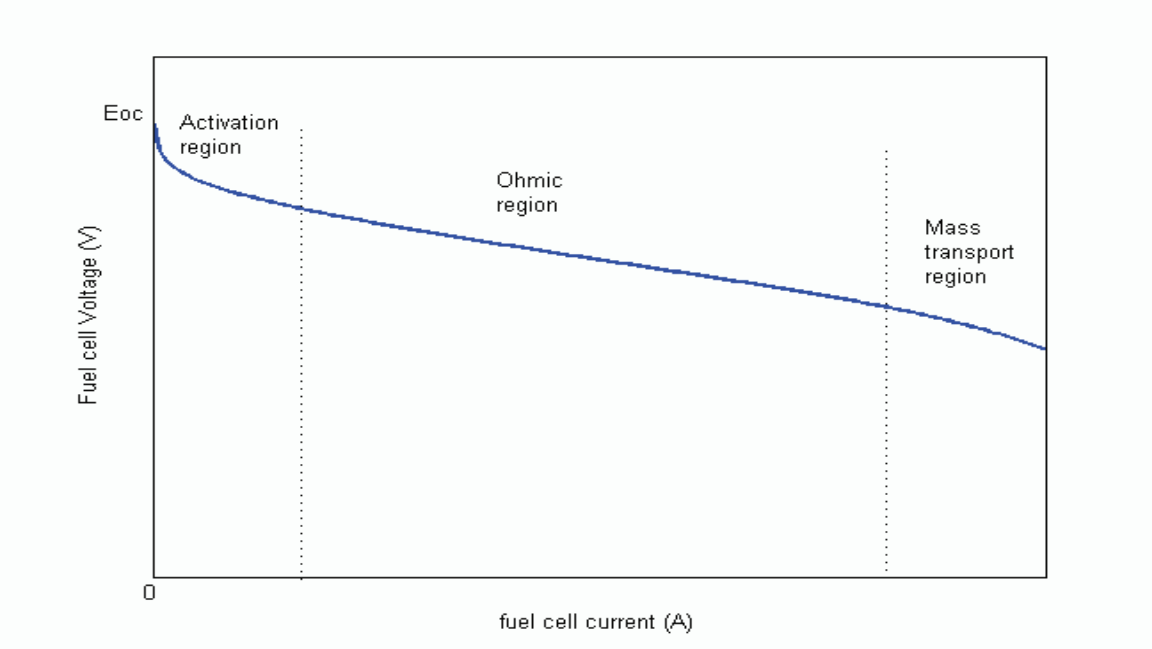

Figure 2.3 A model polarization curve showing the three regions of losses: activation losses at low current density; the ohmic region where there is a proportional increase in overpotential with increases in current; and the mass transport region that occurs at high current densities. Note that high current is associated with low cell voltages. Source: www.mathworks.com

2.10 Some challenges in MFC development

2.10.1 Scale up

Although good power performance up to 1.55 kW m^3 has been demonstrated at the lab scale, power outputs of pilot scale sized MFCs have, however, proved disappointing (Rozendal *et al.*, 2008). Researchers from the Advanced Water Management Centre in Australia operated a pilot sized (1 m^3) MFC at the Yatala brewery, in Queensland. Poor performance of 40 mA m^2, fell considerably short of their 1kA m^2 target. The reported losses were caused by high IR resulting from the 'very different' properties of the wastewater being treated compared to laboratory media (Rozendal *et al.*, 2008). The difficulty of scaling up MFCs to unit sizes of a cubic meter suggests that stacking smaller units together represents the best strategy for scale up.

By connecting MFCs together the voltage and current can theoretically be increased to desired working voltages and current. Connecting microbial fuel cell in series (n) will add voltage and connecting them in parallel (m) should add current. Stack designs consisting of a number of MFCs connected both in series and in parallel (n x m) can be considered as a single MFC with voltage and current as a function of stack size (Aelterman *et al.*, 2006; Oh and Logan, 2007; Lefebvre *et al.*, 2009; Lefebvre *et al.*, 2011). Researchers from the Centre for Water Research at the National University of Singapore presented an interesting study of MFC stacking (Lefebvre, 2009). They suggest that MFC design strategies pursuing low internal resistance as a priority for intensive MFC research because, based on the principle of the maximum power theorem (Equation 2.8), power outputs in an MFC are highest when R_{EXT} and R_{INT} are equal and low R_{EXT} is synonymous with high current densities and therefore reduced stack sizes (Lefebvre *et al.*, 2009)

$$P = OCV^2 \{R_{EXT}/[A(R_{EXT} + R_{INT})^2]\}$$

Equation 2.8

Lefebvre *et al.* (2009) reasoned that at a stack size of 2400 cells, based on the lowest MFC internal resistances reported at the time (10 Ω), would provide enough power to operate a 40 W pump (pump specifications: 12v at 3.3A). In a recent paper, the argument has been refined by assuming an internal resistance of 5 Ω, which is based on a state of the art reported by Shimoyama *et al.* (2008) and lowering the pump specification to 4W (5V at 0.8A) (Lefevbre *et al.*, 2011). With this revised model, a 'self-sustaining' fuel cell (one that could power its own pump), would require a stack of 130 MFC units (10 n x 13 m) each with a volume of 0.6 L resulting in a 78 L (minimum) stack volume.

The argument for minimising R_{INT} in MFCs is logical but fails to recognise the inherent properties of wastewater which, typically, have low conductivity (around 1 mS cm^{-1} or equivalent to a resistivity of 1000Ω cm^{-1}) and whose raw composition is difficult to control. Electrolyte losses contribute significantly to R_{INT} and in an MFC and R_{INT} is magnified with volumetric increases and increased electrode spacing (He *et al.*, 2006; Clauwaert *et al.*, 2008; Fan *et al.*, 2008; Rozendal *et al.*, 2008). If MFCs were to be

operated at high current and low voltage, then the energy efficiency is not likely to be optimum as cell overpotentials caused by concentration and turnover losses will increase disproportionately at high current (Harnisch & *Schröder*, 2010). Furthermore, high currents densities are, reportedly, only possible in MFCs operated at high organic load (Lyon *et al.*, 2009). Therefore in considering MFC stack sizes, stack volume is in conflict with the number of units in a stack because low energy efficiency will require larger MFC volumes for equivalent power outputs.

Lefebvre *et al.* (2011) used the following parameters: E_{cell} = 800 mV (OCP), 80% CE and an Alita N3 pump. These parameters are unrealistic as the OCP of 800 mV is more than the OCP reported by Shimoyama *et al.* (2008) of 560 mV and 80% CE is optimistic in field conditions. The pump that they have chosen, an Alita N3, can only cope with a 2.5 cm hydraulic head at the specified flow rate of 0.1 L min^{-1}. An MFC stack of 130 units and a volume of 70L replete with pipe fittings that will impede hydraulic conductivity is likely to exceed the shut off head for the pump (www.alita.com). Without being overly critical of what is an extremely important paper, both in its novelty and the insights it provides, a stack size of 130 MFCs, at current state of the art, is optimistic and the pump specifications chosen are too low for the suggested application. To their credit, they do state that this is a 'pedagogical example' and in this respect their paper is exemplary and cogently illustrates the challenges that are inherent in MFC scale up.

The ability of MFCs to be stacked is, therefore, of crucial importance if MFCs are to be scaled up to provide useful power outputs in WWT applications. It is impossible to constrain power requirements of pumping equipment for MFCs of unknown stack sizes because of poorly constrained energy efficiency. The voltage requirement for pumping equipment can reasonably be assumed equal to one of the world standards. Assuming a low 12V standard, we can constrain the minimum number of MFCs that need to be stacked in series (each with and an assumed operational voltage of between 0.4-0.8 V) at between 30-60 MFCs.

A search on the *Web of Knowledge* database using the terms 'MFC + Stack*' yields only 31 results compared to 2178 for the term 'MFC'. Only 14 of these records are relevant and although the average number of citations for each relevant record is 16 this is skewed by one paper with 137 citations (Aelterman *et al.*, 2006; www.isiknowlege.com). Furthermore, some of these studies did not investigate stacking per se but have used small stacks as an experimental convenience (e.g. Woodward *et al.*, 2010). A well known phenomenon, publication bias (also referred to as the file drawer effect) is the tendency for only positive results to be published or, to put it formally, 'A publication bias exists if the probability that a study reaches the literature, and is available for combined analysis, depends on the result of the study' (Scholey & Harrison, 2003). Practitioners of medical science, where the effect of publication bias can be grave, have adapted ways to counter its effects. The absence of studies investigating stacking in the literature is therefore ominous and we can conclude that either a large number of MFC stacking studies have not been carried out or, that when they have they are subject to publication bias.

The most cited, and important, study on stacking to date was conducted by Aelterman *et al.*, (2006). Peter Aelterman and his colleagues observed three interesting phenomena: voltages can be increased by connecting MFCs is series but they suffered from a phenomenon known as cell reversal (a spontaneous change in the polarity of an MFC); enhanced treatment efficiency was not associated with MFCs stacked in series; stacked cells did not deliver higher power densities than individual MFCs. Cell reversal will cause instability in MFC stacks and poor treatment efficiency will increase the hydraulic retention time required for WWT which in turn will increase the effective reactor size required therefore adding to pumping power requirements. The instability of stacked cells caused by the phenomenon of cell reversal has been described by several authors and is poorly understood but is likely the result of differential COD concentration and ORR capabilities between individual cells in the stack (Aelterman, 2006; Oh & Logan 2007; Dekker *et al.*, 2009; Ieropolous, 2010). Small stacks with a maximum of four units have been successfully connected to improve power outputs and studies show that different separators may decrease incidences of voltage reversal although this has only been

demonstrated with bench scale units (Wang *et al.*, 2009; Ieropolous, 2010). The problems of scale up are not just electrochemical and some studies have reported hydraulic short circuits or plug flow in MFC stacks further suggesting the need for sophisticated design of MFC plant (Dekker *et al.*, 2009; Zhuang & Zhou, 2009).

Thus, to date, nobody has convincingly demonstrated an MFC design that can be stacked to meet requirements of operating large scale WWT plants over extended periods. If this hurdle cannot be overcome, and useful voltages and current cannot be achieved, MFC technology is unlikely to ever be useful for powering anything more than small sensors or in other niche applications.

2.10.2 CATALYSIS

Many authors agree that the cathode presents a challenge to the advancement of MFC technology as it must to provide a reactive site that acts as an interface across three phases: gaseous oxygen, aqueous protons and solid electricity (Logan, 2009).

For electrochemical purposes the platinum electrode is the ideal material on account of it being corrosion resistant and having superlative catalytic properties and a higher oxygen reduction reaction (ORR) activity than any other metal (Jaouen *et al.*, 2010). The catalytic potential of graphite, a common low cost electrode, has a low ORR activity and it is often doped with catalysts for MFC applications. Pt is a common catalyst for doping electrodes to enhance their ORR activity. Pt is unsustainable, however, because of poor ORR kinetics at neutral pH and ambient temperatures and also because of its prohibitive cost and global scarcity (Yu *et al*, 2007; Kim *et al.*, 2007; Logan, 2009). Non precious metal catalyst (NPMC) alternatives to platinum have been investigated, mainly Co, Fe & Mn which are often bound in the macrocyles of porphyrins and phthalocyanines (Jaouen *et al.*, 2010). These have been shown to perform better than Pt in half cells under MFC conditions: pH 7, ambient temperature, and moderate buffering (You *et al.*, 2007) although the durability and high activity of NPMC has yet to be unequivocally demonstrated along with their temporal stability in MFCs fed with wastewater (Jaouen *et al.*, 2010; Lefebvre *et al.*, 2011). Christgen (2010) showed that the activity of a number of catalysts (iron

phthalocyanine (FePC), FePC & Manganese oxide, Nitric acid treated carbon black and Pt on carbon) declined significantly before the end of 100 day period. Whilst the carbon black supports and Pt particles commonly used in cathodes of MFCs are nanosized, the way they are loaded onto the electrode assembly does not commonly involve advanced techniques and it is likely that future developments in nanotechnology will offer at least partial contribution to developments in cathode research (Higuchi *et al.*, 2009).

The use of NPMCs in realistic conditions over an extended duration need to be fully characterised as what may be marginal economic or performance gains at the lab scale may not translate to improvements under extended periods of operation. Similarly, the high cost of materials may be insignificant at the lab scale but be magnified to an unrealistic extent when scale up is calculated. For example, the highest output of an air cathode MFC was reported as 1.55 kW m^3 with a cathodic surface area of 280 m^2 m^{-3} (equivalent to 180 m^2 kW^{-1}) (Fan *et al.*, 2007a). The loading rate of Pt catalyst on the electrodes used by Fan *et al.* (2007a) was 0.5 mg cm^{-2} working out at 900g Pt kW^{-1} (Fan *et al.*, 2007b). The spot price of platinum at the time of writing is $1800 per troy ounce making the cost of platinum in this application a prohibitive $55,000 for a 1 kW device (www.kitco.com).

Harnisch & *Schröder* (2010) recently proposed a framework for assessing cathode suitability that considers eight criteria: selectivity, periphery costs, processing costs, product quality and value; thermodynamic performance, kinetic performance, longevity, and catalyst cost. It may be the case that rough and ready alternatives to Pt, such as the absence of any catalyst, can offer field stability and lonegevity, and meet some of the other assessment criteria proposed by Harnisch & *Schröder* thus making them a better option than NPMC or Pt although this will be at the expense of good MXC performance. Christgen (2010) observed that untreated carbon black was the most stable cathode in wastewater fed MFCs compared with a number of alternatives including Pt suggesting that close attention needs to be paid to weight up gains in performance over stability and economics. The future is likely to see great refinements in methods of catalyst

assessment and provide an objective means of assessing what we can really expect from MFC technology. It may be the case that all types of catalyst have niche applications that will eventually be realised but for the moment WWT using MFC technology seems economically far off the mark considering the current high cost and unknown stability of catalysis.

2.11 HORIZONS IN MFC DEVELOPMENT

2.11.1 ADVANCED CONTROL SYSTEMS

As MFCs develop, the need to consider how they are operated in the field is likely to be of widening research interest. Picioreanu and his colleagues have conducted two studies that model MFC behaviour, one on biofilm MFCs and another that describes pH and electrode geometry (Picioreanu *et al.*, 2007; Picioreanu *et al.*, 2010). As our understanding of MFCs evolves modelling capabilities will advance too and open the possibility of enhanced and rapid investigations aimed at optimising MFC performance for any number of scenarios. The conditions inside an MFC – such as organic load, internal resistance, electrode potential and so forth – are temporally dynamic during operation and are also influenced by environmental factors such as temperature and influent composition. For this reason, persistent, consistent and optimal performance during operation is generally not possible as MFC parameters, once selected, remain static (Premier & Kim, 2011; Woodward *et al.*, 2010).

New methods for real time optimisation of MFCs exist. These target external resistance (the only realistic parameter for field control of MFCs because it is readily manipulated after design and instalation) which instead of being static, is changed according to MFC conditions. Woodward *et al.* (2009) compared three optimisation techniques - two Maximum Power Point Tracking Methods (MPPT) and a novel multiunit optimisation (MU) method – and found that the MPPT perturbation and observation method and the MU method were useful for real time optimisation of MFCs and that the MU method allowed faster convergence to optimum. The study also showed that different perturbations (changes in organic load and temperature) induce different optimisation

behaviour suggesting that real world perturbations will need careful and targeted management strategies that arise only from intimate understanding of MFC behaviour.

Advanced control methods will be of vast importance in real world MFC applications, particularly where large stack sizes are required, both to manage process perturbations (changes in temperature, influent composition and conductivity etc.) and complications of stacking MFCs such as voltage reversal (Woodward *et al.*, 2009). The multi unit optimisation described is applicable to MFC stack operation but it relies on *a priori* information which is difficult to obtain and will require additional sensing equipment to be designed into MFC architecture. The cost implications of the sensory equipment, and indeed, the hardware to operate the multi-unit optimisation system are as yet unknown but are likely to add to the already challenging economics of MFC scale up. One of the problems of Woodward's comparison study is that the perturbations were introduced to the system over short time scales (seconds) which is likely too fast for microbial redox adaptations. This was addressed in a different study by Woodward *et al.* (2009) where acclimation times between perturbations was increased to 10–15 minutes although Watson & Logan (2010) observed that microbial acclimation to changes in external resistance was slow and occurs in its entirety over hours or days rather than minutes. A batch study using a parsimonious logic-based control algorithm for MFC optimisation and conducted over 600 hours, showed increased power output in load controlled cells over a more sustained period compared with a static load MFC (Premier & Kim, 2011). This was accompanied by a reduction in biomass on the load controlled anodic biofilm and a fivefold increase in coulombic efficiency in the load controlled cell over the static load MFC. Furthermore, the authors assert that load control may increase operational stability and longevity in MFCs and can be implemented at low cost.

Intelligent control studies for MFCs such as those described above are only recently emerging in the literature. There is considerable potential in these techniques, particularly the simple model proposed by Premier & Kim (2011) and they are likely to be

useful as research tools to facilitate scale up and stacking as well as offering fundamental insights into MFC technology.

2.11.2 MXCs

The high cost of catalysis in MFCs relative to the wholesale cost of electricity, which is currently trading at an average of around £50 per MWh (www.wrap.com, March 2011), has driven researchers to consider the application of microbial fuel cell-based technologies for the generation of products other than electricity. The electrons harvested at the anode can be used to drive almost any electrochemical process at the cathode given favourable redox potentials, and the prospect for novel cathode reactions is high. The versatility of the technology is such that a variety of catalysts can be used in an MXC (enzymatic, chemical and biological) and by considering a number of cathodic end products, matching specific catalyst properties to the requirements of the bioelectrochemical reaction will be possible. Whilst it is still likely that Pt will be too costly for many applications, the production of high value chemicals may mean cost considerations are less restrictive (Harnisch and *Schröder*, 2010).

Many cathode reactions have been considered in MXCs including the production of caustic soda, methane and hydrogen as well as the removal of pollutants from wastewaters such as the reductive dechlorination of organic solvents, the reduction of nitrobenzene and decolourisation of azo dyes (Logan, 2008; Rabaey *et al.*, 2010; Mu *et al.*, 2009; Mu *et al.*, 2009). Four common cathodic reactions are considered in Equation 2.8 to Equation 2.12 below:

$$O_2 + 4H^+ + 4e^- \rightarrow 2H_2O \;\; \Delta E^{\theta'} = 0.805V$$

Equation 2.9

$$O_2 + 2H^+ + 2e^- \rightarrow H_2O_2 \;\; \Delta E^{\theta'} = 0.62\,V$$

Equation 2.10

$$CO_2 + 8H^+ + 8e^- \rightarrow 2H_2O + CH_4 \;\; \Delta E^{\theta\prime} = 0.098\,V$$

Equation 2.11

$$2H^+ \, 2e^- \rightarrow H_2 \;\; \Delta E^{\theta'} = -0.414\,V$$

Equation 2.12

The ORR (Equation 2.9); hydrogen peroxide evolution (Equation 2.10); methanogenic CO_2 reduction (Equation 2.11); and the hydrogen evolution reaction (Equation 2.12) are shown with their corresponding standard potentials (Fetzer & Conrad 1993; Logan, 2008; Rabaey, 2010). Reactions with a positive potential are exergonic and can occur with the release of energy, conversely, negative potentials denote endergonic reactions and require energy for them to proceed. The ORR is the standard reaction in MFCs and has is the focus of the discourse in this study (Equation 2.8) although the partial reduction of oxygen of H_20_2 is an unwanted reaction that can contribute to cathodic overpotentials in MFCs. All but the reaction shown in Equation 2.12 are exergonic which, theoretically, means that they can proceed in a galvanic cell (an MFC) whereas the reaction shown in Equation 2.12 can only proceed in an MXC where there is an input of energy. If hydrogen evolution at the cathode of an MEC is coupled to the oxidation of acetate at the anode (-300 mV) then theoretical cell voltage is -0.14 ($E_{cell} = E_{cat}$ (-414) – E_{an} (-300) = -0.14). The cell voltage of -0.14 V represents the voltage that will need to be overcome to produce hydrogen at the cathode, the fact that it is lower in MECs as opposed to the standard potential of -0.414 V (Equation 2.12) is what makes MECs attractive as a way to produce hydrogen with less input of energy than standard electrolysis of water. The potentials quoted above are ideal potentials and any overpotential in the MXC will have the effect of decreasing the energy output (in the case of an MFC) or requiring the input of more energy for an BES. See Logan *et al.* (2008) for a good review of the hydrogen evolution reaction in MECs.

Methanogenesis has traditionally been thought to proceed only at very low redox potentials of around -200 to -350 mV (Khanal, 2009). It is, however, the extreme sensitivity of methanogens to oxygen rather than the redox potential per se that inhibits methanogenesis. Oxygen concentrations of only 0.005% (corresponding to an E_h of ≈50 mV) are sufficient to inhibit methanogenic reactions. Fetzer & Conrad (1993) demonstrated that a pure culture of the methanogen *Methanosarcina barkeri* could

produce methane at redox potentials as high as 50 mV and that the methanogeneis was not impeded even in media with a high initial E_h of over 400 mV, clearly demonstrating that the absolute oxygen concentration limits methanogenesis rather than the redox potential. It is realistic to have operational anode potentials significantly below 50 mV and, given that methane production is exergonic, it possible to generate methane at the cathode with the production of small current. The redox potential for the CO_2 methane couple shown in Equation 2.11 is 98 mV. Given the relatively low Gibb's free energy for the reaction in Equation 2.11 compared to, for instance, the ORR (Equation 2.9), even small overpotentials will lead to either a very sluggish reaction or require the input of energy. Both hydrogenotrophic and acetoclastic methanogens have been shown capable of accepting electrons from an electrode although to date this has not been shown to proceed where the energy balance is positive (Cheng, *et al.*, 2010; Cheng *et al.*, 2011).

The area of methanogenic MEC research is in its infancy and offers potential for the same rapid development in understanding that has occurred with MFCs over the last decade. AD is a well-established, comparatively well understood and stable technique for producing methane so methanogenic MECs must provide a benefit over AD for them to find a proper use in society. AD suffers from instability when changes to organic load or feedstock composition are introduced; some biomass is unsuitable for direct AD and the process is usually limited by hydrolysis (Khanal, 2009). These problems are often addressed with a multi stage processes. The first stage is designed to solubilise material (this can reduce toxicity, solubilise components that require particular degradation conditions or simply concentrate the feedstock) that can be then fed into an anaerobic digester. The first or early stages of multistage AD processes require an input of energy and it is here that methanogenic MXCs may be competitive and the requirement for small current inputs mitigated. One could imagine a central methanogenic cathode receiving electrons from multiple units able to solubilise any type of biomass simultaneously.

2.12 FUNDAMENTALS

In 1962, Berk & Canfield doubted that biological fuel cells could ever yield useful energy but recognised their potential as useful research tools – particularly in relation to corrosion science at the bacterial metal interface. This was a great insight and MFC research has undoubtedly advanced our understanding in unexpected ways, particularly regarding exocellular electron transfer at microbiological solid interface and the discovery of electrically conductive pili (Reguera *et al.*, 2005; Gorby *et al.*, 2006). These discoveries have been incidental but important in describing MFC interactions and it is likely that this interesting field of research, particularly with the emergence of new technologies such as MECs, will continue to provide novel scientific insights. This can be stimulated by using MFC techniques as research tools in the form of bioelctrochemical reactors.

Perhaps the most dramatically fundamental example of MFC technology is the study by Abrevaya *et al.* (2010) who proposed using MFCs as 'life detectors' for space missions to other planets. As a case for using MFCs as life detectors, they cite the example of the false positive obtained from a suite of life detectors on board the 1972 Viking Lander mission to Mars. They propose an MFC that samples Martian soils and the proof of concept was demonstrated by higher current densities in soil samples that contained living bacteria when compared with a sterilised control soil sample. Whilst this does not rule out false positives from, for example, mineral driven redox chemistry, biological redox reactions will have a well defined electrochemical signature that can be determined from abiotic redox processes.

Recently, bioelectrochemical techniques have been used to study the role of microbes in marine sediment biogeochemistry. Nielsen *et al.* (2010) showed that benthic microbes isolated from the ocean sediments in Aarhus Harbour and Aarhus Bay, Denmark, could oxidize H_2S coupled to oxygen reduction in the overlying seawater over distances greater than 12mm at rates which could not be explained by diffusion and only by the transmission of electrons. This is the first time that extracellular electron transfer has been demonstrated over distances greater than a few microns and is explained by the

flow of a current through sediments facilitated by a proposed interaction between the sediment, made conductive by pyrite, and microbes that can transmit electrons to the sediment matrix via cytochromes, external redox shuttles and nanowires – the latter of are proposed as a means for microbes to interact with one another within the electrically conductive sediment matrix. The observation of naturally occurring electric currents in marine sediments brings us closer to understanding why the reactions that are exploited in MXCs occur in nature and it is likely that the benthic environment is a naturally occurring analogue of an MFC. Benthic MFCs have been studied for some time as a means to power remote sensing equipment for indefinite periods and it is an interesting example whereby a technology has driven fundamental understanding of a natural phenomenon rather than the other way around (Nielsen *et al.*, 2008; Rabaey *et al.*, 2010). It is likely that Research into the bio(geo)electrochemical processes that occur naturally is a potentially fruitful area for novel research findings, in particular it may provide insights as to why organisms that inhabit benthic environments, such as *Geobacter spp* are equipped with complex redox apparatus and how these are deployed in response to environmental conditions (Humphrey-Smith & Hecker, 2006).

2.13 SCOPE

September 2011 marks the centenary of Professor Potter's paper describing 'Electrical effects accompanying the degradation of organic compounds' (Potter. 1911). Many of the observations that Potter made are still valid. For instance he noted that biomass influences potential difference (he standardised his yeast solutions); potential rises proportionally to the concentration of glucose (fuel); that potential is inhibited by excessive glucose concentrations; that scale may be problematic (he found that 1L vessels showed a decrease in performance – perhaps because they were mediator limited); and that potential was greater at elevated temperatures. He even attempted to optimise his system for temperature, fuel concentration and biomass. All these problems are still considered important.

Microbial fuel cell research is a relatively new discipline emerging from electrochemistry, microbiology, biotechnology, materials science and environmental engineering. In the past MFC research has suffered from lack of a common language but workers in their respective disciplines have made progress towards communicating in a standardised manner (Ieropoulos *et al.*, 2005). Despite the huge promise of MFCs and formidable research advances in field, we are still far away from realistic, commercially feasible manifestation of this technology, particularly for wastewater treatment (WWT) applications. Whilst workers are naturally prone to believe that their respective disciplines will provide the greatest advances in MFC technology, in truth a united front is the only way forward (Ieropoulos *et al.*, 2005; Schubert, 2006).

This thesis is concerned with MFCs in the context of wastewater treatment. The technical work is presented in three chapters: the first is an investigation into inoculum effects on MFC performance; the second and third chapters are closely related an examine how a well known statistical technique, Design of Experiments, can be applied to MFCs to better understand the effects of MFC operational parameters, and any interactions that occur between them, on MFC performance.

3 MATERIALS AND METHODS

3.1 MATERIALS & METHODS

3.2 MFC ARCHITECTURE

Single chamber MFCs were based on the cube reactors described previously (Liu & Logan, 2004). The reactors consisted of a Perspex tube with an internal diameter of 44 mm and a length of either 40 mm (Chapter 4) or 20 mm (Chapters 5 & 6) giving an anode chamber volume of 50 ml and 25 ml respectively. Two square end plates (80 x 80 x 6 mm) were attached to either end of the Perspex tube, one end plate was solid with a 60 mm diameter circular recess for the anode and the second had a 40 mm aperture to expose the cathode to air. Threaded sampling ports were drilled into the wall of the anode chamber – two at the top and one at the bottom – these were fitted with rubber bungs (VWR, UK), nipples, or gas sampling units depending on the experimental requirements. Nipples were fitted with lengths of silicone tubing to allow a syringe to be attached for injection of media or inoculm. Gas sampling units were made from a length of glass tube threaded at the top and secured with an open-holed screw cap fitted with a butyl rubber septum (Supelco, USA). An exploded isometric drawing of the MFC construction and specifications can be found in Figure 3.1A & Figure 3.1B.

3.2.1 ANODES

Plain weave (221 g m^{-2}) carbon cloth anodes (E-Tek, USA) were used for the experiments in Chapter 4 whilst plain carbon cloth was used for the experiments in chapter 5 & 6 (Chemviron Carbon, UK). The anodes for the tubular MFCs were circular (59 mm diameter) and had an active surface area of 12.5 cm^2.

3.2.2 CATHODES

The MEA was constructed from Toray carbon paper with 20% wet proofing (TGPH-090, E-Tek, USA) painted with a gas diffusion layer of Ket Jen Black (E-Tek, USA) at a loading of 0.5 mg cm^2. This was followed by a catalyst layer of 0.3 mg cm^2 of Pt on Vulcan® carbon black (Cabot, USA) and 1 mg cm^2 of Nafion® solution (Sigma, UK). The MEA was completed by

binding a layer of Nafion 117® by hot pressing at a pressure of ≈70 kg cm^2 at 132^oC for 5 minutes. The untreated side of the MEA was exposed to the air.

3.2.3 ELECTRICAL LOAD

An electrical load was applied across the MFC circuit by connecting solid state resistors to complete a stainless-steel wire circuit. For the experiments presented in Chapter 4, 1000 Ω resistors were used in all instances. For the work presented in Chapter 5 and Chapter 6 resistances of 200, 2600 or 5000 Ω were used according to the requirements of the experimental design and detailed in Tables 5.1 and 6.1.

3.2.4 DATA ACQUISITION

Cell potential was measured using an ADC 16 high resolution datalogger (Pico Technology Ltd., UK) set for differential input and connected to a PC using a BS32 high resolution analogue cable (Pico Technology Ltd, UK). The cell potential was logged every thirty minutes returning a mean value from multiple sampling points collected over each 30 minute time interval.

3.3 ANOLYTE AND INOCULUM

3.3.1 ANOLYTE SOLUTION

Mineral salts medium in 50 mmol L^{-1} phopshate buffer (pH 6.8) with ammonium chloride as the nitrogen source was used as the anolyte solution in all tests presented in this thesis. The solution was prepared in bulk in 5 L Duran® bottles (Duran group GMBH, Germany) with distilled water and subsequently sterilised using an autoclave. The final composition of the medium is given in Table 3.1.

Table 3.1 The composition of the stock mineral solution used to make up the anolyte to the final concentration shown in the table. * denotes AnalR® grade reagent and † general purpose reagent both from British Drug House Ltd.

Mineral	Concentration (mg L^{-1})
NH_4Cl^*	0.31
$CuS0_4^*$	0.1 mg
$ZnCl^†$	0.120 mg
$MnSO_4^*$	0.1024
$CaCl^*$	5.04
$KCl^†$	0.1
$MgCl6H_2O^*$	0.1
$FeCl^*$	0.01

3.3.2 SOURCES OF INOCULUM

Return activated sludge was collected from Howden and Spennymoor Sewage Treatment Works (grid references: NZ333663 & NZ248355 respectively). Anaerobic digestor sludge was collected from Berwick Sewage Treatment works (NT977527). All sites are operated by Northumbria Water Ltd. RAS Samples were collected in a 10 L bucket and transferred to a 20 L carbuoy for transporting back to the laboratory where they were stored at 4°C. Health and safety regulations were observed throughout. Anaerobic sludge was collected in 500 ml wide necked plastic containers.

Freshwater sediment was collected from the bed of a burn before it drained into Eastend reservoir (NY864451), a man made water body situated 500 m at a bearing of 180° from Allenheads, Northumberland, UK. Sediment was collected using a hand trowel and stored in wide necked 500 ml containers.

3.3.3 INOCULA

The environmental inoculum samples were added directly to sterile mineral salts medium along with concentrated fuel solution (see Paragraph 3.4.3 below) immediately prior to inoculating MFCs. For the experiments presented in Chapter 4, the inocula were standardised for cell numbers by estimating the inoculum density of each sample. The inoculum density of raw environmental samples was estimated from total cell counts (Paragraph 3.6.1) and a weighed sample added to the mineral salts medium to achieve a final inoculum density of 1.29×10^7 cells ml^{-1}. The inoculum used for the experiments presented in Chapter 5 & Chapter 6 was RAS from Spennymoor STW and was diluted 50/50 (v/v) with the mineral salts medium. The final concentration of each inoculum was always 50 mmol L^{-1} phosphate buffer with the trace concentrations equal to those in Table 3.1.

3.4 OPERATION OF MFC REACTORS

3.4.1 STERILISATION

Prior to all work, the MFCs were thoroughly cleaned with soap, rinsed with distilled water, dried and then wiped with absolute alcohol. They were then exposed to UV light for 1 hour in a laminar flow cabinet where they were assembled and sealed ready for receiving the inoculum.

Anodes were suited to autoclaving but the MEA was not. To help maintain aseptic conditions in the MFC, the internal, membrane side of the cathodes were exposed to UV light prior to assembly.

All the equipment used to introduce material to the MFCs, remove samples from them and for sample storage was sterilised using an Autoclave at 121°C for 30 minutes except when they were purchased sterile (e.g. Cryogenic vials, Nalgene, USA).

Media were sterilised at 121°C for 30 minutes. General aseptic technique was used throughout.

3.4.2 DEGASSING

All media was degassed to remove dissolved oxygen prior to inoculating the fuel cells. Nitrogen gas (BOC Ltd., UK) was bubbled through the sample for ≈10 minutes. To maintain sterility and to avoid cross contamination of samples the N_2 was passed through a 0.2 µm Puradisk™ syringe filter fitted to a glass rod that was flamed before use and in between samples.

3.4.3 INOCULATION, REFUELLING AND OPERATION

At the start of each experiment or refuelling event, the inoculum was degassed and made up to the desired fuel concentration using a concentrated, sterile, stock solution of acetate or glucose in phosphate buffer. For the experiment presented in Chapter 4, the working fuel concentration was 300 mg L^{-1} in all instances. For Chapter 5 and Chapter 6 the target fuel concentrations were 50, 175 or 300 mg L^{-1} according to the experimental designs described in Table 5.1 and 6.1. The inoculum was introduced to the fuel cell through the sampling port using a syringe (Figure 3.1A)

When the voltage dropped to its lowest point, the cells were disconnected from the datalogger, the anolyte was carefully removed with a sterile syringe, so as not to disturb the anodic biofilm, and replaced with fresh fuel and inoculum mixture. This procedure was repeated until the microbial fuel cells showed a stable reproducible response between feeding events.

3.4.4 ANOLYTE SAMPLING

Liquid samples were removed from the MFC through the sampling ports using a sterile syringe fitted with a 20 cm, sterile stainless-steel lumbar-needle. The 5ml anolyte sample was dispensed equally into two 5 ml cryogenic vials. Samples for chemical analysis were passed through a 0.2µm Puradisc™ 25 polyethersulfone (PES) syringe filter (Whatman, UK) and stored at -20°C. Samples for microbiological analysis were first fixed in 50% v/v alcohol and stored in a freezer at -20°C.

3.4.5 HEADSPACE GAS SAMPLING

Headspace gas was sampled with a 5 ml gas-tight push-lock syringe (Hamilton, USA). Headspace gas samples (2 ml) were transferred into gas tight evacuated Exetainer® tubes (Labco, UK) and stored in a refrigerator until they were required for analysis.

3.4.6 ANODE SAMPLING

At the end of each experiment whole anodes were removed and transferred to 50 ml sterile centrifuge tubes and stored in 50% (v/v) ethanol in distilled water at -20°C until required for analysis. The anode biofilm was sloughed off from the anode by suspending the anode in ethanol solution and shaking for 20 minutes on a flask shaker at 800 rpm (Voss of Maldon, UK). The biomass suspension was stored at -20°C and used for subsequent microbial analysis.

3.5 ANALYTICAL PROCEDURES

3.5.1 CHEMICAL OXYGEN DEMAND

Chemical oxygen demand (COD) analysis was carried out using commercially available COD kits (Merck, UK). Filtered, frozen anolyte samples were thawed and 1–2 ml of sample was then added to the COD tube and digested at 151°C for two hours. COD values were determined by spectroscopic absorbance using a Spectroquant Nova 60 (VWR, UK) colorimeter. COD Kits with the range 10–150 mg L^{-1} (Cat No: 114895) were used to measure COD at the end of a MFC feeding cycle and 25–1500 mg L^{-1} kits (Cat No: 114541) were used for all other COD measurements.

3.5.2 PH

The pH of anolyte samples was measured using a Jenway (UK) 3310 pH meter fitted with an epoxy membrane probe (VWR, UK). The probe was immersed in the anolyte until a stable reading was returned.

3.5.3 VOLATILE FATTY ACID (VFA) DETERMINATION

All anolyte samples (5 ml) were filtered with a 2µm pore size Puradisk™ 25 (PES) syringe filter (Whatman, UK) prior to storage at -20°C. Prior to analysis, samples were defrosted and 0.5 ml was diluted 1:1 with octanesulfonic acid and sonicated for 45 minutes to remove carbonate. The prepared samples were then transferred to 0.5 ml tubes with filter caps (Dionex, USA) ready for analysis.

Analysis for VFAs was performed on a Dionex ICS 1000 Ion Chromatograph system with Chromeleon® acquisition software and an AS40 auto sampler (Dionex, USA). Separation was achieved with an an ionpac ICE AS1 4 x 250 mm analytical column under the following conditions: flow rate, 16 ml min^{-1}; eluent, 1.0 mM heptafluorobutyric acid; suppressant regenerant, 5 mM tetrabutylammoniumhydroxide; injection loop, 10 µl.

Quantification of VFA was achieved by constructing a four point standard curve (5, 50, 100 & 500 ppm) using a mixed external standard solution (consisting of acetate, propionate, butyrate, isobutyrate, valerate, and isovalerate).

3.5.4 HEADSPACE GAS ANALYSIS

Headspace gas samples were obtained as described above and stored in evacuated containers until analysis. Quantification of CO_2 and CH_4 was performed using a Trio Gas Chromatograph-Mass spectrometer (GC-MS) system (Fisons, UK).

Separation by gas chromatography was achieved isothermally at 36°C with a Chrompak® fused silica capillary column (25 m x 0.25 mm internal diameter) packed with Poraplot-Q (DF = 0.8 µm). The carrier gas flow rate was 1 ml min^{-1} at a pressure of 46 kPa. A 100 µl sample of headspace gas was injected manually at 1 minute intervals using a gas tight syringe with the split open at 100 ml min^{-1} at a temperature of 250°C

Methane was estimated by mass spectrometry from the primary ion (m/z 16) and CO_2 using m/z 44 at the following settings: filament current 4.2A, at 70 eV; Source current 1000 µA; multiplier voltage 500 V and interface temperature 250°C.

Data acquisition was controlled by TVM 4860 computer using Masslab software in full scan mode (1 - 101 amu sec^{-1}).

Calibration of this instrument was carried out using a standard gas mix containing 10% CH_4 and 10% CO_2 in N_2 (Scientific and Technical gases Ltd., UK). A serial dilution of the standard gas mix was performed in sealed serum bottles to obtain a range of gas concentrations for a 3 point calibration in the analytical range of interest.

3.6 MICROBIAL ANALYSIS

3.6.1 TOTAL CELL COUNTS

Inoculum samples were diluted in sterile phosphate buffered saline (0.01M phosphate buffer, 0.0027 M KCl, 0.137 M NaCL, pH7.3, Oxoid UK) using a dilution factor of 10, 50, 100 or 200 according to the expected concentration of cells in the sample in order to give a sample that yielded ca. 30 cells per field of view (those that fell within the area projected by the eyepiece graticule counting grid). After dilution the samples were treated with an aliquot of SYBR® green to achieve a final concentration of 1:10,000 and a pH of 7–8.5. Samples were stained in the dark for 15 minutes and vacuum filtered onto a 0.2 µm Isopore™ membrane filter (Millipore, USA) using a sterile, stainless steel filter unit (Eppendorf®, USA). The membrane filter was transferred to a microscope slide and cells were manually counted using an Olympus BX40 epiflouresence microscope with a 100 x oil immersion objective lens and a λ 300 nm light source. Around 20 – 30 fields of view were counted manually to return an average and standard deviation. The number of cells per ml of sample can be calculated as:

$$n_{cell} = \frac{\overline{X}_{cell} \bullet A_{fil}}{A_{grat} \bullet V \bullet D_1 \bullet D_2}$$

Equation 3.1

Where the X_{cell} is the average number of cells per field of view, A_{fil} is the area of the membrane filter, A_{grat} is the area of the graticule, V is the volume of sample, D_1 and D_2 are the dilution factors used for analysis and preservation respectively.

3.6.2 Analysis of anodic bacterial communities

3.6.2.1 Nucleic acid extraction

DNA was extracted from preserved inoculum samples and anode biofilm samples using a Bio101 FastDNA SPIN kit for soil (QBiogene, USA) according to the manufacturer's instructions using a Hybaid ribolyser.

3.6.2.2 DNA Amplification

The extracted DNA was used as a template for amplification of bacterial 16S rRNA genes using the polymerase chain reaction (PCR). To amplify DNA using PCR, 1 µl of extracted DNA was added to 47 µl of commercially available mastermix (Megamix blue, Microzone, UK) which contains all the reagents required for the PCR reaction to proceed (NH_4^+, 1.1 x reaction buffer (2.75mM $MgCl_2$), all four deoxyribosenucleoside triphosphates (220 µM dNTPs) in a 200 µl centrifuge tube (Eppendorf®, USA). One microlitre each of 10 µM solution of primer 2 and primer 3 (Muyzer *et al.*, 1993) was added to the tube containing the master mix and the extracted DNA. These primers target the variable V3 region of 16S rRNA genes. Negative control reactions were prepared as above but without the addition of any DNA.

The PCR reaction was carried out in a PX2 Thermocycler (Thermo Hybaid, UK) under the following conditions: Intitial denaturation (95°C, 3 min); 24 cycles of denaturation (95°C, 1 min), annealing (65°C, 1 min and reduced by 1°C very second cycle) and extension (72°C, 1 min); a further 15 cycles of denaturation (95°C, 1min), annealing (65°C, 1 min) and extension (72°C, 1 min); and a final extension step (72°C, 10 min).

3.6.2.3 Agarose gel electrophoresis

To confirm that and the amplified DNA was of the expected size (233 bp) the PCR products were visually analysed by agarose gel electrophoresis against a 50-2000 bp standard PCR

marker (Sigma-Aldrich, UK). 5 µl of amplified DNA was loaded onto a 1% (w/v) agarose gel prepared with 1X TAE buffer (40 mM tris acetate 1 mM EDTA, pH 8, Eppendorf Science Ltd., USA) containing 0.18 µg ml^{-1} ethidium bromide. Electrophoresis was conducted for 50 minutes at 100V. DNA bands were visualised under UV illumination with a dual intensity transilluminator (Ultraviolet Products Ltd., UK).

3.6.2.4 Denaturing gradient gel electrophoresis (DGGE)

Eleven microlitres of PCR product was mixed with the same volume of loading buffer (0.25% bromophenol blue, 0.25% xylene cyanol FF and 30 % glycerol in sterile microbiological grade water) and added to the wells of a 10% w/v (160 x 160 x 0.75 mm) polyacrylamide gel (37.5:1 polyacrylamide: bis-acrylamide) containing a chemical denaturing gradient of 30–55% denaturant (100% denaturant is 7M urea and 40% v/v formamide) in 1 x TAE buffer (40 mM tris acetate 1 mM EDTA, pH 8, Eppendorf Science Ltd., USA). Marker samples which comprised a mixture of PCR amplified 16S rRNA genes from 12 cloned 16S rRNA gene fragments with differing GC ratios were run alongside samples to correct for variations in electrophoretic migration across the gel. Electrophoresis was carried out using a D-Code System (Bio-Rad, UK) and a Powerpac 3000 (Sigma, UK) for 900 volt hours at 60°C. The separated DNA was stained with 20 µl SYBR® green in 200 ml 1x TAE buffer for 30 minutes and photographed under UV illumination with a Flour-S® Multi imager and the image captured with Quantity One software (Bio-Rad, UK).

3.6.2.5 Image analysis

Images of DGGE gels were analysed using the Bionumerics software package (Version 3.5, Applied Maths Inc, USA). Images were processed and bands normalised by reference to the marker samples (described in Paragraph 3.6.2.4) that were run alongside samples on the DGGE gel. Bands were assigned and matched automatically but manually verified. Band intensity and presence absence data was generated using the Bionumerics program. Band patterns were compared for similarity between samples using the binary DICE coefficient (presence absence data). Dendograms visually representing the similarity between samples were generated using the cluster analysis function in Bionumerics and selecting the

unweighted pair group method using arithmetic averages (UPGMA). The presence absence data and densiometric data was exported from Bionumerics and used to calculate band richness, species richness and the Simpons' reciprocal index (1/D).

Nonmetric multidimensional scaling (NMDS) was performed using PRIMER version 6 software (PRIMER-E Ltd, UK). Densiometric data was imported from Bionumerics and converted to binary presence absence data for the calculation of the Bray-Curtis index of similarity which were used to generate the ordinations. The statistical significance of each ordination was described using analysis of similarity (ANOSIM), a non-parametric permutation procedure.

3.6.3 CONFOCAL LASER SCANNING MICROSCOPY (CLSM)

Anodes were removed from the MFCs at the end of the experiment and immediately transferred to a petri dish and submerged in sterile PBS (0.01M phosphate buffer, 0.0027 M KCl, 0.137 M NaCL, pH7.3, Oxoid UK) where a 12mm section was randomly cored. The cored section was then transferred to a small petri dish containing 3 ml of a 10 X dilution of Baclight® bacterial viability stain (Life technologies Ltd, USA) and allowed to develop for ten minutes. After the stain had developed, the anode samples were rinsed in PBS fixed in a 50% ethanol solution in distilled water and immediately presented for CLSM. The anodic biofilm was examined with a Leica TCS SP2 UV on a DMRXA upright microscope running LCS 2.61 software (Leica Microsystems GMBH, Germany) with a NX63 NA 0.9 water dipping lens and with the excitation emission filters set to PI and UV. The Baclight® stain is made up of propidium iodide and SYTO stains which fluoresce at 620 and 310 nm respectively.

3.7 ELECTROCHEMICAL TECHNIQUES

3.7.1 INTERNAL RESISTANCE

A GillAC potentiostat (ACM instruments Ltd, UK) was used to measure the internal resistance of the MFCs by Electrochemical Impedance Spectroscopy (EIS). The anode was used as both the counter electrode and the reference electrode and the cathode as the working electrode. Impedance measurements were carried out at maximum potential over

the cell cycle over a frequency of between 3000 and 0.1 Hz with a sinusoidal perturburation of 10 mV amplitude.

3.7.2 POLARISATION

At the end of an experiment, MFCS were refuelled and allowed to acclimatise under open circuit potential (OCP) at which point they were polarised. In the experiments presented in Chapter 4, polarisation was conducted manually by incrementally switching out the external resistance of the MFC from 1 MΩ through to 50Ω and recording the cell voltage and current at each change in external resistance. The MFC was allowed to stabilise for two minutes between changes in external resistance. Subsequent polarisation (Chapters 5 & 6) was carried by means of a potentiostat (GillAC, ACM Instruments) at a scan rate of 1 mV s^{-1}. Anode behaviour under polarisation was recorded with an Ag/AgCl reference electrode.

3.8 DATA HANDLING

3.8.1 RAW DATA

Data was recorded continuously using an AD16 picologger (Pico Technology, UK) and periodically copied from the logging PC into an Excel spreadsheet. Current and power were calculated from the measured potentials using the following equations.

3.8.2 CURRENT

Current was calculated from the measured cell potential using ohms law:

$$E = IR$$

Equation 3.2

Current normalised to surface area as follows:

$$I = \frac{E}{A_{anode} \bullet R}$$

Equation 3.3

Where E = Cell potential in volts (V), I = current in Amperes (A), R = external load in ohms (Ω), and A_{An} is the area of the anode (m^2).

3.8.3 POWER

Power was calculated from the relationship:

$$P = \frac{E^2}{R}$$

Equation 3.4

This is normalised to anode surface area as follows:

$$P_{An} = \frac{E^2}{A_{An} \bullet R}$$

Equation 3.5

Volumetric power density is expressed as:

$$P = \frac{E^2}{V_{cell} \bullet R}$$

Equation 3.6

Where E = Cell potential in volts, R = external load in ohms and V_{cell} is the volume of the reactor (m^3).

3.8.4 COULOMBIC EFFICIENCY

Coulombic efficiency (CE) is a means of assessing what proportion of electrons contained in the substrate are used to generate electricity. It was calculated as the quotient of the theoretical number of electrons contained in the substrate over the electrons recovered over a complete feeding cycle. Since the definition of an ampere is equivalent to a current transfer of 1 coulomb per second, we find CE by integrating the current generated in an MFC over a feeding cycle:

$$CE = \frac{Ms\int_0^{t_b} I\ dt}{F\, b_{es}\, V_{an}\, \Delta c}$$

Equation 3.7

Where M_s is the molecular mass of substrate, I is current in amperes F is Faraday's constant, b_{es} is number of electrons transferred per mole of reactant, V is the volume of the anode in litres (L), and Δc is the change in concentration of substrate over the time for which current was integrated.

3.8.5 Energy efficiency

The energy efficiency (η) can be calculated from the energy recovered in the MFC and the change in energy content of the substrate over a given feeding cycle. Since one joule is equal to the energy expended in applying one ampere of current through a resistance of 1 Ω for one second, energy efficiency can be expressed by first calculating the integrals of MFC potential and current over a complete feeding cycle:

$$\eta_{MFC} = \frac{\int_0^{t} E_{mfc}\, I\ dt}{\Delta H n_s}$$

Equation 3.8

Where E_{MFC} is cell potential, I is current, ΔH is the heat of combustion (J mol^{-1}) of a pure substrate and n_s is the amount of substrate added (mol).

3.9 Statistical techniques

3.9.1 Design of factorial and half factorial experiments

Design of Experiments (DoE) techniques are a way of examining the interactions that exist between experimental variables (factors) and to what extent this affects the experimental output. DoE requires sufficient experience of a process so as to choose suitable factors and make sure that they set within in a suitable range. DoE techniques are suitable for

exploratory (screening), experimental and optimisation studies and are designed to be iterative. The DoE approach should yield more results in fewer studies than conventional experimental approaches.

Factorial and half factorial experimental arays were generated using the design of experiments (DoE) function in Minitab® 15 (Minitab Inc., USA). In order to generate a full factorial design the factors to be examined were chosen along with upper and lower experimental values. Midpoints were automatically calculated. In a full factorial design Minitab lists all of the possible combinations of factors randomly and it is this order that the experiments are conducted to minimise bias. Half factorial designs use half the possible number of permutations but only allows for resolution of two way interactions.

Data from factorial and half factorial experiments were analysed and plotted using Minitab® 15.

3.9.2 ANOVA

Analysis of variance was carried out using Minitab® 15 statistical software.

4 A COMPARISON OF FOUR DIFFERENT INOCULA AND THEIR EFFECT ON MICROBIAL FUEL CELL PERFORMANCE AND ANODE BACTERIAL COMMUNITY COMPOSITION

4.1 INTRODUCTION

One of the most surprising things about exoelectrogenic bacteria is their apparent ubiquity; the seemingly special ability of organisms to produce electricity is relatively common. Since Potter's description of MFC fundamentals, MFC research has followed an intuitive developmental trend based on prevailing scientific dogma (Potter, 1911). Bennetto's work used mediators primarily, one would assume, based on the current understanding of microbial physiology of the time and the accepted maxim that the terminal electron acceptor in microbial electron transport chains was always a dissolved species (Allen & Bennetto, 1993). Even with the epic first descriptions of dissimilatory iron and manganese reducing bacteria and evidence that microbes could reduce a solid phase electron acceptor, nobody could have foreseen that this ability would not be confined to more than a few select genera (Lovley & Phillips, 1988; Myers & Nealson 1988; Lovely, 1991). Everywhere we look, microbes display a diversity of metabolic capabilities that challenge our accepted notions of life.

In MFC research to date, common sources of inocula have been from laboratory grown, pure cultures or environmentally derived mixed consortia. The former has the benefit of being experimentally convenient and the latter provides a wider representation of the electroactive genera that nature has to offer. Earlier work (e.g. Potter, 1911; Cohen, 1931; Karube *et al.*, 1976; Karube *et al.*, 1977; Allen & Bennetto, 1993) relied on defined, pure-cultures to describe the electrogenic potential of microbes. This reflects the prevailing dogma - classical microbiology relied on the isolation and culture of microbes to unravel their mysteries. At the time of these studies modern molecular techniques which allowed microbiologists to study a number of genera simultaneously did not exist, or were in their infancy. Even before the advent of using microbial consortia or environmental samples as MFC inocula, Stirling, as part of Bennetto's research group, noted in 1983 that a number of organisms, including *E. coli, P. aeuringosa, S. cerevisiae* & *Alcaligenes eutrophus* (all workhorses of the classical microbiology laboratory) can be used to catalyse the anodic reaction and "…provided effective mediation of electron transfer can be obtained the choice of organism largely depends on the nature of the substrate" (Stirling *et al.*, 1983). Note here

Stirling used ‘organism’ in the singular and that he refers to a mediated mechanism of electron transfer. Prior to this, Cohen (1931), compared the reduction potential arising from pure cultures of *Bacteriodies dysenteriae*, *Bacteriodes coli*, *Bacillus subtilis*, *Corynebacterium diphterea,* and *Proteus vulgaris* - all medically important microbes. Potter noted that half cells inoculated with *B. Subtilis* and *P. vulgaris* gave the highest potential (0.6V and 0.9 V respectively) when compared with uninoculated controls and that such a microbial half-cell could, conceivably, be used to perform work. Other early research reflected the same trends (Bennetto *et al.*, 1985; Allen & Bennetto, 1993) and *S. cerevisiae* and *E.coli* were the experimental organisms used by Potter in his pioneering work here at Newcastle (Potter, 1911).

Later, inocula of pure organisms that could reduce an anode without the addition of mediators became de rigueur. Kim *et al.* (1999) demonstrated this phenomenon with *Shewanella putrefaciens* and much research followed confirming the ability of other *Shewanella* spp. to confer ‘unmediated’ reduction of the anode in microbial fuel cells (Park & Zeikus, 2003).

By the turn of the millennium it was common to use environmental inocula such as marine sediment and sewage sludge as MFC inocula and Dulon *et al.* (2007) suggested that many natural environments may contain electrochemically active genera and demonstrated the evolution of electrogenic biofilms from compost and bottled water. Many species were identified from anode enrichments of MFCs that were inoculated with a range of environmental samples these included *Aeromonas hydrophilia* (Pham *et al.*, 2003), *Desulfromonas*, (Reimers *et al.*, 2001; Bond *et al.*, 2002) and *Geobacter* (Bond *et al.*, 2002; Jung & Reagan, 2007). Dissimilatory iron reducers, such as *Geobacter* spp. (from a terrestrial inoculum) and *Shewanella* spp. (from marine sediment), were commonly identified as the putative electrogens in the anodic communities of microbial fuel cells inoculated with environmental samples. In an attempt to harness the electrogenic capabilities of microorganisms from natural environments, these organisms were isolated and subject to investigation using pure culture (e.g. Min *et al.*, 2005). Although many studies now show

that MFC performance is usually superior in MFCs using mixed species consortia (Ishii *et al.*, 2008; Wang *et al.*, 2010), Derek Lovley's group refute this assertion suggesting that the apparent enhanced performance of mixed consortia in an MFC is a facet of fuel cell design rather than inherently superior electrogenic properties of mixed communities (Nevin *et al.*, 2008). This is an interesting point and Nevin *et al.* (2008) demonstrated that MFCs inoculated with *G. sulfurreducens* performed better than an MFC inoculated with anaerobic sludge. Whilst it is possible to design studies and to manipulate MFC conditions that suit a particular microbe it is debatable as to whether these idealised conditions (e.g. using a poised electrode and small anodic volumes of 7 ml) are applicable to scale up.

In an attempt to enhance the electrogenic capability of environmental inocula, researchers have described enrichment strategies such as heat treatment to select for an acidogenic culture (Venkata Mohan *et al.*, 2007) and selective enrichment with media containing iron hydroxide (Kim *et al.*, 2005; Liu *et al.*, 2008) or electrogenic enrichment in MFCs (Kim *et al.*, 2005). The rationale for serial enrichment with media containing ferrous hydroxide is the assumption that the metal reducing capabilities of organisms from environmental inocula are a good proxy for electrogenic activity. Although serial enrichment with ferrous hydroxide met with some success, both Kim *et al.* (2005) and Liu *et al.* (2008) reported that selectively inoculating MFCs from the anodic community of other MFCs was a better enrichment procedure. Therefore, the ability of microbes to reduce solid metal oxides is not precisely analogous to the ability to reduce an electrode and that the ultimate enrichment procedure for electrogenic activity is cultivation on the anode of an MFC. Recently, Wang *et al.* (2010) combined enrichment on ferric medium with a serial dilution enrichment strategy of a Microbial Electrolysis Cell (MEC) anode derived biofilm which showed improved performance compared with inocula from both activated sludge and the original biofilm.

The intensive investigation of electrogens in MFCs has revealed much about the fascinating ability of microbes to interact electronically with solid interfaces and has led to greater understanding of MFC technology and its applications. Scientists at the J. Craig Venter institute have manufactured the first living organism using an entirely synthetic genome

(Gibson *et al.*, 2008) and the genome of *Geobacter sulfurreducens* (an electrogen that is effective in MFCs) has been fully sequenced and is, reportedly, amenable to genetic manipulation (Franks & Nevin, 2010). It seems likely, therefore, that we will be able to engineer the perfect electrogenic organism or consortium once we fully understand what properties it is we need to engineer. Whilst this will be an academically interesting exercise, nobody is sure if these advances will be of use in 'dirty' applications, such as wastewater treatment, which has been the focus of the vast majority of MFC research, and which are open systems, where the integrity of an engineered anodic community will almost certainly be challenged by the immigration of organisms from the fuel medium.

Intuitively, it seems that similarity between the community in the fuel and that of the anodic community would confer the greatest degree of stability to the anodic community. However, highly specialized environments are insular and are more influenced by the seed community and replacement of lost community members from local reproduction events than immigration (Goodhead, 2010). In which case, we can expect the composition of the anodic community to exhibit a high degree of stability regardless of the community composition of the fuel. Microbial electron transfer over distances greater than 12 mm has been shown to proceed in natural systems. However, the ability of microbes to generate excess electricity is not energetically favourable and may not represent a true climax community or steady state population in ecological terms – whether or not this has implications for community assembly remains to be investigated (Nielsen, 2010).

To date, a systematic comparison of the effectiveness of different inocula on the performance of MFC has not been conducted. This study compares the electrochemical performance and the composition of anodic community in MFCs inoculated with different environmental inocula using a novel procedure developed by the author to overcome the confounding effects of inoculum density by standardising the inoculum when seeding MFCs.

4.2 Aim

The work in this chapter aims to examine differences in MFC operation and climax anode communities brought about from seeding MFCs with different inocula. Understanding the

characteristics of various environmental inocula and their effect on MFC performance will be of immense practical importance in both field situations (for seeding or reseeding MFCs) and for bench-scale research systems. Four inocula were chosen: return activated sludge (RAS) from two sites, anaerobic sludge, and freshwater sediment (Section 3.2.2). The RAS was chosen to represent the probable microbiological status of feedtsocks that MFCs used in wastewater treatment applications will be exposed to in the future. Anaerobic sludge is often used as an inoculm source in MFCs and was chosen as a benchmark for comparison with the literature, freshwater sediment was chosen for its ubiquity and to represent a natural inoculum source. Other than manipulating the seed inoculum, the operational conditions of the single-chamber air-cathode MFCs used in this study were identical and described in Section 4.5 and in greater detail in Chapter 3.

4.3 OBJECTIVES

- Examine and compare the difference in electrochemical properties (E_{cell}, *I* & CE) of fuel cells operated with inocula from the following media: Freshwater Sediment, Return Activated Sludge from two sites & Anaerobic Sludge.
- Measure the change in COD (Δ_{COD}) over the course of the experiment and the fate of organic carbon by estimating VFA concentration in the anolyte and the evolution of CO_2 and CH_4.
- Compare the treatment efficiency between inocula.
- Determine and compare the community fingerprints of the seed inoculum with the climax anode community in each cell.

4.4 HYPOTHESIS

The aims and objectives of this particularly study were designed to test the hypothesis that different seed inocula will result in the following observations between treatments:

- Differential electrochemical performance between treatments
- Differential treatment efficiencies

- Differential carbon oxidation pathways
- Differential colonisation of the anode

4.5 EXPERIMENTAL

Single chambered, air-cathode MFCs with 50 ml bed volume and fitted with gas collection ports were used in this study (Figure 3.1A). The cathode was constructed of a membrane electrode assembly that consisted of a Nafion 117® membrane hot pressed to carbon paper with a final Pt catalyst loading of 0.3 mg cm^{-2} and a gas diffusion layer of carbon black between the Nafion membrane and the carbon paper. The Anode was constructed of carbon cloth. Both electrodes had an active surface area of 12.5 cm^2. The electrodes were connected under a static electrical load of 1000Ω and the drop in potential across the load was measured using a Pico ADC16 datalogger connected to a PC where the E_{cell} was logged half hourly using PicoLog software.

The fuel cells were set up and inoculated in duplicate with Freshwater Sediment, Return Activated Sludge (RAS) from Spennymoor Sewage Treatment Works (RAS-1), RAS from Howden Sewage Treatment Works (RAS-2) and Anaerobic Sludge from Berwick Sewage Treatment works. The inocula were standardized to 1.29 x 10^7 cells ml^{-1} based on total cell counts determined using epiflouresence microscopy. The original environmental sample was diluted in sterile artificial wastewater nutrient medium (pH 6.8) and amended with sterile stock glucose solution to a working concentration of 300 mg L^{-1} (Section 2.5.1). Feeding events were instigated at the nadir of the voltage curves when the MFCs were refuelled by removing the anolyte — some of which was preserved for later analyses — and replacing with fresh medium.

The degradation of organic matter was expressed in COD, analysis was carried out using commercially available COD kits (Merck, UK) on anolyte samples that were collected at the start and finish of each experiment and passed through 0.2 µm syringe filter. The method is described fully in Section 3.4.1.

Analysis for VFAs was performed on a Dionex ICS 1000 Ion Chromatograph system with Chromeleon® acquisition software and an AS40 auto sampler (Dionex, USA).The method is described fully in Section 3.4.3.

Headspace gas was collected through the septa of the gas sampling ports using a gas-lock syringe (Hamilton, USA). Composition of headspace gas was analysed by Gas Chromatography Mass Spectrometry (Section 3.4.4).

DNA was extracted from frozen anode suspensions, prepared from shaking anodes in a solution of ethanol and water (50/50 v/v), using a FastDNA® Spin Kit for soil. Bacterial 16S rRNA gene fragments were amplified from the DNA extract by the PCR using primers 1 and 3 targeting the V3 region of the 16S ribosomal RNA gene (Muyzer *et al.*, 1993). The amplification of DNA of the correct length was confirmed by agarose gel electrophoresis. The amplified DNA samples were loaded directly onto a 10% polyacrylamide gel with a 30-55% denaturing gradient and run for 900 volt hours at 60 °C in TAE buffer. DGGE gels were stained using SYBR® green and visualized using a Flour-S multiimager and Quantity One software. DGGE fingerprint analysis was carried out using the Bionumerics software package. Full details can be found in Section 3.5.2.

Statistical analyses were carried out using Minitab 15. The electrochemical and efficacy parameters were calculated according to the formulae in Section 3.7.2 – 3.7.5.

4.6 RESULTS

4.6.1 CELL POTENTIAL, CURRENT AND CHARGE

The cell potential (E_{cell}) against time for four sets of duplicate MFCs inoculated with freshwater sediment (A), RAS 1 (B), RAS 2 (C) and anaerobic sludge (D) is shown in Figure 4.1 for six feeding events starting at t = 0. Feeding events were instigated at the nadir of the voltage curves (t ≈ 1.8, 4.0, 6.3, 8.6 & 11 days), represented graphically in Figure 4.1 by E_{cell} = 0, which is not a true value, but a consequence of disconnecting the dataloggers whilst the fuel cells were manipulated. The observed value of E_{cell} = 0 at 12.7 days is an experimental artefact and not a feeding event.

With the exception of the MFC inoculated with anaerobic sludge between day 0 and 6 (Figure 4.1D) the cell potential rose rapidly after each feeding event with the maximum potential ($E_{cell(max)}$) was typically reached between 0.2–0.8 d ($\bar{x}$ =0.4 d) and was sustained for 1.99–2.41 days ($\bar{x}$ =2.28 d). The highest mean $E_{cell(max)}$ was observed in cells inoculated with RAS from Howden STW (42.27 mV, RAS-2), followed by RAS from Spennymoor STW (39.78 mV, RAS-1), freshwater sediment (24.70 mV) and finally, anaerobic sludge (19.89 mV), these maxima were all observed during the fourth feeding cycle (starting at around 6.3 days) and the data (from highest to lowest) are shown in Figure 4.1C, B, A & D respectively. Those cells inoculated with anaerobic sludge (Figure 4.1D) appear to go through a lag or acclimation phase and, in contrast with the other treatments (Figure 4.1 A, B, C), there was no marked response to the initial three feeding events t = 0–6.3 days. The response to subsequent feeding events appeared generally similar to the other treatments with a trend to increasing $E_{cell(max)}$ over time. A summary of the data is shown in Figure 4.1.

A fully nested analysis of variance (ANOVA) confirms that the effect of each treatment is significant for all runs although this is so with the most confidence the fourth feeding event (P= <0.0000, n = 8, df = 7), between days 6.3 and 8.6. The boxplot in Figure 4.2 shows the relationship between the measured and expected values of the sample means for each treatment. Note the better performance of the MFCs inoculated with RAS, compared to MFCs inoculated with Freshwater Sediment and Anaerobic Sludge where the $E_{cell(max)}$ is small but, nonetheless, significant.

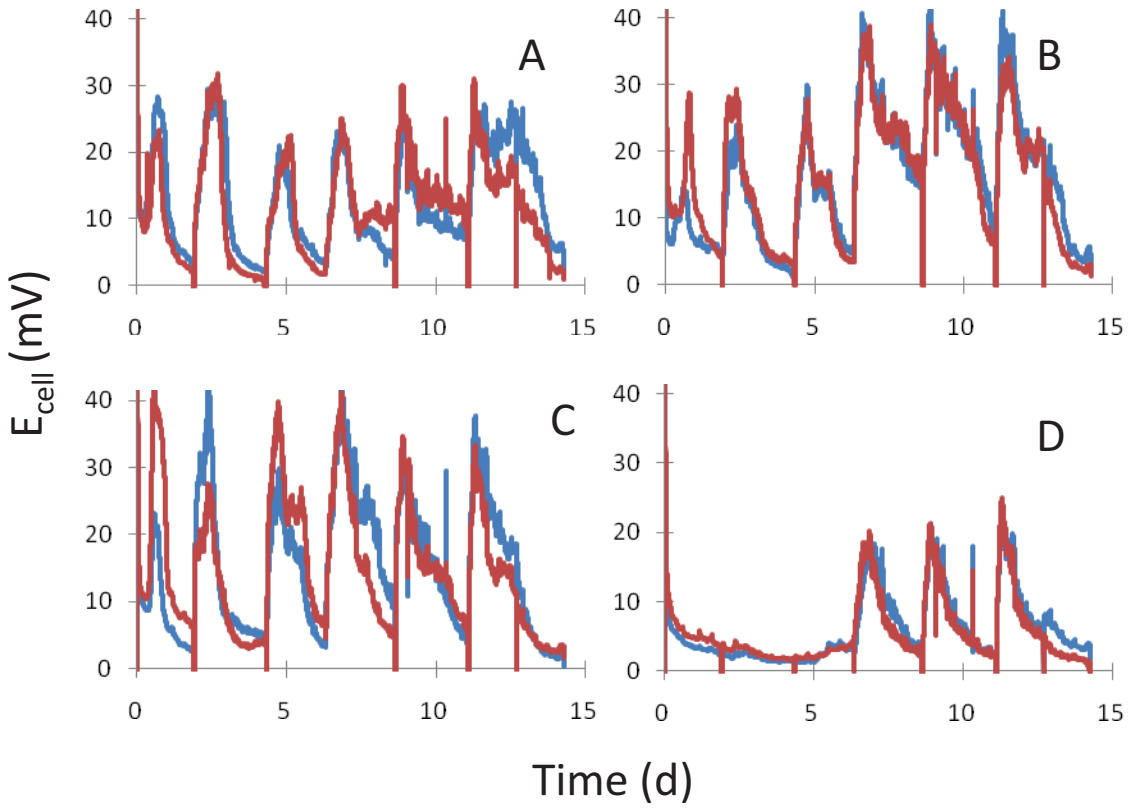

Figure 4.1 Voltage generation in four sets of duplicate MFCs inoculated with freshwater sediment (A); RAS 1 (B); RAS 2 (C); and anaerobic sludge (D).

In addition to the statistical significance between treatments, there is good parity between duplicate reactors with mean (n = 5) Pearson correlation coefficients of 0.91 (± 0.091), 0.91 (± 0.05), 0.95 (± 0.04) and 0.95 (± 0.08) between replicates MFC for the Freshwater sediment, RAS-1, RAS-2 and anaerobic sludge inocula respectively. In all instances, there is a weak trend towards greater reproducibility and increased performance in terms of E_{cell} as the experiment progresses. Where there are anomalies in the data, this is generally consistent across the dataset, for example at t ≈ 10.3 d there is a spike in E_{cell} which occurs in all cells and is an experimental anomaly. Additionally, $E_{cell(max)}$ is observed during feeding event 4 and 5 (with the exception of the Freshwater Sediment treated MFCs) and the longest feeding event (2.41 d) and most reproducible data (Mean Person Coefficient = 0.97 ± 2.5%) all occur during the fifth feeding event (t= 8.63 – 11.08 d). The above trends are identical for this dataset when expressed in terms of current.

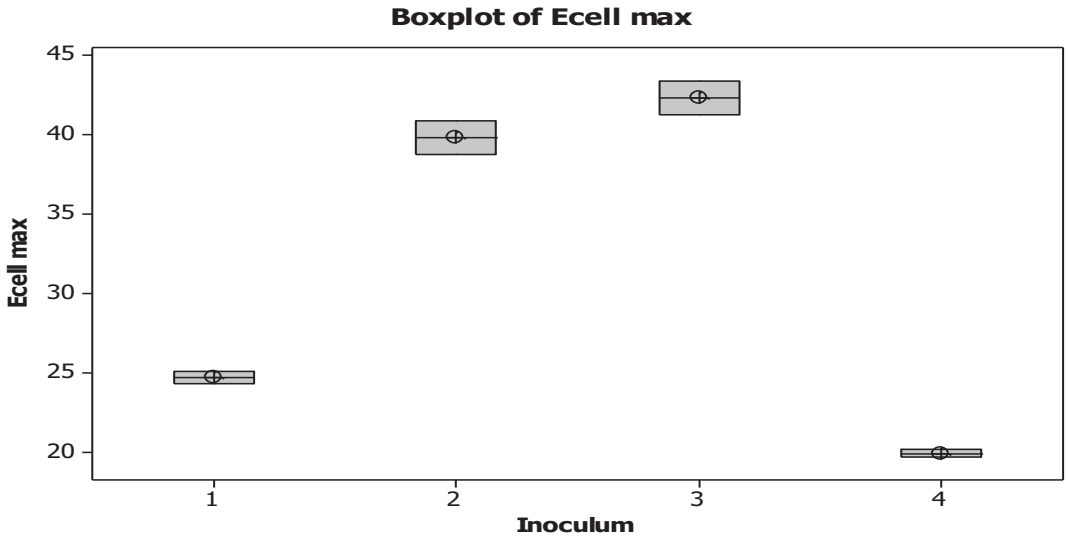

Figure 4.2 Boxplot of E_{cell}(max) observed in duplicate MFCs inoculated with 1, freshwater sediment; 2, Spennymoor RAS; 3, Howden RAS; & 4, anaerobic sludge with mean value shown as crossed circle and data range by boxes.

Table 4.1 A summary of the electrochemical outputs from eight duplicate cells operated with four different inocula. Standard deviation (±) and mean n = 2.

	Inoculum											
	Freshwater Sediment			Spennymoor RAS			Howden RAS			Anaerobic Sludge		
Feeding event	E_{cell}(max) (mV)	Imax (mA m^{-2})	Charge (C)	E_{cell}(max) (mV)	Imax (mA m-2)	Charge (C)	E_{cell}(max) (mV)	Imax (mA m^{-2})	Charge (C)	E_{cell}(max) (mV)	Imax (mA m^{-2})	Charge (C)
2	30.69	25.58	6.01	26.70	22.28	5.48	35.79	30.05	6.32	3.68	3.07	1.16
	(±1.70)	(± 1.42)	(±0.80)	(±3.93)	(±3.28)	(±0.97)	(±11.4)	(±9.59)	(±1.38)	(±1.07)	(±.10)	(±0.24)
3	21.76	18.13	4.01	28.97	24.17	5.51	34.88	29.29	7.62	4.35	3.62	1.10
	(± 1.05)	(±0.88)	(±0.04	(±1.51)	(±1.26)	(0.08)	(±7.06)	(±5.95)	(±1.89)	(±0.04)	(±0.95)	(±0.04)
4	24.70	20.58	5.77	39.78	33.18	11.89	42.27	35.50	10.33	19.89	16.58	4.32
	(±0.59)	(±0.49)	(±0.67)	(±1.46)	(±1.22)	(±0.00)	(±1.51)	(±1.25)	(±1.92)	(±0.34)	(±4.22)	(±0.34)
5	27.91	23.26	7.13	40.61	33.88	12.02	34.35	28.84	8.45	20.83	17.36	4.18
	(±3.03)	(±2.53)	(±1.25)	(±2.24)	(±1.87)	(±0.46)	(±0.33)	(±0.30)	(±0.20)	(±0.74)	(±4.16)	(±0.19)

4.6.2 POWER

Table 4.2 shows the theoretical and observed open circuit potential (OCP_T, OCP_O), along with the internal resistance data (R_{Int}) used to calculate the maximum theoretical power (P_{maxT}) and the system specific maximum power (P_{maxS}) – the maximum power that can be generated from this system based on the observed OCP internal resistance and external resistance of each system. Also included in Table 4.2 are the maximum observed power outputs (P_{maxO}).

Table 4.2 A summary of power data for eight duplicate cells operated with four different inocula. ± standard deviation and for mean n = 2.

	Freshwater Sediment	Spennymoor RAS	Howden RAS	Anaerobic Sludge
OCP_T (V)	1.23	1.23	1.23	1.23
OCP_O (V)	0.50 (±0.00)	0.47 (±0.02)	0.37 (±0.03)	0.33 (±0.01)
R_{Int} (Ω)	53.5 (±0.35)	43.5 (±0.35)	40 (±1.41)	49.50 (±0.35)
P_{maxT} (mW m^{-2})	1082	1104	1105	1126
P_{maxS} (mW m^{-2})	176 (± 3.40)	164 (±12.37)	102 (±15.56)	81. (±3.73)
P_{maxO} (mW m^{-2})	22.24 (±1.21)	32.48 (±0.90)	27.48 (±0.13)	16.66 (±0.29)

The mean difference between the OCP_T (1.23 V) and the OCP_O represents the cell overpotential and is 0.73, 0.76, 0.82 and 0.9 V for Freshwater Sediment, Spennymoor RAS, Howden RAS and Anaerobic Sludge inocula respectively (Table 4.2). The difference between the system-specific maximum power (P_{maxS}) relative to the maximum theoretical power (P_{maxT}) reflects the same trends as the overpotential with the R_{INT} having little apparent effect on predicted power both because of the low currents observed in the MFCs and because the R_{Int} is similar (± 6 Ω) for all cells. MFCs inoculated with Spennymoor RAS gave the highest output of 32.48 mW compared to 27.48, 22.24 & 16.66 mW m^{-2} for the MFCs inoculated with Howden RAS, Freshwater Sediment and Anaerobic Sludge respectively, this is between 1.5–3 % maximum theoretical power (P_{maxS}) of 1082, 1104, 105, & 1126 mW m^{-2}.

The MFCs with the lowest overpotentials do not give rise to the highest observed output as expected, for example, Freshwater Sediment has the lowest overpotential yet is the second worst performer in terms of maximum observed power output of 22.24 mW m^{-2} (Table 4.2). MFCs inoculated with Freshwater sediment had the highest internal resistance of 53.5 Ω against a mean of 46.6 Ω (n=8). The data shown in Table 4.2 & Table 4.3are for run 5 only as COD data exists for this feeding event only and are crucial to calculating the efficiency parameters and hence the only feeding event that has a complete dataset.

4.6.3 COULOMBIC EFFICIENCY AND ENERGY EFFICIENCY

Table 4.3 shows a summary of coulombic, treatment and energy efficiency data (CE, COD_{SD}, η_E) and the COD data used to arrive at these values. The data in Table 4.2 are for run 5 (8.63 –11.08 days) as COD degradation data are only available for this feeding cycle. The treatment efficiency of these systems was, from lowest to highest: 33% (Anaerobic Sludge), 80% (Freshwater Sediment), 82% (Howden RAS) and 87% (Spennymoor RAS) thus substrate destruction was respectable and comparable for all treatments with the exception of Anaerobic Sludge (Table 4.3). The same trend is true for coulombic efficiency at 12, 8, 7, & 4% for Freshwater Sediment, Howden RAS, Spennymoor RAS and Anaerobic Sludge respectively. Energy efficiency data does not follow this trend although the RAS inocula were still the best performers with 8% for Howden followed by 7% for Spennymoor, the energy efficiency for freshwater sediment and Anaerobic Sludge was 3% and 2% respectively.

4.7 CARBON FATE

Table 3.4 shows the pH, VFA concentration and headspace CO_2 for run 5 (8.63 – 11.08 days). From the headspace gas concentration and pH of the anolyte it is possible to estimate dissolved CO_2 (H_2CO_3) and determine the fate of carbon in the system. The theoretical carbon dioxide yield is the maximum molar yield of CO_2 given the amount of substrate degraded which was estimated from the efficiencies presented in Table 3.3 based on the stoichiometry in Equation 2.1.

Table 4.3 COD at the beginning of run 5 (COD_{TOT}), that which remained in the anolyte at the end of feeding event 5 (COD_{SD}) and the amount of COD degraded throughout the course of the feeding event (ΔCOD) along with summary data of efficiency metrics for eight duplicate MFCS operated with four different inocula. ± standard deviation, for mean n = 2.

	Freshwater Sediment	Spennymoor RAS	Howden RAS	Anaerobic Sludge
COD_{TOT} (mg L^{-1})	300 (±11.09)	426 (±11.71)	336 (±9.90)	342 (±14.59)
COD_{REM} (mg L^{-1})	60 (±18.48)	56 (±0)	60 (±18.48)	228 (±14.59)
ΔCOD (mg L^{-1})	240 (±18.48)	370 (±13.48)	276 (±16.07)	114 (±14.59)
COD_{SD} (%)	79.91 (±7.41)	86.83 (±1.78)	82.08 (±6,18)	33.33 (±0)
CE (%)	7.13 (±2.42)	12.02 (±0.91)	8.45 (±0.39)	4.18 (±0.37)
η_E (%)	2.94 (± 0.54)	7.62 (±0.47)	8.31 (±1.62)	1.57 (±0.252)

The pH is similar for all cells at ≈ 6.78, except for those inoculated with Freshwater sediment, which also exhibits the greatest change in pH over the course of the experiment. The mole % change in headspace CO_2 concentration was greatest in cells inoculated with Howden RAS (2.31%), followed by Spennymoor RAS (2.00%) Freshwater Sediment (1.85%) and Anaerobic sludge (1.48%) which equates into 786, 679, 628 & 370 µmol L^{-1} of H_2CO_3 in the liquid phase respectively. Keeping the same order, the theoretical carbon dioxide yield was 1089, 1393, 955 & 653 µmol L^{-1} respectively resulting in approximately 327, 713, 293, 283 of µmol L^{-1} dissolved organic carbon that was unaccounted for in these systems.

4.7.1 ANODIC MICROBIAL COMMUNITY COMPOSITION

Bacterial communities were analysed by denaturing gradient gel electrophoresis (DGGE) of polymerase chain reaction (PCR)-amplified 16S rRNA genes from anodic biofilms. The Howden RAS and the Anaerobic Sludge inocula were compared with the final anodic-communities in the corresponding MFCs at the end of run six when the experiment was

terminated. The anodes from the MFCs treated with Spennymoor RAS and freshwater sediment were subject to electrochemical manipulation (polarization) and were not used for microbial analysis.

Table 4.4 pH at the start (pH_s) and finish (pH_f) of a feeding event, the percentage change in headspace CO_2 concentration (ΔCO_2), dissolved $C0_2$ in the anolyte (H_2CO_3), the theoretical CO_2 yield (CO_{2T}), the amount of CO_2 unaccounted for in the system (CO_{2M}) and the change in VFA concentration (ΔVFA) for eight duplicate cells seeded with four different inocula over the course of feeding event five (8.63-11.08 days). ± standard deviation, for mean=2. ND= No Data.

	Freshwater Sediment	Spennymoor RAS	Howden RAS	Anaerobic Sludge
pH_s	6.85 (±0.20)	6.79 (±0)	6.78 (±0)	6.76 (±0)
pH_f	6.73 (±0.41)	6.72 (±0.21)	6.74 (±0)	6.75 (±0)
ΔCO_{2HS} (%)	1.85 (±0.24)	2.00 (±0.37)	2.31 (±0.24)	1.48 (±nd)
H_2CO_3 (µmol L^1)	628	679	786	370
CO_{2T} (µmol L^{-1})	955	1393	1079	653
CO_{2M} (µmol L^{-1})	327	713	293	283

The dendrogram in Figure 4.3 shows clustering into groups with more than 90% similarity between duplicate anode communities. The two inocula are different from one another with only about 30% similarity. More amplicons were resolved in the lanes corresponding to the RAS inoculum from Spennymoor than from the lanes corresponding to the Anaerobic sludge inoculum. The anaerobic sludge appears to be dominated by three intense bands having a relative intensity of 30, 60 and 43% respectively with the remaining 7 bands having a relative intensity of less than 8%. Conversely, the Spennymoor inoculum has one band with intensity greater than 71%, one band with intensity of less than 8% and 21 bands with an intermediate intensity of between 8 and 36%. The different inocula gave rise to different anodic communities with around 56% similarity in their DGGE profiles. The community

profiles obtained from the anodes are different from their corresponding inocula, although this is so to a much greater extent for Anaerobic Sludge, and to one another. There are several bands which are enriched in the anodic community profiles of both treatments although this appears to be so to a greater extent in the anodes from MFCs inoculated with anaerobic sludge. The bands circled indicate enriched bands with high intensity that is similar in both duplicates (83 and 81%) from the MFCs inoculated with anaerobic sludge and which had an intensity of 5% in the original inoculum (Figure 4.3). There is a thick dense band that is common to all samples except the anaerobic sludge inoculum. The average Simpson's index of diversity (1-D) for the microbial community recovered from the anodes of MFCs inoculated with both Howden RAS and Anaerobic Sludge was similar, 0.9 and 0.89 respectively, although the microbial community in the MFC inoculated with Howden RAS showed a greater degree of evenness, 0.94 vs 0.89 in the MFCs inoculated with anaerobic sludge. The Simpson's index of diversity for the Howden RAS and anaerobic sludge is 0.95 and 0.75 respectively with a corresponding evenness of 0.96 and 0.72.

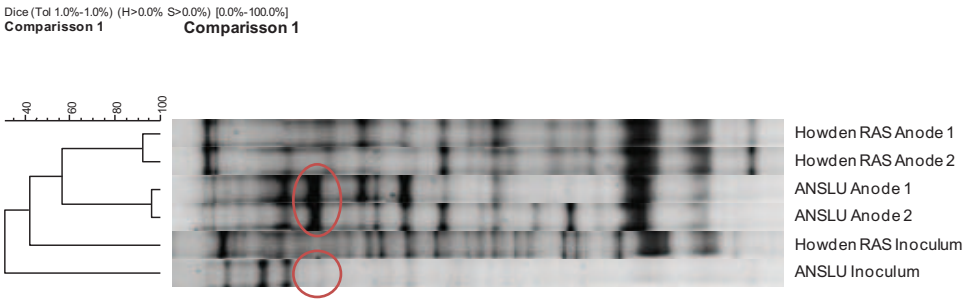

Figure 4.3 16S rRNA DGGE analysis of Howden RAS and Anaerobic Sludge inocula compared with duplicate samples of the anode community at the end of the experiment. Note the obvious enrichment in the circled bands in MFCs inoculated with anaerobic sludge compared to the original inoculum. There is also a thick band common to all of the MFCs and more bands in the MFCs inoculated with Howden RAS than those inoculated with anaerobic sludge.

4.8 DISCUSSION

The superior performance of the RAS inocula from both sites compared with the other two inocula was confirmed by all the electrochemical metrics determined (maximum potential, current, and power as well as charge, coulombic efficiency & treatment efficiency). As the purpose of these tests was to arrive at a comparative observation about the best performing inocula it might be safe to assume that the RAS inoculum is, in performance and start up terms, 'better' than both Freshwater Sediment and Anaerobic Sludge as an MFC inoculum. Further investigation of the data shows that the story is more complicated.

Whilst the performance of the RAS is comparatively good, none of the cells in this study are performing well. Firstly, there is a large difference between the theoretical OCP_T (1.23V, Table 4.2) and the observed OCP_O (0.33-0.5 V) in all instances. This represents the cell overpotential, which is the difference between the OCP_O and that predicted from thermodynamic calculations. The resulting overpotentials of 0.73, 0.76, 0.86, and 0.9 V respectively will reduce the maximum system-specific power (P_{maxS}) which is around 7–16 % of that predicted from thermodynamic data. Polarization was unsuccessful in these tests and without good polarization data it is impossible to tell where these losses arise. The cathodic OCV of MFC with air cathodes and platinum catalysts is typically reported to be around 0.4–0.6 V (Liu and Logan, 2004; Logan *et al.*, 2006; Logan, 2008). It is therefore safe to assume that a large part of the cell overpotential is cathodic in nature although it would be unwise to speculate to what degree this is so. The internal resistance of these cells (40-53 Ω) only accounts for around one percent of the cell overpotential calculated from the OCV.

The observed power (P_{maxO}) was between 1.5 and 3% of the theoretical maximum power and between 12-25% of the system specific power (P_{maxS}, Table 4.2) suggesting that the MFCs were subject to further, extensive losses during operation. As it was not possible to measure the anode or cathode potential in these tests, it is impossible to say with any certainty which electrode is not working efficiently although the modification of the anode potential by the colonizing organisms (or lack of them) as well as oxygen influx into the

anode chamber are potential explanations – the latter of which can easily be investigated qualitatively using chemical data.

The coulombic efficiency ranges between 4–12% (Table 4.3). Whilst other studies report coulombic efficiencies as low as a few percent (Jadhav and Ghangrekar, 2009), coulombic efficiencies greater than 20% are commonplace (e.g. Wang *et al.*, 2010; Shimoyama *et al.*, 2008) and reports exist describing coulombic efficiencies as large as 80% (Rabaey *et al.*, 2004) or even 100% (Nevin *et al.*, 2008). Generally, the higher coulombic efficiencies such as those achieved by Nevin *et al.* (2008) result from MFCs operated with pure cultures and simple electron donors such as acetate. Conversely, operating MFCs under 'realistic' or challenging conditions results in lower coulombic efficiency as is the case with Jadhav and Ghangrekar (2009) who subjected MFCs inoculated with anaerobic sludge to changes in temperature, influent composition and pH. As well as the unremarkable recovery of electrons in these cells, the energy efficiency (η_E) is low, ranging from 1.5 – 8% (Table 4.3). Low energy efficiency is a result of low cell potential and can, theoretically, occur even in instances of high electron recovery. The maximum energy efficiency for these cells, taking into account initial losses, would be around 50%. The poor recovery of electrons by the bioelectrochemical system was in contrast to high treatment efficiencies greater than 79% in all systems except those that were inoculated with Anaerobic Sludge where the treatment efficiency was 33% (Table 4.3). With the exception of anaerobic sludge treatment, the COD removal in these systems met the discharge requirements in the UK for industrial wastewater of less than 125 mg L^{-1} or in excess of 75% treatment efficiency (91/217/EEC). The final COD concentration in the anolyte of the MFCs (excluding those treated with anaerobic sludge) was similar (58-60 mg L^{-1}) despite large differences in the range of starting COD of around 40%. This figure may be close to the upper limit of treatment efficiency for these systems and the lack of VFA detected in the anolyte may suggest that the residual COD is of a refractive nature (Swiderska-Broz, 2011).

The combination of low bioelectrochemical electron recovery and high treatment efficiency demonstrates that the carbon in the system is being consumed and that electrons are being

diverted to a sink other than the electrical circuit. For this to occur there must be another electron acceptor in the system. Headspace gas analysis reveals that the concentration of CO_2 in the headspace is between 1.85–2.31%. This was measured as a means to estimate dissolved organic carbon in the anolyte with a view to elucidating the fate of carbon in the system — essentially the difference between the amount of dissolved organic carbon in the anolyte and theoretical amount of dissolved organic carbon that could be produced from the starting substrate. For the purposes of this experiment and by convention, it is convenient to assume that all dissolved CO_2 is present in solution as carbonic acid (Chang, 1981; Drever, 1997). The estimated concentration of dissolved inorganic carbon in the anolyte (based on headspace CO_2 concentration) is 628, 679, 786, 370 μmol L^{-1} H_2CO_3 for Freshwater Sediment, Spennymoor RAS, Howden RAS, and Anaerobic Sludge inoculated MFCs, which accounts for 65, 48, 73, and 57% of the theoretical dissolved inorganic carbon in solution respectively. The proportion of dissolved inorganic carbon unaccounted for in these systems is low and is strongly indicative of oxygen infusing into the anode chamber through the cathode membrane assembly which this is a frequently observed phenomenon (Cheng *et al.*, 2006, di Lorenzo *et al.*, 2009). Methane was not detected in the headspace gases of these cells, and is further evidence of oxygen being present in the anode chamber both methanogens are sensitive to oxygen and are outcompeted by aerobes (Fetzer & Conrad, 1993).

The absolute amount of carbon unaccounted for in these systems, based on the mole % of carbon in CO_2 and adjusted for reactor volume, is similar (196, 176 & 170 μg) for MFCs inoculated with Freshwater Sediment, Spennymoor RAS, and Anaerobic Sludge respectively and more than double this (428 μg) in the MFCs inoculated with Howden RAS (Table 4.4). The obvious fate of this proportion of carbon is its likely incorporation into biomass given the high treatment efficiency and that that VFAs were not detected in the anolyte. The incorporation of these quantities of carbon into biomass was not measured directly nor is it possible to tell how the quantities are distributed between the planktonic community in the anolyte and those associated with the anode. Carbon accounts for 10–50% of the total biomass of microbial cells (Jones, 1979; Coskuner, *et al.*, 2005). Thus an estimate for

biomass of between 340–4280 µg can be arrived at which, using a conversion factor from Findlay *et al.*, 1989 of 3.4 x 10^6 cells per µg of carbon roughly equates to between 1.16 x 10^9 and 1.47 x 10^{10} cells (Jones, 1979; Findlay *et al.*, 1989; Coskunur, *et al.*, 2005). A low cell potential means that, thermodynamically, more energy is available for bacterial metabolism and a corollary would be that a relatively high proportion of carbon would be incorporated into biomass (Wei *et al.*, 2010). Using a phospholipid assay, Wei *et al.* (2010), estimated the biomass of pure cultures of *Geobacter sullfurreducens* in a microbial fuel cell as being 180 ng P cm^{-2}, which equates to about 2.04 x 10^8 cells cm^{-2} using a conversion factor of 3.4 x 10^9 cells per 100 nmol P (Findlay *et al.*, 1989). By accounting for the anode surface area of 8 cm in Wei's estimate an absolute figure of 1.63 x 10^9 cells in the MFC which is in range of the estimate of cell numbers reported here. Wei *et al.*, (2010) used a pure culture of *G. Sulfurreducens,* acetate and higher fuel concentration (1200 mg L^{-1} vs 300 mg L^{-1}) than that which was used in this study. The COD of glucose and acetate is comparable and the absolute concentrations of COD fuel used in Wei's study, normalised to MFC volume, was 80 mg COD whilst in the study reported in this Chapter it was 15 mg (Lee, 2007, Wei *et al.*, 2010). The cell yield per mg of COD added to each MFC is therefore 2.03 x 10^7 cells g COD^{-1} and 7.77 x 10^7 cells g COD^{-1} for the Wei study and the MFC reported here respectively. Accordingly, the cell yield in this study is almost four times that of those reported by Wei *et al.* (2010). There is a large degree of error associated with this estimate and it would be unwise to make too much of these numbers. The amount of energy available to an organism increases as the anode potential moves towards a more positive potential (because the potential difference between the substrate and the anode becomes greater) this means that MFCs that have a low operational cell potentials may support higher biomass and in this respect may explain the relatively high estimate for biomass yield in this study (Cheng *et al.*, 2011; Aelterman *et al.*, 2008).

Figure 4.1 shows an obvious difference between the start up profile of MFCs inoculated with anaerobic sludge (Figure 4.1D) and the other treatments (Figure 4.1A-C). The fact that the anaerobic sludge inoculum performed relatively poorly in comparison to the other inocula is surprising as it is widely reported as being an effective inoculum source for MFCs (e.g.

Ramasamy *et al.*, 2008; Aelterman *et al.*, 2006). The lag phase observed in Figure 4.1D suggests either different mechanistic electron transfer in these MFCs (direct vs. mediated) or low abundance of electrogens in the anaerobic sludge inoculum. All inocula were standardized for cell numbers to counter any effects that may arise from the differential abundance of microbial species in each inoculum. If low abundance of electrogens is the cause of the observed lag phase with the anaerobic sludge inoculum (Figure 4.1D), there is no way of telling if this is a natural state or if the inoculum has been compromised somehow during handling. Alternatively, the assumption of viability in the total cell counts procedure is invalid or, if oxygen was diffusing through the cathode, it may present a particular challenge for this community of anaerobes resulting in longer acclimation periods for the anaerobic sludge inoculum compared with the inocula sourced from aerobic environments or less strictly anaerobic environments. The fact that overall treatment efficiency in the systems inoculated with anaerobic sludge is lower than with the other inocula (c.a. 33% vs c.a. 80%) does seem to suggest that there is less electrogenically active biomass in the MFCs inoculated with anaerobic sludge. If this is the case, and considering the apparent acclimation phase, it begs the question as to whether or not, given more time, the MFCs inoculated with anaerobic sludge would have undergone further enrichment and subsequent increases in electrochemical performance. In fact, Figure 4.1D shows progressive increases in maximum cell voltage between feeding events which suggests that the further enrichment may have been likely given time although in previous experiments with similar systems MFCs were prone to instability and reduced reproducibility over time (data not shown) and is primarily why the experiments were terminated after 14 days. The community fingerprint analysis data support both these theories (Figure 4.3). In the lane corresponding to the anaerobic sludge inoculum (Figure 4.3), it is apparent that fewer bands are resolved in this lane and that it is dominated by three bands with a strong signal and 7 bands of weak intensity. Conversely, the Spennymoor inoculum has around double the number of bands (23) and 22 of these are present at intensities greater than the minor bands in the anaerobic sludge inoculum. The increased intensity of a number of bands from the anode inoculated with anaerobic sludge compared with the initial inoculum, in

particular the ones circled in Figure 4.3, support the observed lag phase with anaerobic sludge inoculum (Figure 4.1D) in that species that were less abundant in the inoculum appear to have become enriched on the anode. These bands correspond to the putative electrogens and would be natural targets for sequencing. There is weak evidence for different mechanisms of electron transfer too. The fact that almost no lag period was seen in the cells inoculated with RAS and Freshwater Sediment and that, unlike the MFC inoculated with anaerobic sludge, an obvious increase in the magnitude of band intensity or enrichment between the initial inoculum and the anodes was not observed in the RAS community profiles suggests that the mechanism of electron transfer is mediated rather than direct transfer by attached anode electrogens. In terms of diversity indices, the Howden RAS inoculum was more diverse (Simpson's index of diversity (1-D) = 0.94) and even than the anaerobic sludge inoculum (Simpson's index of diversity (1-D) = 0.75). However the anodic communities recovered from the MFCs inoculated with Howden RAS and Anaerobic sludge showed similar diversity, with Simpson's index of diversity (1-D) of 0.89 for Howden RAS and anaerobic sludge inoculated MFCs respectively. The fact that, potentially, anaerobic sludge inoculum has a lower natural abundance of electrogenic microbial species is interesting. Further data would allow us to tell with certainty whether this assertion is true and the degree to which the results observed here are confounded by the relatively low electrochemical efficiencies in the MFCs and the influence of oxygen on the development of the anodic community in MFCs inoculated with an anaerobic environmental sample.

4.9 SUMMARY

The hypothesis set out to test to what degree the different inocula influence MFC performance.

- Each inoculum exerted a statistically significant effect on the MFC performance and the ranked effect of inoculum on MFC performance for all the metrics tested here (E_{cell}, I and C) was Spennymoor RAS> Howden RAS> Freshwater Sediment> Anaerobic Sludge.

- With the exception of MFCs operated with Anaerobic sludge which had a treatment efficiency of 33%, the treatment efficiency all inocula was similar at 79-82 %.
- Despite high treatment efficiency the metrics E_{cell}, current density, coulombic efficiency and energy efficiency in these systems point to poor electrochemical performance.
- The combination of poor electrochemical performance combined with good treatment efficiency is indicative of oxygen infiltration through the cathode
- The anaerobic sludge starting inoculum was less diverse than the Howden RAS inoculum but the resulting community profiles from MFCs operated with each inoculum had a similar diversity shown by a Simpson's index of diversity (1-D) of value of 0.9 and 0.89 respectively. This showed the MFCs inoculated with Anaerobic Sludge inoculum underwent greater enrichment than did the RAS inoculum.

- The RAS form two different sites performed similarly well compared to the freshwater sediment and anaerobic sludge inocula. This is true for all the metrics determined here and is statistically significant.

- The treatment efficiency in all cases was sufficient to meet the trigger value of <125 mg L^{-1} COD for discharge into UK receiving waters as set out in the Urban Wastewater Treatment Directive (91/217/EEC). With exception of the MFCs inoculated with anaerobic sludge, the biological treatment efficiency was greater than the statutory value of 75% set out in the same regulations.
- Evidence suggests that the poor performance of the MFCs inoculated with anaerobic sludge systems is related, at least in part, to low abundance of electrogens.
- Potentially, there may be different mechanisms of electron transfer between the anodes of the MFCs inoculated with anaerobic sludge and the other three inocula. Insufficient molecular data coupled with predominantly non bioelectrochemical removal of COD means that this assertion is difficult to conclude with certainty.

4.10 CONCLUSIONS

The experiments presented in this chapter used a novel procedure to standardise inoculum density when seeding MFCs which provided valuable insights particularly in relation to the effects of inoculum on MFC performance and start up times. The methodological development of standardising inoculum density in MFCs is recommended for future MFC research where inoculum density may be a confounding factor in MFC experiments. Additionally, the findings in this chapter will pave the way for developments in operating full scale MFCs in field situations where seeding will have economic and regulatory implications. Reducing plant down time during start up or reseeding (following bioreactor instability) through proper seed choice will be immensely valuable. The treatment efficiency of the MFCs used in the study presented in this chapter was good and met UK regulatory requirements for the treatment of wastewater.

5 USING STATISTICALLY DESIGNED EXPERIMENTS TO IDENTIFY FACTORS THAT AFFECT THE PERFORMANCE OF MICROBIAL FUEL CELLS OPERATED UNDER SUB OPTIMAL CONDITIONS

5.1 INTRODUCTION

Process optimization focuses on manipulation of those parts of the process, or factors that have the most pronounced effect on the process outcome or performance, and which are simple or economical to control (Antony, 2008). In the case of an MFC a conceptual model can help identify the variables which influence fuel cell performance and categorize them as either those which are beyond our control or uneconomical to manipulate or those which are convenient or economical to manipulate. Figure 5.1 shows a conceptual model of the MFCs used in this study and the factors which one would reasonably expect to influence performance. The readily controlled factors are designated 'X' and more difficult or nuisance variables are designated 'Z'. Z or nuisance variables are the main cause of variability in process performance.

One of the central aims of statistically designed experiments is to optimize the settings of X variables and to minimize the effects of Z variables (Antony, 2008).

There are some obvious targets for manipulating fuel cell performance namely, Fuel Concentration (organic load), External Resistance, and Fuel Type. All of these are easy to control in a microbial fuel cell requiring only minor changes to operational protocol (Figure 5.1).

MFCs must at least be able to generate sufficient power to drive the plant required for their operation. The operating voltage and power in MFCs is typically low (Chapter 2.4) and in order to achieve the voltages and current required to power equipment such as pumps, MFCs will need to be connected in series and in parallel in what is known in conventional fuel cell parlance as a stack. Connecting circuits in series adds voltage whilst connecting them in parallel results in additive current. Operating MFCs at maximum power is one strategy to minimize the number of MFCs in a stack (Lefebvre *et al*; 2009; Lefebvre *et al.*, 2011).

The maximum power theorem states that the external load should be close to that of the internal resistance in order to obtain maximum power. It is explained by the following

expression:

$$P = OCV^2 \{R_{EXT}/[A(R_{EXT} + R_{INT})^2]\}$$

Equation 5.1

Where 'P' is the power density, 'OCV' is the open circuit voltage and 'A' is the electrode area (Jung & Regan, 2011).

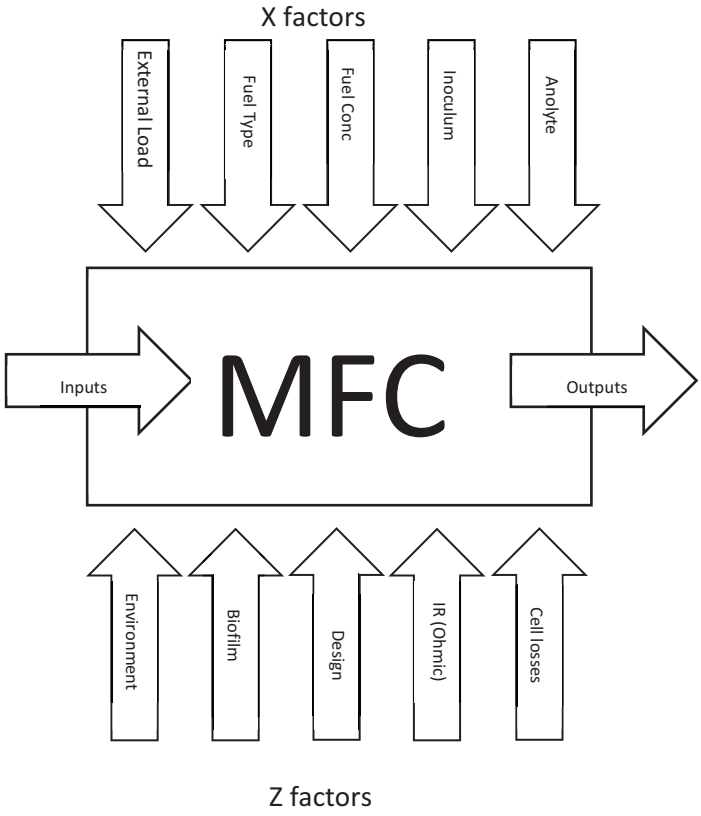

Figure 5.1 A conceptual model of a fuel cell showing examples of some of the factors which may be easily controlled (X factors) and those which are more difficult to control (Z factors). Adapted from Antony (2008). MFC design was beyond the scope of this experiment and designated as a 'Z' factor accordingly. Parasitic losses include internal currents, oxygen diffusion and methanogenesis.

Levebvre *et al.* (2011) reason that to minimize stack size then it is important to minimize internal resistance in an MFC so that maximum power is achieved at lower external resistance (higher currents). Maximum power is not necessarily synonymous with high efficiency as mass transport losses may increase disproportionately as higher currents are drawn from a fuel cell. In conventional fuel cells, the fuel is a valuable commodity and efficiency is much more likely to be an issue than in MFCs. For wastewater treatment, it could be argued that capital expenditure would be more limiting than efficient use of a waste material and hence, minimizing stack size by designing MFCs with extremely low external resistance may be a valid strategy. However, decreased energy efficiency will result in larger volumetric requirements for each MFC in order to achieve both high treatment efficiency and to provide enough reducing power to reach the desired current. Any cost savings in reducing the number of units in a stack will need to be carefully considered alongside additional volumetric requirements to treat each unit of wastewater. There are other problems with this simplistic approach too. Transfer, kinetic, membrane, and biofilm resistances in microbial fuel cells mean that the internal resistance is not static, thus the maximum power transfer theorem may not be applicable and the choice of what external load to use when operating a MFC is, currently, almost arbitrary. However, operating an MFC at low internal resistance may be an attractive proposition worthy of investigation although design advances that confer small reductions in R_{INT} may be insignificant when considering that the conductivity of most wastewaters is typically lower than 1 mS cm^{-2} equivalent to a resistance of 1000 Ω cm^{-2} (Rozendal *et al.*, 2010).

Finkelstein (2006) demonstrated that the anode potential influences microbial fuel cell performance. At relatively high anode potentials, the energetic gain for anodic microbial consortia will be greater. This is explained by thermodynamics — the difference between the reduction potential of the substrate and the anode will be larger thus the free energy available to the organism from metabolizing the substrate is potentially greater too (Torres *et al.*, 2009). This occurs at the expense of fuel cell performance as the potential difference between the anode and cathode will be smaller resulting in electrons passing through the

circuit at lower energy (Aelterman *et al.*, 2006). The energetic gain for bacteria is limited by the upper potential of a microbe's terminal respiratory apparatus and microbes appear to control the potential of an anode to maximize the return on their metabolic investment (Logan, 2009; Wei, 2010). Anode potential may control the metabolic pathway used by the bacterium and even play a selective role in anode colonization as well as influencing biomass yield and MFC startup times (Aelterman *et al.*, 2006; Katuri *et al.*, 2011). As air cathodes are likely to be more sustainable than other cathode designs, it is likely that oxygen will always diffuse from the cathode into the anode chamber to some degree and compete against the anode process. Under such conditions, it may be better to select high rate (low external resistance) anode kinetics to increase the electron flow through the anode and minimize alternative routes for oxidation of the wastewater fuel (Gil, 2003; Jung & Regan 2010). Given the complexity of the anode interactions, it is desirable to control the anode potential at a level that will maximise MFC performance. Poising the anode potential may not practical in field situations so selecting the external load that enables and MFC to operate at a desirable anode potential is a crucial aspect of MFC operation (Aelterman *et al,* 2006). It is still unclear how microbes communicate with the anode but one can expect that the different strategies so far proposed (direct contact, mediated & nanowires) would only serve to complicate the simple relationship between external load, potential and current in conventional fuel cells thus making the choice of external resistance much more critical.

Organic load, in the case of wastewater engineering applications, has a logical maximum (that of the wastewater being treated) but theoretically could be diluted to any required strength if it was shown to be a useful parameter to optimize MFC performance. This would require an effluent recycle step adding an additional level of complexity, would require additional pumping capacity and would need to be justified by gains in performance. Jadhav and Ghangrekar (2009) demonstrated a linear correlation between current and organic load and as the substrate is the ultimate source of electrons it is intuitive that its concentration will be a critical factor in generating current. Moreover, Aelterman *et al.* (2006) demonstrated the preferential degradation of organic matter at low external resistance when current is high. Thus rapid electron transfer can sustain high substrate degradation

rates, particularly if the anolyte is sufficiently conductive to achieve equivalent levels of proton transport across the anolyte to the cathode.

Manipulating fuel type is valid from an experimental point of view but in wastewater applications, the composition of the wastewater of interest will dictate the fuel type. Fuel type is likely to influence the composition of the anode community as some organisms preferentially degrade some substrates, for example *Shewenella putrefaciens* preferentially utilizes non-fermentable carbon sources (Madigan, 2011). Jung and Regan (2011) showed differences in bacterial community composition using 16S rDNA analysis related to fuel type (acetate, lactate and glucose). They observed *Geobacter sulfurreducens* in all instances in the anodic communities in MFCs fed with different fuels but different Geobacter species that were associated with fuel type. *Firmicutes* were only found in the anodic communities fed with glucose and the authors attributed their role as fermentative (Jung and Regan, 2011). Fuel type is, therefore, likely to influence the anodic community in an MFC although not all of these changes will result in changes to the electrogenic capabilities of the anode.

To date, organic load, fuel type and external resistance have been studied using one variable at a time (OVAT) experiments. These give no information about interactions and may lead to false identification of optimum settings (Antony, 2008). As well as correct variable selection, carefully chosen process responses are more likely to ensure the success of designed experiments. To obtain the most value from statistically designed experiments, process responses that are easily measured, continuous, linear and monotonic are preferred.

5.2 AIMS

The aim of the work in this chapter was to investigate if “Design of Experiment” techniques are useful tools for investigating MFC performance by investigating the main effects of three factors: external resistance, organic load, and fuel type and the suitability of process responses for further optimization studies based on the response profile (i.e. continuous, linear and monotonic). It is expected that DoE techniques will allow deeper insights into

how manipulating operational parameters will affect MFC performance. The experiments here will be useful to inform future DoE experiments and even extend to scale up systems.

5.3 OBJECTIVES

- To investigate the main effects of Fuel Type, External Resistance, and Organic Load on E_{cell}, current and coulombic efficiency
- To assess the suitability of E_{cell}, Power, and Coulombic Efficiency as suitable process responses for the use in full factorial experiments
- To compare the performance of each treatment with a view to optimizing MFC performance

5.4 HYPOTHESIS

The aims and objectives were designed to explore the following hypotheses:

- The different factors chosen, external resistance (R_{EXT}), organic load (OL) and fuel type (FT) will influence MFC process performance observed by their effect on cell potential (E_{cell}), Current (I) and coulombic efficiency (CE).
- The output parameters (E_{CELL}, I and CE) chosen for the design of experiments will show differential suitability for use in DOE depending on whether MFCs are operate under high or low R_{EXT}, and OL and also FT.
- The significance of each factor (R_{EXT}, OL and FT) will vary depending on the output (E_{CELL}, I and CE).
- The design of experiment results will inform future, full-factorial DOE studies aimed at examining interactions between factors

5.5 EXPERIMENTAL

The experimental procedures for this chapter are summarized below but can be found in more detail in sections 3.1–3.82.

Single chambered air-cathode MFCs (25 ml volume) were used in this study (Figure 3.1). The cathode was constructed as a membrane-electrode assembly that consisted of a gas

diffusion layer hot pressed between a Nafion 117® membrane and a carbon paper cathode with a final Pt catalyst loading of 0.3 mg cm^{-2}. The anode was made of carbon cloth. Both electrodes had an active surface area of 12.5 cm^2. The electrodes were connected under a load according to the factorial array outlined below (Table 5.1) and the drop in potential across the load was measured using a Pico ADC16 datalogger and connected to a PC to determine OCV and perform half-hourly logging of E_{cell} using PicoLog software.

Electrode potentials were determined by placing an Ag/AgCl reference electrode next to the working anode. The specific overpotentials were determined by polarizing the cell using a GillAC sequencer.

The fuel cells were set up and inoculated with Return Activated Sludge (RAS) from Spennymoor Sewage Treatment Works (3.2.2). The original environmental sample was diluted 1:1 in sterile, artificial wastewater medium (pH 6.8) and amended from a sterile stock glucose solution to a working concentration of 50 or 300 mg L^{-1} (Section 3.3.3) according to the factorial array below (Table 5.1). Feeding events were instigated at the nadir of the voltage curves when the MFCs were refueled by removing the anolyte — some of which was preserved for later analyses — and replacing with fresh medium. Electrochemical monitoring began after an acclimation period of 12 days.

The organic matter concentration was measured as COD, using a commercially available COD kit (Merck, UK) on anolyte samples that were collected at the start and end of each experiment and subjected to the clean up method (Section 3.4.1).

Analysis of volatile fatty acids (VFAs) was performed on a Dionex ICS 1000 Ion Chromatograph system with Chromeleon® data acquisition software and an AS40 auto sampler (Dionex, USA) (Section 3.4.3).

Confocal laser scanning microscopy (CLSM) was performed on the anodes of MFCs upon terminating the experiment and removing them from the MFC. Anode sections were suspended in PBS and stained with BacLight® (propidium iodide and SYTO9) bacterial

viability stain after termination of experiments and presented for confocal microscopy immediately (Section 3.5.3).

A half-factorial design was chosen as a screening experiment for the full factorial design presented in Chapter 6. Eight MFCs were set up according to a factorial design generated using Minitab 15 statistical software (Section 3.8.1). Performance was measured in terms of the process outputs E_{cell} (Section 3.1.5), Current (Section 3.7.2) and coulombic efficiency (Section 3.7.4). All statistical analysis was carried out using Minitab 15.

Table 5.1. DOE Factorial array for eight MFCs. Replication was achieved over two runs and by duplicating the midpoints. The design is formally described as a $2^{(3-1)}$ factorial design with resolution (III) and centre points.

	Standard Order	MFC ID (run order)	External resistance (Ω)	Organic Load (mg L^{-1})	Fuel Type
Run 1	1	4	200	50	Glucose
	2	*5*	5000	50	Acetate
	3	1	200	300	Acetate
	4	3	5000	300	Glucose
	5	2&7	2600	175	Acetate
	6	6&8	2600	175	Glucose
Run 2	7	4	200	50	Glucose
	8	5	5000	50	Acetate
	9	1	200	300	Acetate
	10	3	5000	300	Glucose
	11	2&7	2600	175	Acetate
	12	6&8	2600	175	Glucose

5.6 RESULTS

The results are presented in four distinct sections. Firstly, the MFC process outputs used to measure performance are presented as summary data and include those required for the factorial analysis. Then the results of the factorial analysis are presented followed by an electrode assessment and finishing with some confocal microscopy of the biofilms present on the anodes of the MFCs.

5.6.1 SUMMARY DATA

Table 5.2. A summary of the outputs from MFCs 1-8.

Run	Maxima	MFC 1	MFC 2	MFC 3	MFC 4	MFC 5	MFC6	MFC 7	MFC 8
1	E_{cell} (mV)	1.03	11.22	64.78	0.61	27.41	59.77	11.83	62.06
	I (mA m^{-2})	4.12	3.45	10.36	2.4	4.39	18.39	3.64	19.10
	P(mW m^{-2})	0.21	1.94	33.57	0.07	6.01	54.96	2.15	59.25
	CE (%)	0.70	0.59	1.09	4.38	3.26	1.43	0.40	1.43
2	E_{cell} (mV)	1.14	10.88	60	0.43	29.34	54.15	13.04	61.45
	I (mA m^{-2})	4.56	3.35	9.60	1.72	4.69	16.66	4.01	18.91
	P(mW m^{-2})	0.26	1.82	28.80	0.04	6.89	45.11	2.62	58.09
	CE (%)	0.76	0.85	1.03	4.01	2.50	1.90	0.82	2.59

Table 5.2 shows a summary of output maxima cell potential current, power density and, coulombic efficiency (E_{cell}, I, P and CE) from MFCs 1-8. The factorial array used in the statistical analysis (Table 5.3) was generated from the data in Table 5.2 according to the method described in Section 5.5 using Minitab 15.

Table 5.3 Factorial array of a duplicated half-factorial design with midpoints. Duplication was achieved by including data from two simultaneous runs treated as two separate blocks in this array. The midpoints were duplicated as a monitoring exercise.

Std Order	Run order	External resistance (Ω)	Organic Load (mg L^{-1})	Fuel Type	Ecell (mV)	I (mA m^{-2})	CE (%)
1	4	200	50	Glucose	0.61	2.43	5.310
2	*5*	5000	50	Acetate	27.41	4.39	12.450
3	1	200	300	Acetate	1.03	4.12	2.320
4	3	5000	300	Glucose	64.78	10.36	2.260
5	2&7	2600	175	Acetate	11.52	3.54	2.330
6	6&8	2600	175	Glucose	60.09	18.75	5.410
7	4	200	50	Glucose	0.43	1.71	7.370
8	5	5000	50	Acetate	29.34	2.93	1.945
9	1	200	300	Acetate	1.14	4.54	2.270
10	3	5000	300	Glucose	60.00	9.55	2.770
11	2&7	2600	175	Acetate	13.04	3.99	3.550
12	6&8	2600	175	Glucose	61.45	18.82	6.240

5.6.2 Design of experiment analysis

The effect of external resistance and organic load on cell potential (E_{cell}) was positive although the latter to a lesser extent (Figure 5.2A). For fuel type, acetate invoked a much smaller effect on E_{cell} than glucose and the response changed little at different settings (evident from the proximity of the two points in Figure 5.2C). The effect of glucose on E_{cell} is greater than acetate, although the mean response at the midpoints is greater than the sum of the responses at the high and low settings.

The effect of R_{EXT} on E_{cell} was broadly linear and monotonic (Figure 5.2A) whereas the effect of organic load appears to be both non-linear and non-monotonic – this is evident from Figure 5.2B where the midpoints lie at a distance from the line on the main effects plots. The Pareto chart (Figure 5.2D) shows the standardized effects of the three factors ($R_{EXT,}$ OL and FT) on E_{cell}. The red line denotes the value of alpha (set at 0.05%) and shows that R_{EXT} and FT exert a significant effect on E_{cell} above the 95% level whereas the effect of OL is not significant.

Current showed a moderately positive response to external resistance and organic load, however, because of the position of the midpoints, it appears that in both instances the response is neither monotonic nor linear (Figure 5.3A, Figure 5.3B). The effect of glucose on current was greater at the midpoint (175 mg L^{-1}) than the combined effect of glucose on current at 50 and 300 mg L^{-1}. The effect of acetate on current was much smaller than that of glucose and the effect was similar at both the corner point and the midpoint (Figure 5.3C). The Pareto chart shows that only fuel type exerts a significant effect on current in this study (Figure 5.3D)

There was a small negative effect of external resistance on CE (Figure 5.4A) however this was not significant (Figure 5.4D). Organic load and fuel type exerted the greatest effect on coulombic efficiency and the extent of these effects was significant in both instances (Figure 5.4D). Increasing organic load led to a strong reduction in CE (Figure 5.4A) and appears to be monotonic but non-linear with signs of saturation between the midpoint and high settings

(175 and 300 mg L^{-1} COD). Higher CE was obtained with glucose under all conditions (Figure 5.4C).

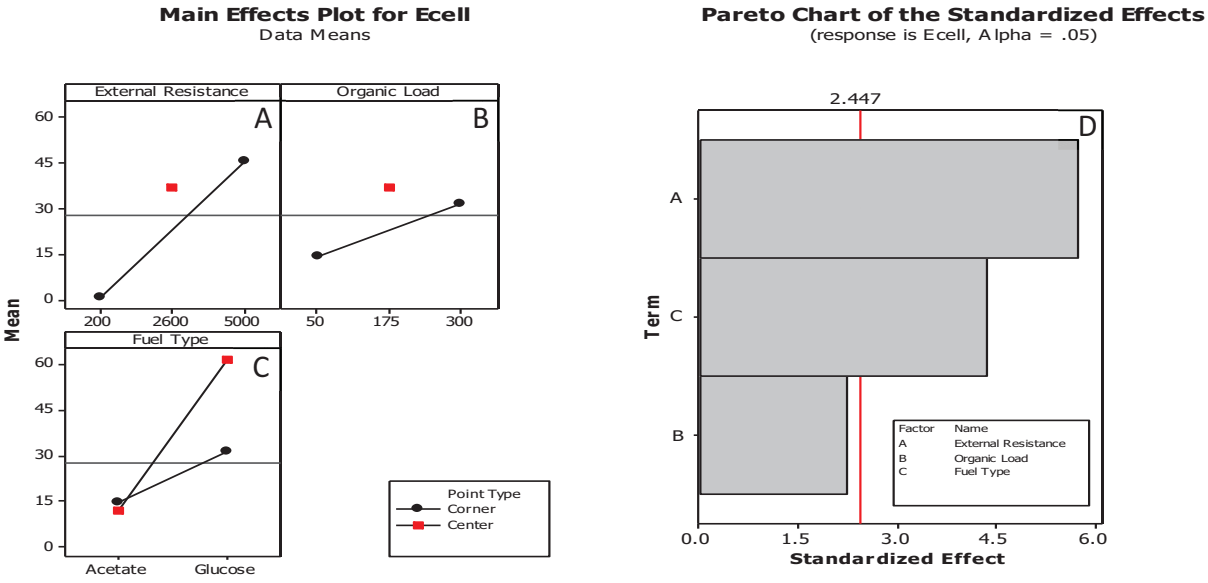

Figure 5.2. Main effects of the factors external resistance (A), organic load (B) and fuel type (C) on potential (E_{cell}) in MFCs. A Pareto chart (D) showing the significance of each factor on the response, potential (E_{cell}). The red line denotes alpha (α) set at 0.05 (equivalent to 95% confidence). If a bar crosses this line, the corresponding effect is deemed significant. Produced using Minitab® 15 statistical software package.

5.6.1 ELECTRODE POTENTIAL

The OCV of MFC operated under the different experimental conditions ranged from 238 to 479 mV (Table 5.4) The anode and cathode potential (E_{AN} & E_{CAT}) at open circuit of MFC 3 was determined using an Ag/AgCl reference electrode and was -204 & 32 mV. The recorded overpotentials for the cell, anode and cathode were 252, -142 & 38 mV respectively against a saturated Ag/AgCl electrode.

5.6.2 CONFOCAL MICROSCOPY

The mean anode biofilm thickness was determined by confocal microscopy (Table 5.5). The standard deviation was large (≥ 14%) in each instance (with the exception of anode 5). The anode biofilm thickness was similar for anodes 3 to 6 at around 140 µm but was lower for anode 2 (116 µm) and lower still for anode 1 (78 µm).

Table 5.4. OCV OF MFCS 1, 3, 4, 5, 7 & 8

	MFC 1	MFC 3	MFC 4	MFC 5	MFC7	MFC 8
OCV (mV)	248	301	479	277	282	238

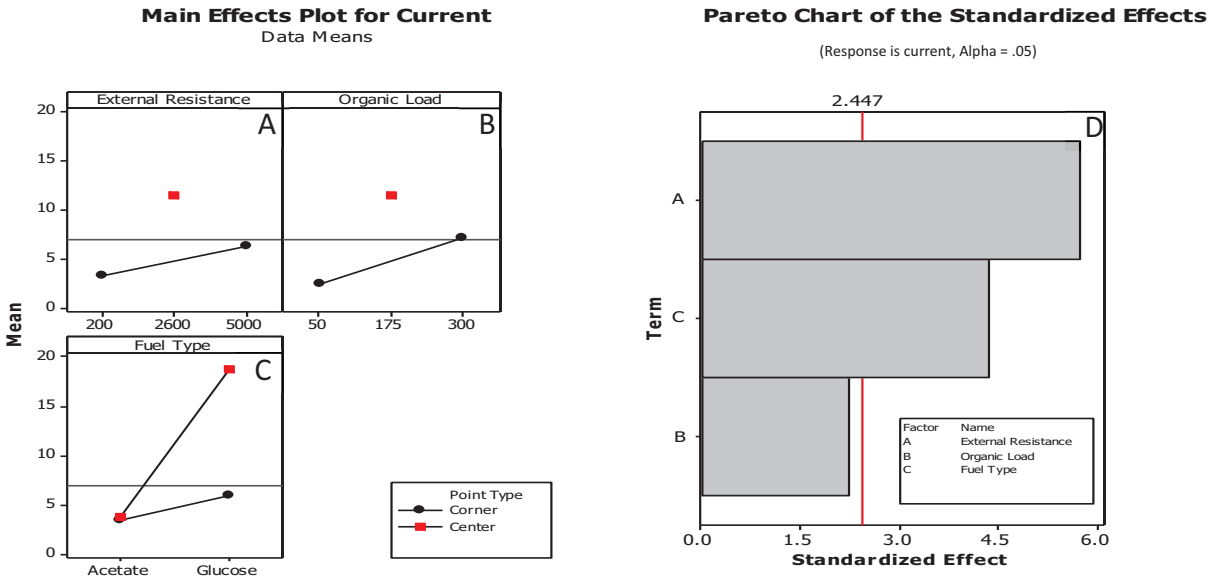

Figure 5.3 Main effects plots of the factors external resistance (A), organic load (B) and fuel type (C) on the response, current (I) in MFCs. A Pareto chart (D) showing the significance of each factor on the response, current (I). The red line denotes alpha (α) set at 0.05 (equivalent to 95% confidence) if a bar crosses this line then corresponding effect is deemed significant. Produced using Minitab® 15 statistical software package.

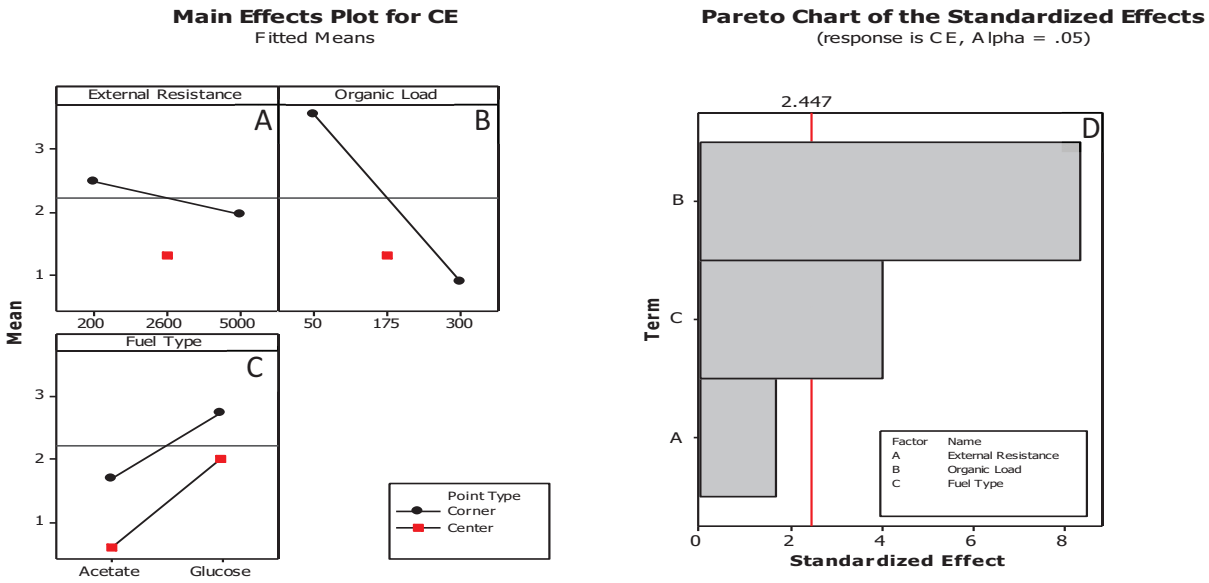

Figure 5.4 Main effects plots of the factors external resistance (A), organic load (B) and fuel type (C) on the response, coulombic efficiency (CE) in MFCs. A Pareto chart (D) showing the significance of each factor on the response, coulombic efficiency (CE). The red line denotes alpha (α) set at 0.05 (equivalent to 95% confidence) if a bar crosses this line then corresponding effect is deemed significant. Produced using Minitab® 15 statistical software package.

Table 5.5. Mean thickness of biofilm on anodes from MFCs 1-6 as determined by confocal microscopy. N= 4 except * n=3.

Anode	Fuel	Organic Load COD (mg L^{-1})	External resistance (Ω)	Mean biofilm depth (µm)
1	Glucose	50	200	78 (±27)
2	Acetate	50	5000	116 (± 31)
3	Acetate	300	200	141 (± 30)
4	Glucose	300	5000	140 (± 20)
5	Acetate	175	2600	137 (± 7)
6	Glucose	175	2600	146*(±32)

The ranked effect of organic load, external resistance and fuel type on biofilm thickness was organic load > external resistance > fuel type (Figure 5.5). As the magnitude of these effects, were below the value for α= 0.05, they did not have a significant effect on biofilm thickness.

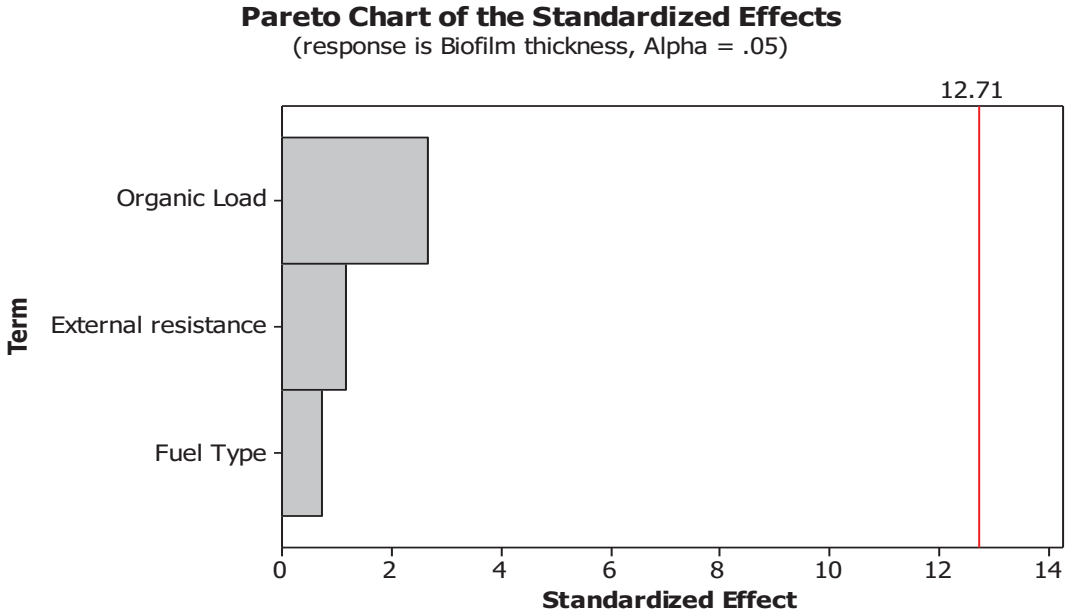

Figure 5.5 Pareto chart showing the magnitude of effect of each factor on biofilm thickness and its significance.

The anode biofilms from MFC 1 (R_{EXT} = 200 Ω, OL = 300 mg L^{-1}, FT = acetate) and MFC 3 (R_{EXT} = 5000 Ω, OL = 300 mg L^{-1}, FT = glucose) were stained using the LIVE/DEAD® BacLight™ bacterial viability stain to distinguish between live and dead cells visualized with a confocal microscope (Figure 5.6 & Figure 5.7). Total cell counts of each of the images in the Z plane (for both MFC 1 and MFC 3), revealed that the biofilm density peaks at approximately 60 µm from the anode surface (Figure 5.8 & Figure 5.9). The percentage of living cells in each Z plane for MFC 1 ranges between 22–66% (Mean = 49%, ± 25, n = 24) and for MFC4 the percentage of living cells ranges from 7–57% (Mean = 37%, ± 40, n = 24). In both MFC1 and MFC 3 the proportion of living cells in the anodic biofilm increases with distance from the anode surface (Figure 5.8 & Figure 5.9). In MFC 1 there is as a strong positive correlation between distance from the anode and the proportion of living cells (R^2 = 0.8) whereas for

MFC3 only a moderate correlation between distance from the anode and the proportion of living cells exists (R^2 = 0.4). This suggests that a large proportion of the anodic biomass is not partaking in the anodic reaction or that, if it is, the mechanism of electron transfer is mediated.

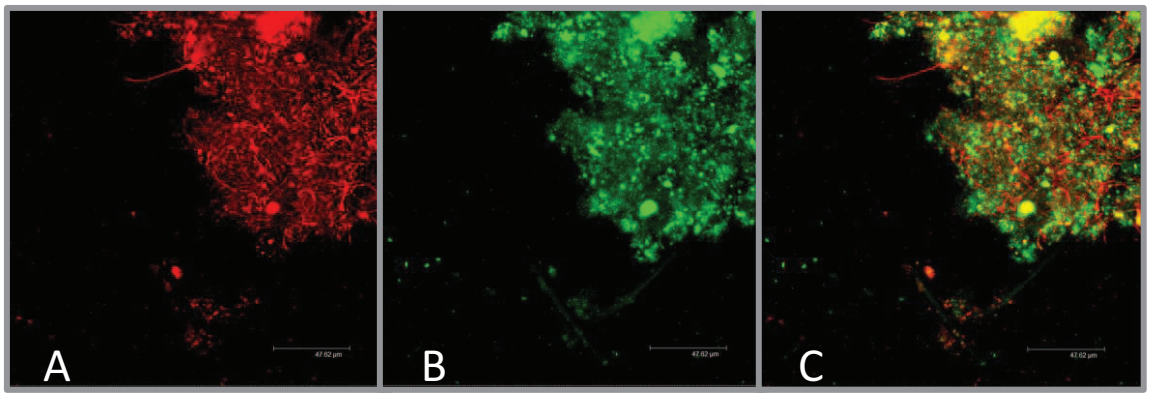

Figure 5.6 Overlays of 24 images of a biofilm from the anode of MFC 1 each taken in the z plane using CLSM microscopy showing red propidium iodide stained dead cells (A), living cells which have taken up the green SYTO 9 vital stain (B) and a composite of these two images (C).The images are taken as if looking down on the anode with cells in the foreground being the furthest away from the carbon cloth anode.

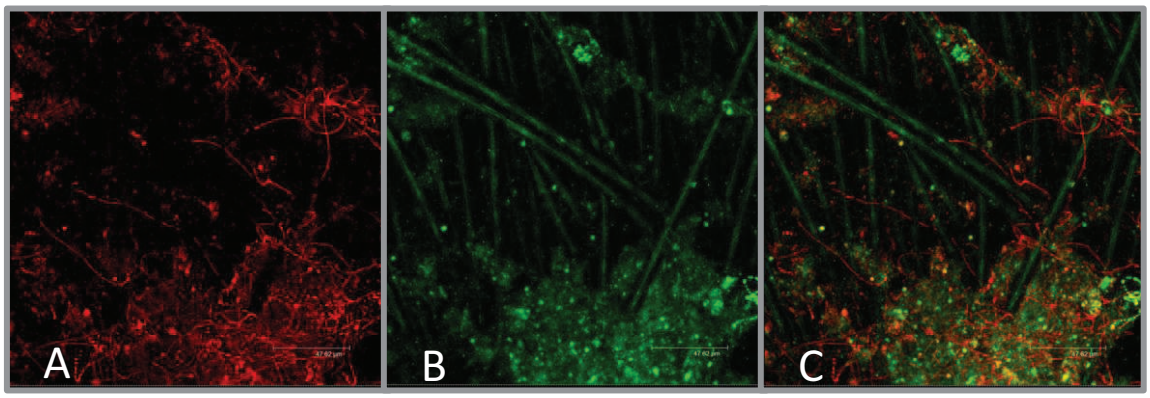

Figure 5.7 Overlays of 24 images of a biofilm from the anode of MFC 3 each taken in the z plane using CLSM microscopy showing red propidium iodide stained dead cells (A), living cells which have taken up the green SYTO 9 vital stain (B) and a composite of these two images (C).The images are taken as if looking down on the anode with cells in the foreground being the furthest away from the carbon cloth anode.

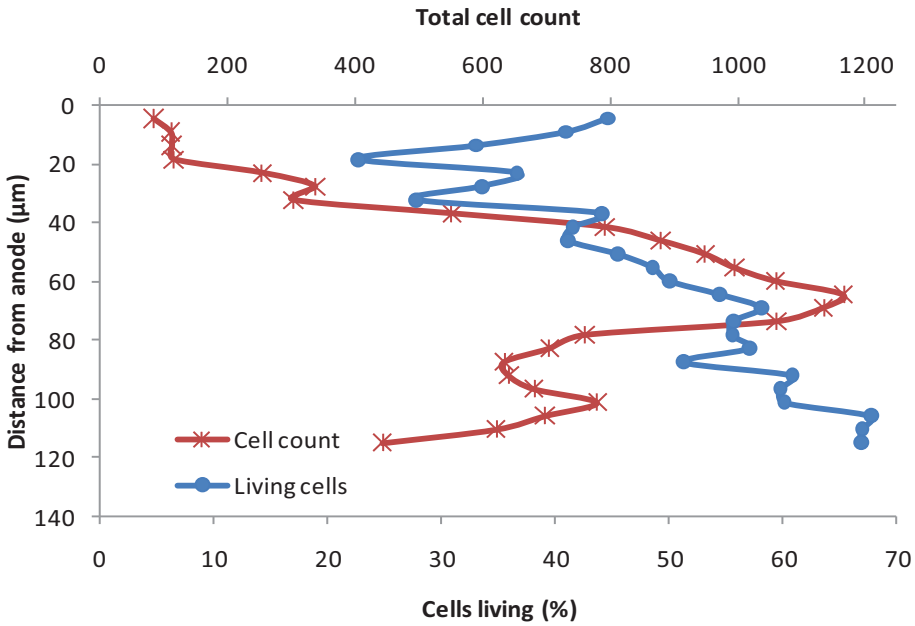

Figure 5.8 Anodic biofilm depth profile for MFC1 showing total number of cells in each z plane (red line) and the proportion of these which are living (blue line).

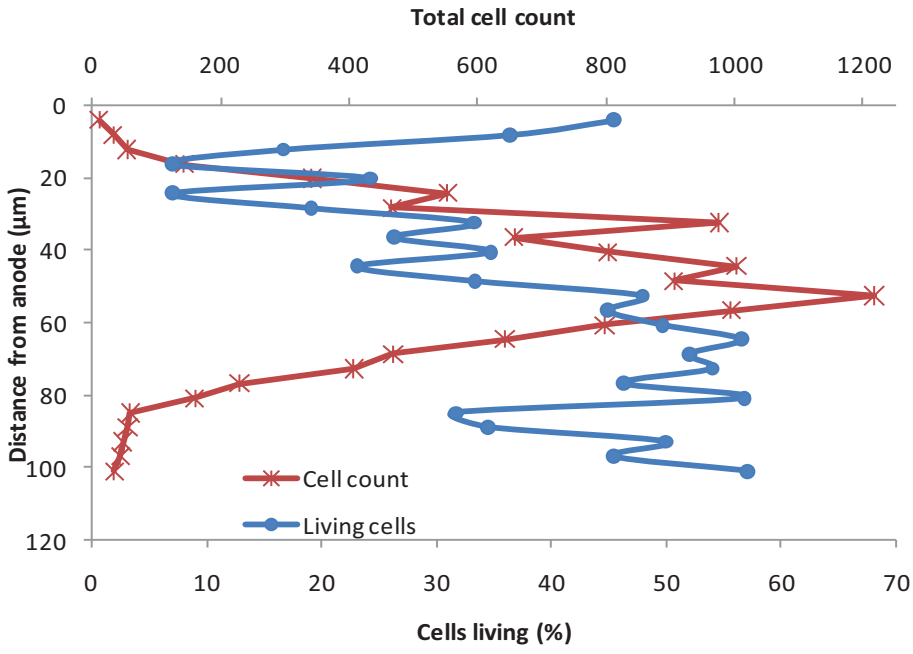

Figure 5.9 Anodic biofilm depth profile for MFC3 showing total number of cells in each z plane (red line) and the proportion of these which are living (blue line).

5.7 DISCUSSION

5.7.1 DESIGN OF EXPERIMENTS

The MFC performance metrics presented in Table 5.2 and Table 5.3 do not lend themselves well to casual comparison as they form part of a factorial array where direct comparison cannot be made between the corner point data (MFCs 1, 3, 4 & 5 are corner points) as they do not share the same values for each factor. The midpoints (MFCs 2, 7, 6 & 8) only vary in fuel type, with the setting for external resistance and organic load remaining constant. Comparing the mid points, glucose outperforms acetate as a fuel in all three metrics – the E_{cell} and current maxima are five times greater for glucose than acetate and the coulombic efficiency is about double. The lowest recorded cell potential of 1.03 mV was observed in MFC1, which operated under 200 Ω external resistance with acetate at 300 mg L^{-1}, conversely the highest E_{cell} of 64 mV was observed in MFC 3, which was operated with Glucose at 300 mg L^{-1}, and an external resistance of 5000 Ω (Table 5.2 and Table 5.3).

The factorial analysis yields more in depth information about the effects of each factor on the process outputs. For cell potential, the effect of external resistance was positive and monotonic. The relationship does not appear to be linear, however, and the majority of the effect of R_{EXT} on cell potential occurs between 200 Ω and 2600 Ω (Table 5.2A). At external resistance higher than 2600 Ω, the effect plateaus and future DoE studies should be limited to external resistances below 2600 Ω. This is much more likely to ensure a linear response from E_{cell} thus making it more useful output parameter for use in DoE techniques. The relationship between E_{cell} and R_{EXT} observed in this experiment (Figure 5.2A) is regular as E_{cell} is expected to increase with increased R_{EXT} as observed here (Logan 2008, Rabaey *et al.*, 2010). Theoretically, further increasing the external resistance should result in a linear increase in cell potential until the cell becomes polarized and $E_{cell} \approx$ OCV. In practice, the linear increase only occurs in the mid-range of external resistances as electrochemical losses prevail at the extremes of low current (when E_{cell} is high) or high current (when E_{cell} is low) (Logan, 2008; Rabaey *et al.*, 2010).

The effect of external resistance on current was non-linear and dynamic (Figure 5.3A) but the magnitude of the effect was not significant and external resistance exerted less of an effect on current than did fuel type or organic load. Most authors report a negatively linear relationship between R_{EXT} and current density in MFCs. This predictable and commonly observed relationship between R_{EXT} and current is described in Figure 2.3 (Bard & Faulkner, 2001; Logan, 2008; Rabaey *et al*, 2010; Harnisch & Schröder, 2011). The relationship between R_{EXT} and current presented in Figure 5.3A is unexpected because it does not conform to the negatively linear pattern described in Figure 2.3. The two points between 2600 Ω and 5000 Ω do appear to conform to the expected negative linear pattern and accordingly one may conclude that the point at 200 Ω is potentially aberrant. The non linear relationship observed in Figure 5.2 between R_{EXT} and E_{CELL} suggests that current is not an ideal process output for which to assess the effect of R_{EXT} using DoE techniques. Theoretically, the negatively linear relationship between (R_{EXT}) and current makes them ideal as a choice of factor and process output in DoE. Because the effect of R_{EXT} on E_{cell} is not as expected and because it is not statistically significant (Figure 5.2D) it is fair to conclude that the MFCs are not performing well and that it would be unwise to disregard current as a useful process parameter for assessing the effect of R_{EXT} in future DoE studies.

The positive, monotonic and non-linear effect of organic load on E_{cell} (Figure 5.2B), is in line with the predictions described by the Nernst equation. The concentration terms in the Nernst equation show that as the concentration in solution of a reduced species increases (equivalent to high organic load) then the reduction potential of that solution will become more negative. For these systems, being as the fuel is a constituent of the anolyte, a lower solute reduction potential will influence the anode potential (causing it to become more negative). Therefore, as the OL increases the anode potential will decrease resulting in a larger potential difference between the anode and the cathode and hence a higher $E_{cell.}$ Between the organic loads of 175 mg L^{-1} and 300 mg L^{-1} there is a decrease in cell potential (Figure 5.2B) which runs counter to the trend discussed above. Some authors have reported that the relationship between organic load and cell potential exhibits saturation kinetics as a function of substrate concentration which may account for the tailing off of the cell

potential at high organic load in Figure 5.2B (Catal *et al.*, 2008; Kim *et al.*, 2007). However, the effect of organic load on cell potential is not statistically significant so it is safe to conclude that organic load is not the main factor modulating E_{cell} and that the relationship between E_{cell} and organic load recorded in Figure 5.2B is incidental.

The effect of R_{EXT} on current appears to obey saturation although three data points are insufficient to delineate between first order and zero order kinetics (Figure 5.2B). Assuming the cathode is not limiting, the kinetics in a MFC depend on the rate at which the anode bacteria can oxidize substrate as well as the external resistance and mass transfer limitations, some of which will relate to the porosity, tortuosity and thickness of the anodic biofilm (Logan, 2008). Liu & Logan (2005) observed that half saturation constants for glucose in an MFC were higher when current transfer was high too and the relationship between glucose concentration and current obeyed saturation kinetics. It is not possible to demonstrate saturation kinetics in this study, but the effect of organic load on current (Figure 5.3B) appears to mirror the effect that external resistance exerts on current (Figure 5.3A) suggesting that a saturation effect at increased substrate concentrations at least partly defines this relationship. The Pareto chart (Figure 5.3D) shows that the effect of organic load on current is insignificant therefore the relationship revealed by the DoE analysis (Figure 5.3B) is likely to be a feature of these systems rather than a broadly applicable trend. There is a tendency of organic load to display saturation kinetics with current as organic load increases (Liu & Logan, 2004). Therefore, careful consideration of the concentrations for organic load before further DoE studies are undertaken is a necessary prerequisite for future DoE tests to ensure a linear response and better conformity to the requirements of DoE.

The effect of organic load on coulombic efficiency is monotonic, broadly linear and negative (Figure 5.3B). The relationship between organic load and coulombic efficiency is intuitive, and can be explained in terms of the biocatalytic capacity of the anode (Rabaey *et al.*, 2010). As the organic load increases beyond the catalytic capacity of the anode (saturation) the coulombic efficiency will decrease because a larger proportion of the substrate will be

available for competing processes (Figure 2.3). For coulombic efficiency to be a useful process output for assessing MFC performance in following DoE experiments the concentration settings for organic load should be selected to ensure, as far as possible, that a linear response for CE will is observed.

Fuel type is the only factor to have a significant effect on all three of the process outputs (E_{cell}, I and CE). The main effects plots for the effect of fuel type on E_{cell} (Figure 5.2C), current (Figure 5.3C) and coulombic efficiency (Figure 5.4C) are presented in a way that is unintuitive. By DoE convention, the effect is presented either as a 'corner point' (the combined mean effect of fuel type for each of the tests where the settings for R_{EXT} and OL where both high and low) or 'centre' points (the combined mean effect of fuel type for each test where R_{EXT} and OL where held at the midpoint). The effect of fuel type is similar for both E_{cell} and current – acetate elicits a smaller response than glucose and the effect of acetate on E_{cell} and current does not change much at either the corner or the centre points. The mean effect of glucose on E_{cell} and current, however, is greater at the midpoints than it is for the corner points. This observation is difficult to interpret although it has a simple mathematical explanation. Taking E_{cell} as an example, the centre point value for glucose of 32 mV (Figure 5.2C) is generated from mean E_{cell} values of 0.61 and 64.78 mV for MFC 3 (R_{EXT} = 5000 Ω, OL = 300 mg L^{-1}, FT = glucose) and MFC 4 (R_{EXT} = 200 Ω, OL = 50 mg L^{-1}, FT = glucose) respectively (Table 5.2). The value of 32 mV for the glucose corner point is much smaller than the centre point value of 60.9 mV which is the mean of MFCs 6 & 8 (R_{EXT} = 2600 Ω, OL = 175 mg L^{-1}, FT = glucose) presented in Table 5.2 because, simply, it is the mean of both the peak and the lowest output. An additional problem is highlighted by the fact that that E_{cell} appears almost completely unresponsive to changes in R_{EXT} and OL with acetate as a fuel (Figure 5.2C). However, this is not the case as MFC 5 (R_{EXT} = 500 Ω, OL = 50 mg L^{-1}, FT = acetate) shows a higher peak voltage (27.41 mV) than the peak voltage of 1.03 mV for MFC 1 (R_{EXT} = 200 Ω, OL = 300 mg L^{-1}, FT = acetate). Figure 5.2C leads one to conclude that MFCs fed with acetate do not respond to changes in R_{EXT} and OL. This is erroneous and stems from the fact that the mean E_{cell} for MFC 1 and MFC 5 is 14.22 mV (referred to as the corner in Figure 5.2C) which is similar to the centre point value of 11.52 mV (Table 5.2, Figure 5.2C).

The difficulty of using categorical factors for half-factorial DoE studies along with the fact that some effects can be masked in standard DoE analysis is clearly demonstrated above and needs to be taken into consideration for future DoE studies. Put simply, glucose outperforms acetate as a fuel as the effect of fuel type is greater at both the corner and centre points for glucose than for acetate for E_{cell}, I and CE.

Some of the outputs chosen for this experiment, E_{cell} and current, are unsuitable for factorial experiments under the range of factor settings investigated. However, all outputs are potentially useful as they conform to the requirements of a suitable process output under a particular range or suitable operational conditions. There are problems with choosing suitable ranges and conditions prior to starting DoE studies and the need for screening tests or, as in this case, fractional-factorial designs to inform future studies is crucial. Perhaps the best example to demonstrate this is organic load. Saturation kinetics have been described in MFCs for both E_{cell} and current in response to organic load and the observations made in the factorial analysis in this study are, therefore, unsurprising (Liu and Logan, 2005; Kim *et al.*, 2007; Catal *et al.*, 2008). This does not rule out using E_{cell} and current as a factor in future Design of Experiments approach, but emphasizes that care must be exercised when choosing the range of values used for the factors to ensure that a linear process output is observed under the conditions chosen. The conditions chosen here were conservative but realistic – i.e. 300 mg L^{-1} (COD) is within the lower range expected for domestic wastewater strengths (Mara, 2003). Another problem encountered in the DoE approach executed here is that some effects cannot be separated from one another caused jointly by the limitations of a half factorial design combined with selecting categorical factors such as fuel type rather than continuous ones. The limitations caused by the fractional design and the use of a categorical factor are exacerbated by nonlinear responses particularly in the case of acetate.

Aside from assessing the suitability of different factors for measuring process performance in MFCs, the factorial analysis highlighted three interesting observations:

- Poor performance of acetate relative to glucose
- Low operational cell potential and current

- An unexpected relationship between External Load and Current

Each is addressed in turn below.

5.7.2 PERFORMANCE RELATED TO FUEL TYPE

The fact that MFCs operated with acetate performed worse than those operated with the glucose is surprising. Many accounts in the literature show that MFCs operated with acetate generally perform better when compared with fermentable fuels like glucose (Logan 2008; Jung & Regan, 2011; Yuan *et al.*, 2010). The observations in this experiment run counter to the accepted notion that in MFCs, acetate outperforms glucose raising the question of why this may be the case. Logically, a sound basis supports the case for acetate being a better MFC substrate than glucose. Glucose is a fermentable substrate and its anaerobic conversion to simpler compounds (such as acetate) results in the release of energy that fermentative organisms use for growth (See Equation 5.6 - Equation 5.8 for an explanation). This energy, by definition, does not result in simultaneous reduction of the anode since the fate of the reducing equivalents used to drive ATP synthesis in fermentative respiration is the fermentation products themselves rather than the anode (Madigan, 2011). Furthermore, acetate is a significant electron donor in anaerobic systems including MFCs and can be respired directly with a range of electron acceptors including MFC anodes.

Oxygen diffusion across the membrane is common in single chamber MFCs (Axe *et al.*, 2009). Oxygen in the anode chamber will provide a sink for the degradation of acetate and aerobic organisms will be in competition with anaerobic organisms reducing the anode. In MFCs where oxygen is present in the anode chamber, aerobic acetate oxidation occurs to a greater degree than aerobic glucose oxidation suggesting that the anodic consortium can more effectively compete for glucose than acetate (Jung & regan, 2011). VFAs were not detected in the anolyte of any of the MFCs in this study the quantification limits of 0.08 mmol L^{-1}, which, along with coulombic efficiencies below 10%, is indicative of aerobic oxidation of substrate. The aerobic oxidation of acetate explains why current generation in the MFCs fed with acetate is low. For the glucose fed systems, any current generated above that of the acetate systems would logically come from electrons produced by the oxidation

of fermentation products other than acetate. The results quite clearly show that glucose outperforms acetate as the midpoint data, which are directly comparable and well duplicated, show an operational current of 19 mA for glucose and only 11.83 mA for acetate. Thus, glucose produced about twice as much current as acetate and, by extension, at least half of the current in the glucose fed MFCs is coming from electrons produced by the oxidation of other fermentation products such as hydrogen (Madigan, 2011). Another explanation is that glucose conversion is coupled to the reduction of the anode. This alternative explanation is unlikely and both Freguia *et al* (2008) and Jung & Regan (2011) reported that direct glucose oxidation coupled to the reduction of the anode is not the main degradation pathway in MFCs, the latter quantifying it as ≈ 10% of total current at current densities similar to those observed in this study.

In MFCs, the model of substrate degradation is analogous to that of methanogenic systems. In an MFC the availability of the anode as an electron acceptor is high at low external resistances and can support high electron fluxes (equivalent to high growth rates) which means electrogens can outcompete slow growing methanogens (Jung & regan, 2011). Interspecies hydrogen transfer is a mechanism whereby organisms converting fermentable substrates can maximize their energy gain by shifting their metabolism to hydrogen production in the presence of organisms that are able to consume hydrogen (Winter & Wolfe, 1980; Zhender, 1988; Madigan, 2011). The stoichiometric conversion of hexose sugars to acetate at a ratio of three to one is not an inevitable, intermediate catabolic-step in the anoxic degradation of sugars and hydrogen is a product of glucose fermentation. The molar yield of hydrogen per mole of hexose sugar is generally accepted as being 4 moles H_2/mol of glucose (Ren, 2007; Freguia, 2008) although theoretically it can be a yield of four, eight or twelve moles of hydrogen per mole of glucose. The higher yields are only possible if the partial pressure of hydrogen in the medium is kept low ($<10^{-4}$ atm) by syntrophic organisms otherwise the reaction becomes endergonic (Zhender, 1988). Oxidation of hydrogen at the anode is well documented in MFCs and the additional performance in the glucose fed MFCs can be explained by this mechanism (Ren, 2007; Logan, 2008; Mehta *et al.*, 2009). The possible stoichiometry of hexose sugar fermentation is given below:

$$C_6H_{12}O_6 \rightarrow 3CH_3COOH$$

Equation 5.2

$$C_6H_{12}O_6 + 2H_20 \rightarrow 2CH_3COOH + 2C0_2 + 4H_2$$

Equation 5.3

$$C_6H_{12}O_6 + 4H_20 \rightarrow CH_3COOH + 4C0_2 + 8H_2$$

Equation 5.4

$$C_6H_{12}O_6 + 6H_20 \rightarrow 6C0_2 + 12H_2$$

Equation 5.5

Adapted from Dolfing, J in Zehnder (1988) p433

Given the stoichiometry shown in Equation 5.2 to Equation 5.5 above, we can deduce that in comparable systems operated with acetate and glucose, performance should be comparable whatever the catabolic fate of the hexose sugar because the same number of electrons are involved in the oxidation of acetate (8) as in the oxidation of the equivalent molar yield of hydrogen (Equation 5.2–Equation 5.5). If however, the oxidation of acetate at the anode was a limiting step then, assuming the simultaneous oxidation of H_2 and acetate and a linear relationship between substrate and current, we could expect that for glucose fed systems current output would increase as stoichimoetry shifts towards hydrogen (moving from Equation 5.2 to Equation 5.5 above). In the systems under study for this chapter, given that double the amount of current flows in the glucose fed systems, it is likely that the stoichiometry in Equation 5.3 represents the breakdown of the proportion of glucose that accounts for current production and is the stoichiometry quoted by other MFC researchers (e.g. Ren, 2007). In methanogenic systems, the scenario represented in Equation 5.2 is often observed and is the result of syntrophic relationships between organisms; Freguia *et al.*, (2008) demonstrated the phenomenon of syntrophy as a mechanism of glucose oxidation in MFCs for the first time. There is good evidence for

syntrophic interactions in the systems under study in this chapter and it may explain why the performance of the glucose fed systems (MFCs 6 & 8) is double that of the acetate fed systems (MFCs 2 & 7). This is likely a result of either exclusive hydrogen oxidation or simultaneous acetate and hydrogen oxidation, and possibly the direct oxidation of glucose, at the anode of the glucose fed MFCs by electrogenic organisms. Both scenarios explain the additional performance and the consumption of hydrogen is indicative of syntrophy.

An alternative explanation is that the presence of organisms in the anodic community that utilise glucose modify the environment making it possible for electrogens to better oxidize substrate and reduce the anode, perhaps by limiting competition for fermentation products, because of a spatial relationship between species or the ability to create anaerobic microenvironments (Stams *et al.*, 2006; Jung & regan, 2011).

5.7.3 General performance considerations

The MFCs displayed overall poor performance with peak operational E_{cell}, current and Power ranging between 0.61 – 65 mV, 2.43 – 19 mA m^{-2}, and 0.07 - 59.25 mW m^{-3} respectively. Although other studies exist that report similar current densities (e.g. Lyon *et al.*, 2009; Katuri *et al.*, 2010) much higher current densities are possible and have been observed up to 10 – 15 A m^{-2} (Fan *et al.,* 2007). The maximum E_{cell} value of 65 mV in these tests is comparable but slightly higher than the maximum E_{cell} of 42 mV observed in MFCs inoculated with RAS in previous experiments (Chapter 3). Although in the DoE tests presented in this chapter, the maximum E_{cell} was obtained with a load of 5000 Ω compared to 1000 Ω in the RAS inoculated MFCs (Chapter 3) representing an overpotential of 145 mV for MFC3 (R_{EXT} = 5000 Ω; OL = 300 mg L^{-1}; FT = Glucose) in this study. The peak current is lower in these experiments than the peak current observed for the RAS inoculated systems presented in Chapter 3 (20 vs 35.5 mA m^{-2}). Power outputs in excess of 10-15 A m^{-2} have been documented (Torres *et al.*, 2009) and even studies not concerned with MFC optimization consistently report higher power densities (Fan *et al.,* 2007; Torres *et al.*, 2009). A possible explanation for the relatively poor power outputs observed in the systems

presented here may be insufficient colonization of the anode as a positive correlation between biofilm thickness and power output is usually observed (Logan, 2009).

Confocal micrographs show the biomass present on the anodes from MFC 1 (R_{EXT} = 200 Ω, OL = 300 mg L^{-1}, FT = acetate) and MFC 3 (R_{EXT} = 5000 Ω, OL = 300 mg L^{-1}, FT = glucose) Figure 5.6 and Figure 5.7 respectively. Both live (green) and dead (red) cells were present in approximately equal proportions in the biomass from the anode of MFC 1 (mean living cells = 49%) but, on average, there were less living cells in the biofilm from MFC 3 (mean living cells = 37%). The dead material appears to be oriented towards the anode and there is a positive correlation between the proportion of living cells and the distance from the anode surface exists (R^2 = 08 and 0.4 for MFC 1 and 3 respectively, Figure 5.8 & Figure 5.9). The anode material is stained non specifically by the SYTO 9 stain which can clearly be seen on the micrographs (Figure 5.6 & Figure 5.7). In Figure 5.7, the anode fibres are clearly seen stained green. This micrograph was taken after Figure 5.6 and suggests that the stain leeches into the anode over time even though the stained anodes were fixed in fresh medium. Logan *et al.*, (2006) showed a similar arrangement with live cells more distant from the anode although dead cells were more evenly distributed throughout the biofilm. Mclean *et al.* (2010) devised an optically compatible MFC configuration that allowed real time microscopy of developing anode biofilms. They observed that high current production was consistent with thin biofilms (≈ 5µm thickness) and that thick biofilms, which they described as having 'tower morphology' (>50 µm) produced lower peak currents and were associated with high external resistance. Conversely, Logan (2009) asserts that high power densities can only be maintained by 'thick biofilms'. The apparently conflicting observations by Mclean *et al* (2010) and Logan (2009) is testament to the fact that anodic biomass may vary between electrogenically active species that can successfully deliver electrons to the anode across a thick biofilm and an electrogenically inactive 'anodic clump' that is consistent with low current densities in MFCs operated at high organic load (Mclean, 2010; Katuri *et al.*, 2011). Figure 5.6 and Figure 5.7 along with Figure 5.8 and Figure 5.9 show that the majority of the living biomass was not in direct contact with the anode and may explain why the areal power densities were low. Nevertheless, Freguia *et al.* (2008) suggested that cell

proximity to the anode is important irrespective of the mechanism of electron transfer. Thick anodic clumps on the anodes of MFCs are consistent with high energetic gain from microbial metabolic activity as biomass growth is at the expense of coulombic efficiency (in cases where alternative electron acceptors exist) or energy efficiency in the MFC. Of note however, is that there appears to be no obvious differences between the topography of MFCs operated on acetate (MFC 1) or glucose (MFC 3). Both biofilms are around 120 µm thick regardless of the external resistance used and this is concordant with low current densities and high biomass growth.

At the lab scale, we can nurture electrochemically active biofilms that can deliver high power outputs up to 1.55 kW (Fan *et al.*, 2007a). Nobody has looked seriously at the stability of model biofilms over extended periods and in real wastewater applications. This is important for any MXC application whether it be power generation from wastewater in a conventional MFC or in an MEC producing a cathodic product. By definition, resident anodic biofilms that confer high power outputs in MFCs are being manipulated to live on thin margins in energetic terms as a large part of the free energy available from the oxidation of substrate is expended in driving the anodic reaction. In biologically open systems (such as WWT applications) these highly specialised biofilms will be subject to continuous assault from competing organisms that are resident in the influent wastewater or fuel and the long term effect this is likely to have on biofilm stability remains unknown (Woodcock *et al.*, 2007; Premier & Kim, 2011). An attempt was made in this study to use 'realistic' conditions and not manipulate the biofilm to a great extent. One of the limitations of these systems that contributed to poor operational cell potential, low current densities and poor CE may have been caused in part by an electrogenically immature biofilm as well as oxygen infiltration into the anode chamber (Chapter 6; Logan, 2010). Confocal microscopy of the anodes was unable to confirm the presence of a convincing anodic biofilm in close proximity to the anode (Figure 5.4) however, suggesting that poor biofilm formation is a likely contribution to overall poor MFC performance. Thus the ability to develop a stable biofilm in biologically open systems is imperative.

5.7.4 CURRENT

The observation that current was lower in systems operated under low external load is cause for concern as the converse is generally reported (Freguia *et al.*, 2008; Jung & Regan 2011). The relationship between current and external resistance should be inversely proportional (Figure 2.3). In the experiments presented here, a statistically significant relationship was not observed. The relationship between current and R_{EXT} at 2600 Ω and 5000 Ω appears typical, suggesting that low external load is responsible for the errant data and reduction of the anode is almost entirely arrested under these conditions. Furthermore, both the OCV and the operational potential of the cells in these experiments were low (≈ 250 mV & ≈65 mV (max) respectively). The open circuit anode and cathode potential for MFC 3 (R_{EXT} = 5000 Ω, OL = 300 mg L^{-1}, FT = glucose) was -7 and 229 mV against SHE respectively (measured as -204 and 32 mV against Ag/AgCl). The cell and anode overpotential was estimated at 142 mV indicating that the anode modulated E_{cell} with the cathode remaining relatively stable between 32 – 36 mV respectively at the range of current densities reported here (1.71 – 18.82 mA m^{-2}) and is also in keeping with the observations from other research (Katuri & Scott, 2011). It is possible to estimate the operational range for E_{AN} from the difference of the open circuit E_{CAT} and the maximum and minimum E_{cell}. The operational potential of the anode of MFC 3 (R_{EXT} = 5000 Ω, OL = 300 mg L^{-1}, FT = glucose) was estimated at approximately 160 mV against SHE and about 1 mV below the E_{CAT} (assumed to be more or less stable in the range reported here) for the MFCs with the lowest cell potential (MFCs 1 and 4 which were operated at 200 Ω) which explains the poor charge transfer capacity. The amount of energy that a microbe can conserve from a redox reaction is proportional to the difference between the reduction potential of the substrate and that of the terminal reduction apparatus in the organism's electron transport chain (Finklestein *et al.*, 2006). The higher this potential difference, the more Gibb's free energy that is available for anabolic processes. Therefore, anode potentials that are more positive are energetically favourable from the anodophile's point of view although this results in poor energy efficiency in an MFC. Anodic microorganisms can modulate the anode potential to maximize energetic gains and select for favorable thermodynamics (Finklestein *et al.*, 2006;

Logan, 2008, Wang *et al.*, 2009). The mechanisms that confer this property are poorly characterized but some microbes are capable of regulating the relative intercellular concentrations of reduced and oxidized redox species (Logan, 2008). Additionally, the large number of redox active cytochromes in some species of known electrogens – >70 for *G. sulfurreducens* and ≈ 39 for S.*oneidensis* (Humphrey-Smith & Hecker, 2006) – is a means by which some organisms can effectively control the potential at which the terminal redox exchange takes place (Wei *et al.*, 2010). The properties of redox species at the interfacial region of electrodes determines the potential of the electrode, therefore the ability of microbes to regulate the potential of their redox apparatus can regulate E_{cell} in an MFC (Bard and Faulkner, 2001).

The ideal state for microorganisms growing in an MFC, therefore, would be one of high electron flux (current) brought about by high availability of the anode at low external resistance. This is analogous to high current and an anode potential tending to positive potential. A low E_{cell} of 0.61 mV and 1.03 mV for glucose and acetate fed cells respectively was observed in MFCs operated under a low external resistance of 200 Ω (MFCs 4 & 1 respectively, Table 5.2). This corresponds to an estimated anode potential of around 230 mV against SHE. This initially suggests that the highest energy gain is available for these organisms but low current densities and coulombic efficiencies suggest that the anodic reaction is unfavorable under these conditions because the potential difference across the electrodes is not large enough to support sufficient charge transfer. Wei *et al.* (2010) suggested that the amount of energy and organism can gain from a redox reaction is limited by the upper potential of an organism's terminal electron donor. They observed an increase in biomass for an *G. sulfurreducens* in a two chambered MFC at anode potentials between -160 and 0 mV against SHE but not between 0 and 400 mV against SHE and concluded that that the upper limit of the terminal reductases in this organism was close to 0 mV against SHE. Aelterman *et al.* (2006) studied current output in mixed anodic consortia at poised anode potentials of -400, -200 and 0 mV against Ag/AgCl and observed that the consortium operated at -200 mV against Ag/AgCl (≈ 0 mV against SHE) produced the most current. Thus, both Aelterman *et al.* (2006) and Wei *et al* (2010) observe enhanced activity at anode

potentials close to 0 mV against SHE. The operational anode potential for MFC 3, for example, was approximately 160 mV when operated at 5000 Ω. The absence of a significant increase in cell or anode potential between 2600-5000 Ω suggests that a constraint on the maximum $E_{cell,}$ perhaps the presence of oxygen in the anode chamber, exists in these systems. The performance of the MFCs was considerably reduced when operated at 200 Ω, suggesting that the upper limit of the terminal redox apparatus in these MFCs is between 140-230 mV vs SHE. The oxidation potential of cytochrome C1 is 230 mV (Madigan, 2011; Weber *et al.*, 2006). Finklestein *et al.* (2006) showed that the microbial consortium in his benthic MFCs consistently maintained their potential at 35-55 mV more negative than the anode. This suggests the requirement of an electron gradient between the terminal electron donor and the receiving anode. Assuming cytochrome C1 is the terminal reductase in the system under study, electron transfer would not be possible even with small cathodic overpotentials. It seems therefore that an upper E_{AN} is reached whereby anodic transfer does not proceed because the R_{EXT} forces the anode potential close to that of the cathode and beyond the capabilities of the anodic consortia to regulate the anode potential. This may be responsible for the unconventional relationship between R_{EXT} and current observed in this study.

The reduction potentials of glucose, hydrogen and acetate are -428, -414 & -284 mV respectively (Logan, 2008; Torres *et al.*, 2009). The following Gibb's free energy is available for these substrates at an anode potential of 200 mV vs SHE:

	$\Delta G^{\circ\prime}$ $(KJ.mol)$
$C_6H_{12}O_6 + 6H_2O \rightarrow 6CO2 + 24H^+ + 24e^- \quad \Delta G^{\circ\prime}$	-1438
	Equation 5.6
$CH_3COO^- + 2H_2O \rightarrow 2CO_2 + 7H^+ + 8\,e^-$	-375
	Equation 5.7
$H_2 \rightarrow 2H^+ + 2e^-$	-118
	Equation 5.8

Thus for the direct oxidation of glucose 1438 kJ mol^{-1} is available for the microbe whereas the fermentative pathway (Equation 5.3) will yield two moles of acetate (2 x -375 KJ mol (Equation 5.7)) and four moles of hydrogen (4 x -118 (Equation 5.8)) resulting in 1222 KJ mol^{-1} available for the anodic reaction after the fermentation of glucose. The standard reduction potential of hydrogen (-414 mV) is lower than that of acetate (-284 mV) and more energy available from the oxidation of the molar equivalent of hydrogen than acetate (472 KJ for four moles of hydrogen versus 378 KJ per mole of acetate). Thus is a thermodynamically and energetically more favourable anodic substrate than acetate and further supports the idea of dual anodic reactions.

5.8 SUMMARY

The half-factorial experiment presented in this chapter was a useful screening exercise for that full-factorial experiment presented in chapter 6. In addition to the insights into the suitability of the factors and process outputs for DoE techniques, the study provided some useful insights into substrate degradation pathways and microbial interactions.

- The influence of each factor (R_{EXT}, OL, FT) on the process outputs (E_{cell}, I and CE) are as follows in decreasing rank order:
    - E_{cell}: R_{EXT}> FT >OL
    - Current: R_{EXT}> FT >OL
    - Coulombic efficiency: OL>FT> R_{EXT}

- The statistical significance of each factor varied depending on output. Fuel type was the only factor that had a statistically significant effect on all three process outputs ($E_{cell,}$ I and CE). In each case, the two factors exerting the greatest effect on each process output were significant. Thus, the statistically significant factors (α = 0.05) for each process output are given below:
    - E_{cell}: R_{EXT} and FT
    - Current: R_{EXT} and FT

  - Coulombic efficiency: OL and FT
- It was difficult to demonstrate the suitability of process outputs (E_{cell}, I and CE) with a linear response to either R_{EXT}, OL, FT however current demonstrated the least linear response to either external resistance or load. Fuel type is a categorical factor and thus the response cannot be assessed in terms of linearity.
- Glucose outperformed acetate. The maximum E_{cell} was five time greater for glucose than it was for acetate (60 mV and 30 mV respectively), maximum current was about five time higher for glucose fed MFCs than acetate (18.75 mA and 3.54 mA respectively) and coulombic efficiency was about 50% higher for glucose than it was for acetate (5.4% and 3.4% respectively).
- The half-factorial experiment was useful to inform future DoE studies:
  - Categorical factors complicate data analysis and future DoE studies should be limited to continuous factors
  - Acetate performed poorly relative to glucose and should be omitted from future DoE studies.
  - No significant changes in E_{cell} were observed between R_{EXT} values of 2600 – 5000 Ω. Future DoE studies will use a maximum R_{EXT} of 2600 Ω.
  - Although OL gave a non-linear response in all instances, the upper concentration of organic load (300 mg L^{-1}) represents the strength of only weak wastewater and therefore should remain in future DoE.
- There is evidence that both hydrogen and acetate (or only hydrogen) is oxidized by electrogens reducing the anode in glucose fed MFCs. This explains the enhanced performance of glucose relative to acetate in the system under study in this chapter.
- Operational current was lower in these systems at low external resistance than at high external resistance. This is counter to general observations.
- An upper operational anode potential of between 140-200 mV was identified. Under these redox conditions, hydrogen is a thermodynamically and energetically more favourable substrate than acetate for the anodic reaction.

5.9 CONCLUSIONS

The results presented in this chapter represented the first known use of DoE experiments in MFC research to date and yielded some novel insights that went beyond the expectations of the DoE technique as well as proving to be a useful basis for further DoE experiments. The finding that low current is observed at low cell potential is unexpected and worthy of further investigation and will be addressed using DoE techniques in Chapter 6. The findings in this chapter suggests that both acetate and hydrogen were contributing to current flow at the anode simultaneously and accounts for the unexpected observation that glucose fed MFCs outperformed those fed on acetate further demonstrating the versatility of the DoE approached in this chapter. Finally, the results suggest the redox potential of the terminal electron donors in these MFCs is between -140 and -230 mV against SHE which implicates C type chromosomes as the terminal reductases in the electron transport chain of the anodophiles.

6 A FULL FACTORIAL, DESIGN OF EXPERIMENTS STUDY TO EXAMINE THE INTERACTIONS BETWEEN ORGANIC LOAD AND EXTERNAL RESISTANCE IN MICROBIAL FUEL CELLS

6.1 INTRODUCTION

One rationale for the Design of Experiments (DoE) approach is that the technique yields information more efficiently (i.e. in fewer experiments) and reveals information hidden in one variable at a time (OVAT) experiments. DoE also confers a higher degree of certainty about the experimental findings than comparable effort in OVAT experiments. DoE techniques are suitable for exploratory, confirmatory and predictive experimentation (Antony, 2008). The main difficulty in DoE techniques is that at the design stage prior knowledge of the system is needed to successfully select suitable factors and the level at which they are set at in order to satisfy the assumptions central to the success of this technique – that the process outputs are linear, monotonic and easily measured. One way of overcoming this experimental requirement is to conduct screening experiments or fractional factorial designs to understand important process variables. Screening experiments allow a large number of variables to be examined but because there were only few controllable variables (X factors) in the MFC systems studied here (Figure 5.1), a half factorial experiment was chosen as the experimental screening strategy in Chapter 5.

For the success of DoE, ideal process variables should be, as far as possible, continuous and the process output should be linear. The data reported in Chapter 5 demonstrated that the process outputs did not give a linear response in the range chosen and for this reason the setting for some of the factors were modified slightly for the experiment presented in this chapter. The experiment in Chapter 5 also demonstrated the difficulty of working with categorical variables (i.e. Fuel type), which require more experiments for the same level of sensitivity. For example, the fractional factorial design used in Chapter 5 (using eight MFCs) was a resolution III design which cannot resolve interactions between main effects. Using the same number of MFCs with continuous variables only would have resulted in a resolution IV design and the experimental resolution between main effects and interactions would have been possible.

One of the central tenets of DoE studies is that they are iterative and that subsequent tests build on those they are preceded by (Antony, 2008). Full factorial designs using

continuous variables offer the highest degree of resolution and are able to readily distinguish between main effects and interactions between factors. An interaction occurs when the effect of one variable is dependent on the setting of another – i.e. when the mean response for a particular variable or factor is different at different settings of another factor (Antony, 2008). The effect of a two way interaction can be calculated thus:

$$I_{A,B} = \frac{1}{2}\left(E_{A,B(+1)} - E_{A,B(-1)}\right)$$

Equation 6.1

From Antony (2008)

The interaction (*I)* between two factors (A and B) is calculated as half the difference in effect (E) of factor A at the high level of factor B (+1) and the effect of factor A at a low level of factor B (-1). The effects and interactions between organic load (OL) and external resistance were investigated using a single fuel (glucose) and the results presented in this chapter.

The results from Chapter 4 and Chapter 5 indicate that O_2 infiltration through the membrane electrode assembly adversely affected MFC performance. Furthermore, in Chapter 5, the MFCs operated with acetate showed lower cell potential, current and coulombic efficiency compared with glucose (Table 5.2 & Table 5.3). The poor performance of acetate compared with glucose is likely indirect and symptomatic of sub optimal MFC conditions rather than the direct cause of poor performance as it is commonly shown that acetate generally gives rise to superior MFC performance when compared with non fermentable substrates (e.g. Velasquez-Orta *et al.*, 2011). Because of the poor performance of acetate relative to glucose, and the complications associated with using categorical factors in DoE studies, only glucose was used as a fuel in this experiment. In this study, the high setting of external load was changed from 5000 Ω to 2600 Ω because the observations from the fractional factorial analysis in Chapter 5 (Figure 5.2) indicated that there was little change in E_{cell} between external resistances of 2600 and 5000Ω. Whilst there was evidence of saturation at high organic load in the

experiments presented in Chapter 5 (Figures 5.2 – Figure 5.3) the high setting for organic load was kept at 300 mg L^{-1} for the full factorial DoE experiments presented in this chapter. This high setting of organic load (300 mg L^{-1}) was retained in these experiments for two reasons. Firstly, the choice of OL should remain realistic and represent wastewater strengths encountered in the environment. Wastewaters with strength lower than 400 mg L^{-1} are considered weak and therefore the upper limit of 300 mg L^{-1} seems reasonable and realistic (Mara, 2003). Furthermore, the non linear responses of E_{cell}, I and CE to organic load observed in the half factorial DoE study presented in chapter 5 (Figures 5.2 – Figure 5.3) are a combination of effects from both glucose and acetate. In this study it was expected that more linear response would be observed owing to the relatively higher MFC performance expected from glucose fed MFCs.

6.2 AIMS

The work in this chapter is a continuation of the work presented in chapter 5 the results of which have led to fuel type being disregarding as a factor and making adjustments to the settings of the factor, external resistance (R_{EXT}). The aim of the work in this chapter was to conduct a full factorial experiment using MFCs and to explore the effect that any interactions between organic load and external resistance have on MFC performance which are important in defining operational conditions for MFCs in field conditions.

6.3 OBJECTIVES

- Perform a full factorial experiment using glucose fed microbial fuel cells
- Explore interactions between organic load and external resistance on cell potential, current and coulombic efficiency
- Perform bacterial community analysis using DGGE analysis of 16S rRNA gene fragments to relate bacterial community structure to the influence of each factor
- Explore the data in its entirety as well as within the confines of factorial analysis in order to explain observations as fully as possible

6.4 HYPOTHESES

- External resistance is expected to have a strong and significant effect on E_{cell}, Current, and external resistance.
- Organic load is expected to have a strong and significant effect on all factors but to exert the biggest effect on current and coulombic efficiency.
- A full factorial design will reveal previously undisclosed interactions between external resistance and organic load in MFCs and their effect on E_{cell}, I and CE. These interactions will affect each process output to a different degree. There is likely to be a saturation effect of organic load at low currents that will be described by a significant interaction between R_{EXT} and OL for the process outputs I and CE in particular.
- The experimental design modifications presented here – using a full factorial experimental design along with the modifications to the factor settings (only using glucose in this experiment along with and smaller range of external resistance of 200 – 2600 Ω) – are likely to represent an experimental improvement. In particular, the relationship between current and external resistance is likely to follow the expected relationship of high current at low external resistance because of the enhanced performance expected from operating the MFCs with glucose.
- The microbial composition of the anodic consortia from the MFCs in this study will be heavily influenced both by organic load and the external resistance. Being as the external resistance is most likely to affect cell potential this will too exert the greatest effect on the anodic community. .

6.5 EXPERIMENTAL

The experimental procedures for this chapter are summarized below but can be found in more detail in sections 3.1–3.82.

Single chambered air-cathode MFCs (25 ml volume) were used in this study (Figure 3.1). The cathode was constructed as a membrane-electrode assembly that consisted of a gas

diffusion layer hot pressed between a Nafion 117® membrane and a carbon paper cathode with a final Pt catalyst loading of 0.3 mg cm^{-2}. The anode was made of plain carbon cloth. Both electrodes had a surface area of 12.5 cm^2. The electrodes were connected under load according to the factorial array outlined below (Table 6.1) and the drop in potential across the load was measured using a Pico ADC16 datalogger connected to a PC. Open circuit voltage (OCP) and half-hourly logging of E_{cell} was done using PicoLog software.

The fuel cells were set up and inoculated with Return Activated Sludge (RAS) from Spennymoor Sewage Treatment Works (Section 3.2.2). The original environmental sample was diluted 1:1 in sterile, artificial wastewater medium (pH 6.8) and amended from a sterile stock glucose solution to a working concentration of 50 or 300 mg L^{-1} (Section 3.3.3) according to the factorial array below (Table 6.1). Feeding was instigated at the nadir of the voltage curves and the MFCs were refuelled by removing the anolyte – some of which was preserved for later analyses – and replacing it with fresh medium. Electrochemical monitoring began after MFCs had acclimated to reproducible voltage between runs.

The organic matter concentration was measured as COD, using a commercially available COD kit (Merck, UK) on anolyte samples that were collected at the start and end of each experiment and filtered using a 0.2 µm syringe filter (Section 3.4.1).

Analysis of volatile fatty acids (VFAs) was performed on a Dionex ICS 1000 Ion Chromatograph system with Chromeleon® data acquisition software and an AS40 autosampler (Dionex, USA) (Section 3.4.3).

DNA was extracted from frozen anode suspensions, prepared from shaking anodes in a solution of ethanol and water (50/50 v/v), using a FastDNA® Spin Kit for soil. Bacterial 16S rRNA gene fragments were amplified from the DNA extract by PCR using primers 1 and 3 targeting the V3 region of the 16S ribosomal RNA gene (Muyzer *et al.*, 1993). The amplification of DNA of the correct length was confirmed by agarose gel electrophoresis.

The amplified DNA samples were loaded directly onto a 10% polyacrylamide gel with a 30–55% denaturing gradient and run for 900 volt hours at 60 °C in TAE buffer. DGGE gels were stained using SYBR gold and visualized using a Flour-S multiimager and Quantity One software. DGGE fingerprint analysis was carried out using the Bionumerics software package (Applied Maths Inc.) to generate a dendogram based on DICE presence/absence data and band intensity data for calculating Simpson's reciprocal index. Primer version 6 (PRIMER-E Ltd.) software package was used to generate NMDS plots from band intensity data imported from Bionumerics. Full details can be found in Section 3.5.2. Pairwise comparison of the ordinations in the NMDS plots was determined by Analysis of Similarity (ANOSIM) in using the Primer version 6 software package. Anosim generates an R statistic between 0 and 1. The null hypothesis can be rejected with increasing confidence the closer the R statistic is to 1.

Diversity of the anodic microbial community was calculated from band intensity data generated using Bionumerics software as Simpson's reciprocal index (1/D) according to:

$$D = \Sigma(\mathrm{n}/\mathrm{N})^2$$

Equation 6.2

Where n = the total number of organism of a particular species and N = the total number of organisms of all species.

The factorial design was generated in Minitab 15 statistical software package. A full factorial 2^2 design with resolution IV was generated using Minitab® 15 statistical software package and replication was achieved by running duplicate cells and repeating the experiment twice (Table 6.1). Statistical analyses were carried out using Minitab 15. The current and coulombic efficiency were calculated according to the formulae in Sections 3.71–3.75.

Table 6.1. Full factorial array showing the experimental set up.

Std Order	Run order	External resistance	Organic Load
7	1	2600	50
5	*2*	200	50
8	3	2600	300
6	4	200	300
1	5	200	50
4	6	2600	300
3	7	2600	50
2	8	200	300

6.6 RESULTS

6.6.1 ELECTROCHEMICAL OUTPUTS AND EXPERIMENTAL ARRAY

Cell potential ranges were between 2.14–60mV with higher E_{cell} observed in MFCs 3 and 6 where the settings for both organic load and R_{EXT} were high (OL = 300 mg L^{-1} COD, R_{EXT} = 2600 Ω; Table 6.2). Low external resistance (200 Ω) was associated with low cell potential as observed in MFCs 2, 4, 5 and 8 (Table 6.2) and there was little difference in E_{cell} (which ranged from 2.06 to 3.76 mV) between MFCs operated at low external resistance at either high organic load (MFCs 4 and 8, OL = 300 mg L^{-1} COD, R_{EXT} = 200 Ω) or low organic load (MFCs 2 and 5, OL = 50 mg L^{-1} COD, R_{EXT} =200 Ω). Current density ranged between 8.9 to 19.26 mA m^{-2}, the higher current densities were associated with high organic load (300 mg L^{-1} COD) and high external resistance (MFCs 3 and 6). Coulombic efficiencies ranged between 1.7–12.89 % and the highest coulombic efficiencies were observed in MFCs 2 and 5 which were operated with the combination of low organic load (50 mg L^{-1} COD) and low external resistance 200 Ω (Table 6.2). The means for the repeat experiments (Run 1 and Run 2) were calculated and used as inputs for the factorial analysis using Minitab 15 (Table 6.3). The data presented in this section are, on the whole reproducible. The relative standard deviation ranges between 4–6% for the duplicates in each run 9–17 % for the repeat runs showing that the reproducibility is high. The lower

reproducibility between runs is likely the influence of minor differences in substrate and variable ambient conditions between the two runs.

Table 6.2. Electrochemical data summary for MFCs 1–8.

	COD/Ω	MFC 1 50/2600	MFC 2 50/200	MFC 3 300/2600	MFC 4 300/200	MFC 5 50/200	MFC 6 300/2600	MFC 7 50/2600	MFC 8 300/200
Run 1	E_{cell} (mV)	34.57	2.06	59.27	3.76	2.23	62.60	32.56	3.59
	Current Density (mA m^{-2})	10.63	8.23	18.24	15.05	8.93	19.26	10.01	14.34
	Power Density (mW m^{-2})	18.39	0.85	54.04	2.83	1.00	60.28	16.31	2.57
	CE (%)	7.12	12.89	2.00	3.98	13.00	1.94	6.55	3.58
Run 2	E_{cell} (mV)	29.73	2.55	59.24	4.53	2.34	48.85	22.57	4.29
	Current Density (mA m^{-2})	9.14	10.19	18.23	18.12	9.348	14.93	6.94	17.18
	Power Density (mW m^{-2})	13.6	1.30	54.00	4.11	1.09	36.72	7.84	3.69
	CE (%)	5.34	15.89	2.03	4.60	13.00	1.77	4.21	4.46

Table 6.3. Factorial array showing outputs as mean values of duplicate fuel cells (standard deviation given in brackets). The array is presented in two blocks; block 1 includes MFCs 5–8 and block 2 is MFC 1–4. Both blocks were run simultaneously.

Std Order (MFC)	Run order	External resistance	Organic Load	E_{cell} (V)	I (mA m^{-2})	CE (%)
7	1	2600	50	33.57 (±1.42)	10.32 (±0.44)	6.83(±0.06)
5	*2*	200	50	2.15 (± 0.12)	8.58(± 0.50)	12.94 (±0.01)
8	3	2600	300	60.93 (± 2.36)	18.74(±0.73)	1.97 (±0.019)
6	4	200	300	3.67 (±0.12)	14.70 (±0.50)	3.77 (±0.073)
1	5	200	50	2.44 (± 0.15)	9.77 (±0.60)	14.44 (±0.14)
4	6	2600	300	53.89 (±7.56)	16.58 (±2.32)	1.90 (±0.10)
3	7	2600	50	26.15 (±5.06)	8.04 (±1.56)	4.77 (±0.17)
2	8	200	300	4.41 (±0.17)	17.65 (±0.67)	4.52 (±0.02)

6.6.2 Design of experiments analysis

The effect of both organic load and external resistance is considerable and positive (Figure 6.1A) with higher E_{cell} observed in microbial fuel cells operated at the high setting for both factors (R_{EXT} = 2600Ω, OL = 300 mg L^{-1}). There is an interaction between external resistance and organic load on E_{cell} which is shown by the divergence of the two lines on the interaction plot (Figure 6.1B). The interaction is such that the effect of organic load on E_{cell} is similar at both the high (300 mg L^{-1}) and low settings (50 mg L^{-1}) when the external resistance is also low (200 Ω) but a pronounced effect is evident when the external resistance is high (2600 Ω) with higher values for E_{cell} observed at the high setting for organic load (300 mg L^{-1}). This indicates that external resistance exerts a greater effect on E_{cell} than organic load (Figure 6.1A). Furthermore the effect of both external resistance and organic load on E_{cell} along with the interaction between them is statistically significant (Figure 6.1C).

Current density (mA m^{-2}) is greatly influenced by organic load and the effect is positive. External resistance has a small but moderately positive effect on current density (Figure 6.2A). However, there was only a weak interaction between the two factors demonstrated by a moderate difference in current density in MFCs operated at 200 or 2600 Ω for a given organic load (Figure 6.2B). Furthermore, current density was consistently higher when organic load was high (300 mg L^{-1}) (Figure 6.2B). This analysis indicates that organic load exerts a greater effect on current density than external resistance and that it was the only factor that exerted a statistically significant effect on current density. The effect of external resistance and the effect of the interaction between external resistance and organic load on current density was both small and not significant (Figure 6.2C).

The effect of organic load and external resistance on columbic efficiency was both large in magnitude and negative (Table 6.3A). There was an interaction between organic load and external resistance with the response for organic load converging at higher external resistance (Table 6.3B). Thus the difference in coulombic efficiency was greater between

high (300 mg L^{-1} COD) and low (50 mg L^{-1} COD) organic load when the external resistance is low (200 Ω). Conversely, the difference in response between the high (300 mg L^{-1}) and low (50 mg L^{-1}) setting of organic load was less (as is the overall response) when external resistance was high (2600 Ω).

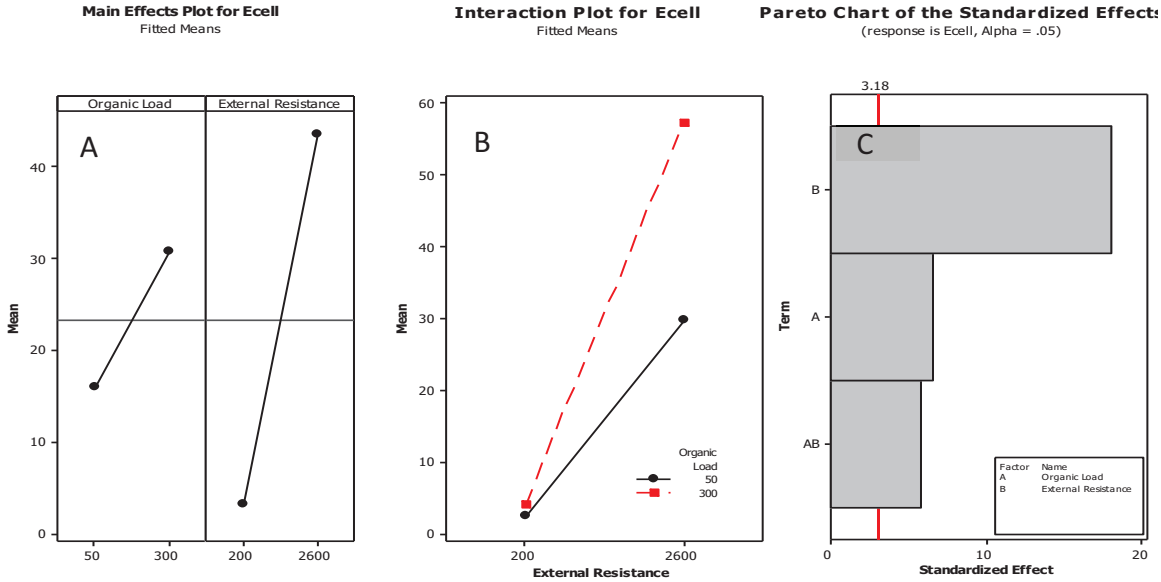

Figure 6.1 Factorial plots showing main effects plot (A) and interaction plot (B) of two factors organic load (300 & 50 mg L^{-1} COD) and external resistance (2600 & 200 Ω), on E_{cell}. The magnitude of each effect and the interaction between them and their statistical significance is shown in the Pareto chart (C). The red line on chart C denotes statistical significance (α = 0.05) and bars that cross the red line have a statistically significant effect on the process output.

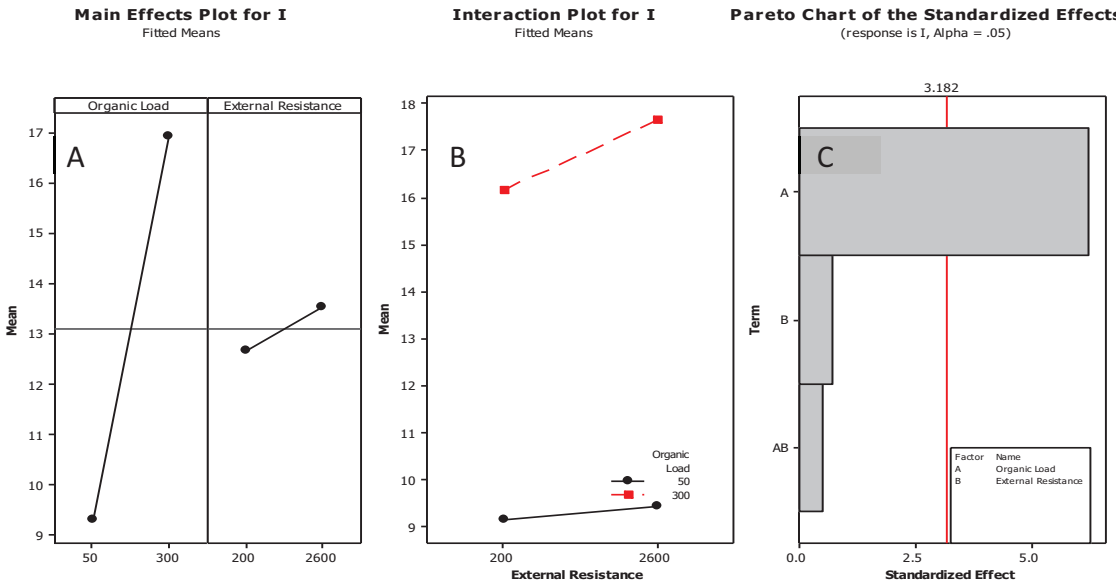

Figure 6.2 Factorial plots showing main effects plot (A) and interaction plot (B) of two factors organic load (300 & 50 mg L^{-1} COD) and external resistance (2600 & 200 Ω), on current . The magnitude of each effect and the interaction between them along with their statistical significance is shown in the Pareto chart (C). The red line on chart C denotes statistical significance (α = 0.05) and bars that cross the red line have a statistically significant effect on the process output.

6.6.1 Open circuit voltage and anode potential

The cell and anode open circuit potential of MFCs 1-4 only were determined. These were considered to be representative because of the good performance reproducibility in terms of E_{cell} and current density (generally >5% RSD, Table 6.3) and because they represented the full range of experimental conditions. The open circuit potential of representative MFCs from each set of conditions ranged between 266 and 293 mV (mean = 280 ± 13, n = 4) (Table 6.4). The anode potential ranged between -172 and -202 mV vs Ag/AgCl (mean = -191 ± 16, n = 4; Table 6.4) and -5 to 14 mV against SHE. The inferred cathode potential (OCP_{AN} + OCP_{CELL}) ranged between 81–95 mV vs Ag/AgCl (mean = 88 ± 6, n = 4; Table 6.4) and 289–292 mV against SHE. The highest E_{cell} was observed in MFCs operated with low organic load (50 mg L^{-1} COD) and the highest E_{cell} values at high organic

load (300 mg L^{-1} COD). A one way analysis of variance (ANOVA) showed that the influence of organic load is statistically significant on both the OCP_{cell} ($p = 0.02$, $df = 1$, $F = 49.39$) and OCP_{AN} ($p = 0.047$, $df = 1$, $F = 19.87$) where no statistical difference exists between R_{ext} and OCP_{cell} and OCP_{An} ($P = 0.978$ and 0.718 respectively).

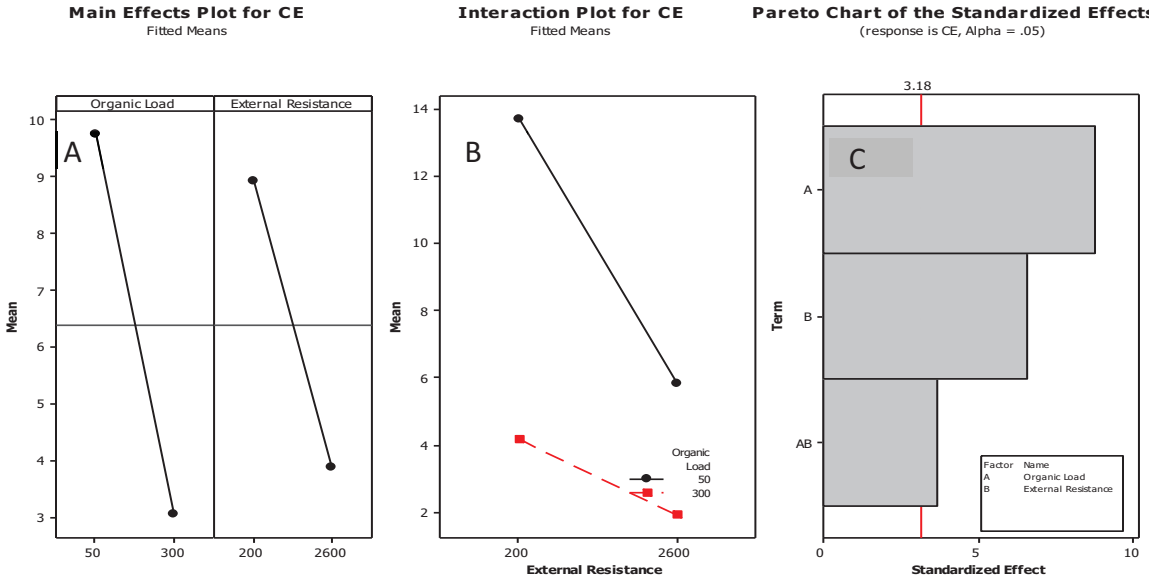

Figure 6.3 Factorial plots showing main effects plot (A) and interaction plot (B) of two factors organic load (300 & 50 mg L^{-1}) and external resistance (2600 & 200 Ω), on coulombic efficiency . The magnitude of each effect and the interaction between them along with their statistical significance is shown in the Pareto chart (C). The red line on chart C denotes statistical significance (α = 0.05) and bars that cross the red line have a statistically significant effect on the process output.

Table 6.4 Open circuit anode potential of MFCs 1-4 vs Ag/AgCl* and SHE†

MFC	Conditions (mg L^{-1}/Ω)	OCP_{AN}(mV)*	OCP_{AN}(mV)†	OCP_{CAT}(mV)*	OCP_{CAT}(mV)†	OCP_{cell}(mV)*
1	50/2600	-202	-5	92	289	293
2	50/200	-207	-10	81	278	289
3	300/2600	-172	25	95	292	266
4	300/200	-183	14	88	285	271

6.6.2 MICROBIAL COMMUNITY ANALYSIS

The composition of the bacterial community recovered from destructive sampling of anodes at the end of each experiment shows that community composition is influenced most by the organic load of the MFC. The dendogram (Figure 6.4) is based on a DICE presence absence matrix generated using the Bionumerics software. It is split into two main clusters: one comprised anode communities from MFCs fed an organic load of 50 mg L^{-1} COD and the other comprised anode communities from MFCs fed 300 mg L^{-1} COD. A third cluster comprised the inoculum community which was distinct from the samples taken from the anodes of the MFCs.

The communities subject to high organic load show greater diversity compared to those treated with low organic load. This is demonstrated by an average Simpson's reciprocal index (1/D) of 21 (± 1.63) and 16 (± 3.1) for the high and low organic load clusters respectively compared with a value of 27 for the inoculum.

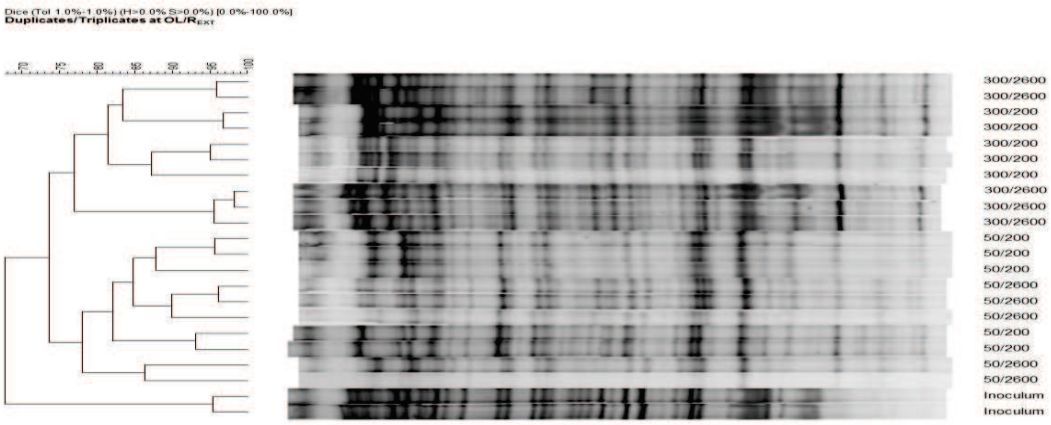

Figure 6.4. Dendogram based on presence/absence DICE analysis of bands and UPGMA cluster analysis generated from DGGE profiles of 16S rRNA genes using the Bionumerics software package. Two main clusters are apparent influenced by organic load with weak secondary clustering based on external resistance. The number to the right of the lanes represents the settings of the factors in the format 'organic load/external resistance' in mg L^{-1} COD and Ω respectively.

The Nonmetric multidimensional Scaling (NMDS) plots (Figure 6.5, Figure 6.6) are based on Bray-Curtis similarity matrices and confirm the grouping based on organic load observed in the dendogram above (Figure 6.4). In Figure 6.6A, the large green numbered circles represent high organic load (300 mg L^{-1} COD) and the small green numbered circles low organic load (50 mg L^{-1} COD), two ordinations can be clearly seen with the low organic load (50 mg L^{-1} COD) communities dominating the left of the plot and the high organic load (300 mg L^{-1} COD) communities dominating the right hand side of the MSDS plot. However, by overlaying R_{EXT} data on the NMDS plot in the similar fashion way, we can see that the high R_{EXT} (2600 Ω, large green circles) and the low R_{EXT} (200 Ω, small green circles) are distributed randomly on both sides of the NMDS plot (Figure 6.6B). The inoculum is less than 40% similar to the rest of the samples and, in general, duplicate and triplicate fuels cells typically had a similarity of 80% or more. The stress value for the ordinations in the MSDS plots is 0.17 which means that the general patterns observed in the data are not likely to be misinterpreted but too much emphasis should not be placed on the detail of the plot (Clark and Warwick, 2001). The ordinations shown in Figure 6.4 and Figure 6.6 are based on univariate Bray-Curtis similarity matrices and even though a significant stress value is generated, this is a global value of significance and does not apply to all the relationships in the sample. Pairwise relationships between samples within the MSDs plot can be tested for similarity using the R statistic generated from analysis of similarity (ANOSIM) (Clarke & Green 1988). All the relationships are statistically significant with a high degree of certainty ($R \geq 0.791$, significance = 0.1%) with the exception of 1) OL = 300 mg L^{-1} COD/R_{EXT} = 200 Ω vs OL = 300 mg L^{-1} COD/ R_{EXT} = 2600 Ω ($R = 0.414$) and 2) OL = 50 mg L^{-1} COD / R_{EXT} = 200 Ω vs OL = 50 mg L^{-1} COD / R_{EXT} = 2600 Ω ($R=0.366$). Essentially, this means that the ordinations on the left hand side of figure are likely due to chance (samples 4, 5, 9, 10, 11, 15, 16, 19 & 20) as are the ordinations between samples on the right hand side of the diagram (1, 2, 3, 6, 7, 8, 13, 14, 17 & 18) but the ordinations between the left and right hand side of the diagram based on organic load are of statistically significant.

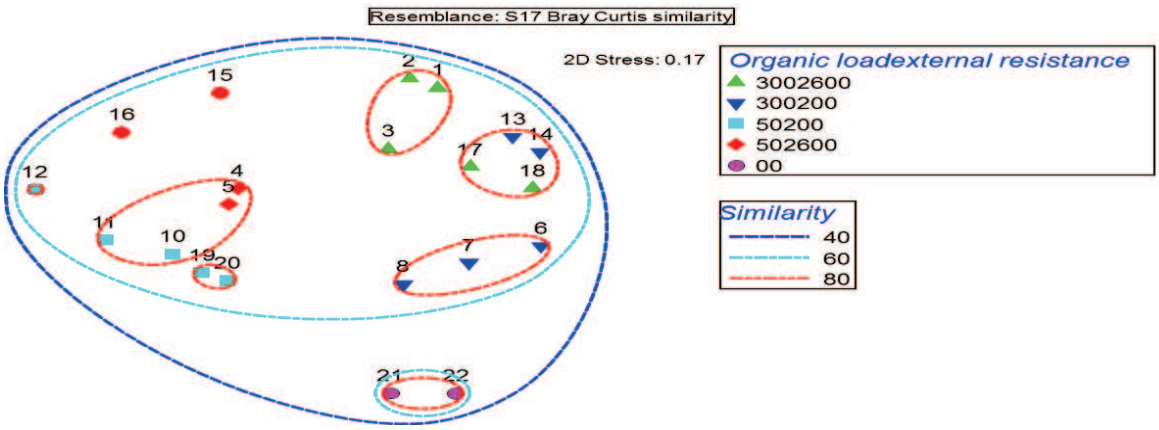

Figure 6.5 NMDS plot of the similarity between microbial communities recovered from the anodes of MFCs operated with different organic loads (50 & 300 mg L^{-1} COD) and external resistances (200 & 2600 Ω). Calculated using the Bray-Curtis similarity index from band intensity data of 16S rRNA DGGE profiles using the Bionumerics software package.

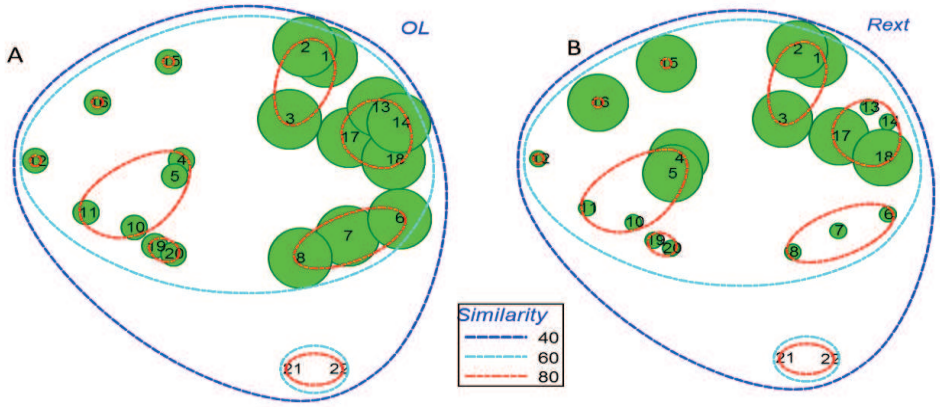

Figure 6.6 NMDS plots of the similarity between microbial communities recovered from the anodes of MFCs operated with different organic loads and external resistances showing the ordinations relative to organic load A, and R_{EXT}, B. Large green numbered circles denote the high setting of each factor (300 mg L^{-1} in plot A, and 2600 Ω in plot B) and the small green numbered circles the low setting of each factor (50 mg L^{-1} COD in plot A and 200 Ω in plot B). Calculated using the Bray-Curtis similarity index from band intensity data of 16S rRNA DGGE profiles using the Bionumerics software package.

6.7 DISCUSSION

6.7.1 GENERAL OBSERVATIONS

Current density ranged between 8–19 mA m^{-2} and the higher values were associated with high organic load. This observation is logical in that the substrate provides the source of electrons which allows current to flow and ultimately limits current. It does not necessarily follow that high organic load will lead to high peak current as current density is influenced by kinetic, operational (e.g. organic load, R_{EXT}), design (e.g. electrode spacing, electrode surface area) and biological features (e.g. biofilm density) of an MFC system. For example, current cannot be generated in an MFC at rates greater than bacteria can oxidize substrate and transfer electrons to the anode. This very much depends on the number and density of active electrogens at the anode surface, mass transport considerations (which may be influenced by electrode spacing and anolyte conductivity) and the influence of R_{EXT} and R_{INT} on anode potential and charge transfer capacities at the anode (Logan, 2008; Harisch and Schroder, 2010). The organic load, however, does govern the total theoretical charge that is available to the system and without sufficient substrate, high current densities cannot be sustained even if the internal conditions in and MFC are favourable (Logan, 2009; Rodrigo *et al.*, 2009). This is illustrated well in a study by Di Lorenzo *et al.* (2009) who showed a positive linear relationship between current and substrate concentration (COD) in an MFC BOD sensor between 0 – 350 mg L^{-1} COD. At COD concentrations greater than 350 mg L^{-1} COD the response plateaued probably due to saturation kinetics.

The unexpected observation of high current density at high external resistance that was noted in a previous experiment (Chapter 5) was observed once more in this set of experiments suggesting that this is a real phenomenon. From the results presented in Chapter 5, the unexpected relationship between R_{EXT} current was statistically significant and, although it was attributed to the high operational anode potentials, the poor performance of acetate as a substrate was thought to exert a dominant effect on the relationship between current and $R_{EXT.}$ In the experiments reported here the effect of

external resistance on current was small and not significant (Figure 6.2A) and need not be considered further.

External resistance and organic load both had a strong negative influence on coulombic efficiency. The largest coulombic efficiencies are observed at low organic loads. This is because increasing organic load above the biocatalytic capabilities of the anode will ultimately result in saturation and a proportional decrease in coulombic efficiency (e.g. Velasquez-Orta *et al.*, 2011). This can be overcome by increasing the surface area of the anode or the density of electrogens in the biofilm (Logan, 2008).

6.7.2 FACTORIAL ANALYSIS – CELL POTENTIAL

The factorial analysis confirmed that both organic load and external resistance have a statistically significant effect on E_{cell} and that there was an interaction between the two factors. The relative importance of the factors were external resistance>organic load>interactions between the two (Figure 6.1C). It was not possible to distinguish the magnitude of effects, nor an interaction, from the data presented in Table 6.1 and Table 6.2 and this could only be determined from the Pareto and significance plots generated from factorial experiments. In particular, without the factorial data analysis it was difficult to identify external resistance as having the dominant effect on E_{cell} as the effect is obscured by the large E_{cell} values observed at high organic loads but influenced to a greater extent by the very low E_{cell} values observed at the low external resistance. This is, in essence, the very definition of an interaction and this relationship would be ill defined or even hidden in regular OVAT experiments. The interaction between external resistance and organic load is such that E_{cell} is influenced to a greater extent by changes in organic load only when external resistance is high (Figure 6.1B). At low external resistance, E_{cell} is comparatively lower and is not responsive to changes in organic load.

Solution chemistry has a well described effect on electrode potentials which is described by the Nernst equation (Bard and Faulkner, 2001; Logan. 2008):

$$E_{AN} = E^{0\prime} - \frac{\mathrm{R}T}{nF}\ln(\Pi)$$

Equation 6.3

Where $E^{o'}$ is the reduction potential at standard biological conditions (pH 7 &, 298 K) R, the gas constant = 8.31447 J mol^{-1} K^{-1}; T, the temperature (K); n, the number of electrons transferred and F is Faraday's constant, 96485 C mol^{-1}, Π is the reaction quotient (Logan 2008).

The reaction quotient, Π, which is the ratio of the activity of the products to reactants raised to the power of their stoichiometric coefficients. The natural log of this expression is used in the Nernst equation meaning that the sensitivity of emf to changes in concentration is low. The $E^{o'}$ calculated from the concentration of glucose in these systems is -444 and -456 mV for glucose concentrations of 50 and 300 mg L^{-1} respectively, this is a difference of 12 mV or 2.6%. Whilst the absolute difference of 12 mV is more than the operational potential of some of the cells here, the Nerst equation is more useful when considering absolute thermodynamic limits at OCP (Logan, 2009). Given the values for OCP_{AN} in these tests ranges between -5 to 25 mV vs SHE , and there was a large anodic overpotential in these MFCs of 439 to 494 mV, it is likely that the chemistry of the anolyte due to changes in organic load, exerts only a minor effect on anode potential. This is consistent with the observations of Rodrigo *et al.* (2009) who did not observe differences in E_{cell} despite large differences in substrate concentration.

On this basis one can conclude that the largest influence on cell potential is external resistance which is unexceptionable. The secondary influence of organic load seems improbable given the large anodic overpotentials of around 450 mV mask the 12 mV influence calculated from the range of organic load in this study (50 and 300 mg L^{-1} COD). An alternative explanation, and also the basis for the interaction, is that the organic load exerts a large influence on the microbial community which in turn is able to influence cell potential. It is commonly documented, and indeed intuitive, that high densities of electrogens will confer superior MFC performance (Picioreanu *et al.*, 2007; Logan, 2009;

Logan *et al.*, 2009; Rodrigo *et al.*, 2009). This is inherently more likely at high organic loads which support the growth of higher biomass densities than low organic loads and, proportionately, higher number of electrogens. However, high organic load it is not though to specifically select for electroactive genera.

6.7.3 FACTORIAL ANALYSIS - CURRENT

Organic load had the greatest effect on current (Figure 6.2D) and it was significant. External resistance and the interaction between organic load and external resistance both had a minor and statistically insignificant effect on current (Figure 6.2A-C). This observation is logical as the electrons that flow in the circuit come from the oxidizing the organic substrate and without it there will be no charge transfer (notwithstanding the occurrence of endogenous metabolism resulting from the metabolism of stored fuel) (Chen *et al.*, 2010; Katuri & Scott. 2011). The absence of an interaction between organic load and external resistance on current, interesting though it is, is not likely to be universally observed in MFCs as changes in anode potential influenced directly by changes in external resistance will affect the capacity of the anode as an electron sink which in turn this will affect anodic charge transfer capacities and the rate at which a substrate can be consumed. The expectation was that the anode would act as a more efficient electron sink at low external loads allowing greater electron fluxes thus saturation effects would have been less apparent at low external resistance (Freguia *et al.*, 2008). A likely explanation for the absence of an interaction effect between organic load and external resistance on current (Figure 6.1B) is that the anode itself is limiting, perhaps because of an insufficient biofilm formation, thus charge transfer is impeded and saturation is reached even at low substrate concentrations. Therefore, increases in organic load above the charge transfer capabilities of the anode will not confer proportionately larger electron fluxes (He *et al.*, 2006; Jiang *et al.*, 20101).

6.7.4 FACTORIAL ANALYSIS – COULOMBIC EFFICIENCY

External resistance, organic load, and the interaction between them, had a significant effect on coulombic efficiency, (Figure 6.3C). The effect of both organic load and external

resistance on coulombic efficiency was strongly negative although organic load exerted a greater influence than external resistance on coulombic efficiency (Figure 6.3A). The relationship between organic load and coulombic efficiency is logical and it is reasonable to expect that coulombic efficiency decreases as organic load increases, particularly if substrate saturation of the anode is reached. The effect of external resistance on CE is negative because increases in external resistance reduce the rate of electron transfer to the anode resulting in a decrease in current (Freguia *et al.*, 2008; Harnisch & Schroder, 2010).

The interaction effect of external resistance and organic load on coulombic efficiency is such that MFCs operated at low organic load (MFCs 1, 2, 5 & 7) were more responsive to changes in external resistance than those operated at high organic loads (MFCs 3, 4, 6 & 8) and had a consistently higher coulombic efficiency (Figure 6.3B). The fact that higher CE was observed at low organic loads is understandable but the CE was higher in MFCs 2 and 5 (12.89 and 13.00 % respectively; Table 6.1) which were operated with the combination of low organic load (50 mg L^{-1} COD) and low external resistance (200 Ω). This in itself makes sense, however it is surprising in relation to the current density data. The higher CE means that more electrons have passed through the circuit of these MFCs yet the current densities for MFCs 2 and 5 (8.23 & 8.93 mA m^{-2} respectively) are lower than for MFCs 1 and 7 which were operated at and organic load of 50 mg L^{-1} COD and an external resistance of 2600 Ω (10.63 & 10.01 mA m^{-2} respectively). These values are, however, for peak current and the sustained low voltage of MFCs operated under 200 Ω and 50 mg L^{-1} (MFCs 2 & 5) results in moderate but sustained currents (over about 30-35 hours) and in turn higher net charge transfer than in MFCs operated under 2600 Ω and 50 mg L^{-1} (MFCs 1 & 7) that only attain meaningful currents (which occur at proportionately higher values of E_{cell}) only briefly (<8h).

6.7.5 MICROBIAL COMMUNITY ANALYSIS

The bacterial community analysis complemented the observations from the factorial analysis of the electrochemical data and demonstrated that the anodic bacterial

community composition was most strongly influenced by organic load. ANOSIM analysis demonstrated that the clustering of bacterial communities based on organic load was statistically significant (Figure 6.5 and Figure 6.6A, R= ≥ 0.791). By contrast there was no statistically significant clustering or ordination based on the external resistance of the MFCs (Figure 6.6B, R = ≤ 0.414). Furthermore, the microbial communities from the anodes of MFCs operated at high organic load were more diverse than communities sampled from the anodes of MFCs operated at low organic load. This was shown by the Simpson's reciprocal indices of 21 and 16 for the high and low organic load ordinations respectively.

Organic load was the only factor that significantly influenced all the electrochemical outputs tested here (E_{cell}, current density and coulombic efficiency) as well as being the main factor that influenced microbial community composition. This serves to confirm the assertion that the effect of organic load on E_{cell} (Figure 6.1A) is largely a result of the influence organic load exerts on the anodic community rather than a direct influence of the solution chemistry itself (discussed under Section 6.7.2 above). That there is no detectable difference in the microbial community structure between the anodic communities in MFCs operated at high and low external resistance shows that the mechanistic influence of external resistance on an MFC, which has a statistically significant effect on both cell potential and coulombic efficiency, has little effect on the microbiology of the MFCs or that the electrogenic actors in this instance are below the detection capabilities of the community fingerprinting technique (DGGE). Studies have examined the effect of a range of external resistances on the composition of anodic communities (e.g. Lyon *et al.*, 2009; Katuri *et al.*, 2010). In a study where MFCs were operated at five external resistances (0.1, 1, 10, 25, and 50 KΩ) a difference in anodic community composition was observed with 16S rRNA DGGE profiles converging into three groups: one operated at the lowest external (0.1 KΩ); the other comprising the anodic communities from MFCs operated at 10 and 25 KΩ and a final group from MFCs operated at 25 and 50 KΩ (Katuri *et al.*, 2010). Another study examined the anodic communities of MFCs operated at 0.01, 0.1, 0.47, 1 and 10 KΩ and found that the

community fingerprint profile of all anodic communities (using Ribosomal Intergenic Spacer Analysis (RISA)) was broadly similar regardless of external resistance with the exception of the anodic communities from the MFC operated at 10 KΩ (Lyon *et al.*, 2009). In a sense, both Katuri *et al.* (2010) and Lyon *et al.* (2009) support the observation reported in this study: that changes in the operational external resistance of an MFC do not always result in a change in anodic community especially at intermediate resistance or when the difference in R_{EXT} is small. The coulombic efficiency in these experiments was less than 15% which suggests that electrogenic organisms were a minor component of the anodic community. Being as there is suspected oxygen diffusion into the anode chamber and that the substrate used in these experiments is glucose, a significant proportion of the anodic community will at least comprise fermentative organisms and possibly aerobes too. Assuming the same electrogenic community is responsible for the range of MFC performance observed in the MFCs, the changes in diversity and abundance linked to organic load are not likely to describe the changes in the electrogenic community. This is also, quite obviously, the case if the abundance of electrogenic organisms is below the detection limits of this technique. Both Lyon *et al.* (2009) and Katuri *et al.* (2010) recognise that changes in the anodic community profiles may not reflect changes in the electrogenic genera in the MFCs both because of potentially low abundance of electrogens compared with the non electrogenic community and because no sequence data to confirm the identity of the organisms in question was obtained.

Despite there being no evidence for anodic community changes related to external resistance we can still assume that there is a biological influence on the operational anode potentials observed. The argument to support this are based on the fact that, solution chemistry is unlikely to control the anode potential in these systems (Section 6.7.2). It has been reported that organisms can control the potential at which electron exchange occurs by regulating the relative intracellular concentrations of reduced and oxidised redox enzymes (Logan, 2009). This mechanism allows organisms to respire at a wider range of potentials than the absolute potential of terminal oxidase that transfers electrons to the anode.

6.7.6 ELECTRODE POTENTIALS

The open circuit electrode potentials of the MFCs in this study range between -10 to 14 mV for E_{AN} and 278 to 292 mV for E_{CAT} against SHE (Table 6.1). The operational anode potential of the MFCs is, therefore, about 230 to 285 mV with the lower anode potential being associated with MFCs operated at high external resistance. The operational anode potentials were estimated from the difference between the mean operational E_{cell} (Table 6.3) and the cathode OCP (Table 6.4) which was assumed to be stable over the operational current range in this study (Katuri *et al.*, 2011; Section 5.7.4). The MFCs that performed the best (MFCs 3 and 6; 300 mg L^{-1} COD, 2600 Ω) had an operational anode potential of ≈233 mV against SHE. The MFCs operated at external loads less than 2600 Ω (and as a result, anode potentials higher than 233 mV) had comparatively low power outputs: 0.85 mW m^{-2} (min for MFC 2; 50 mg L^{-1} COD, 200 Ω) vs 62 mW m^{-2} (max for MFC 6; 300 mg L^{-1} COD, 2600 Ω). A similar, upper operational anode (of around 200 mV) was described in Chapter 5 and Katuri & Scott (2011) describe a 'broad redox wave' at 234 mV characteristic of electroactive biofilms. Thus there is convincing evidence that an upper anode limit of around 230 mV does exist and that this may be determined by the reduction potential of the terminal reductases of the anodic biofilms in this study. Interestingly 233 mV is also the standard potential for C-type cytochromes (Madigan, 2011).

The low cell potentials observed in MFCs operated at low external loads suggest that this upper limit of 230 is being reached or exceeded because the influence of the low external load is forcing the anode potential above 233 mV or too close to the cathode potential so as to inhibit the flow of electrons. The low cell potentials of the MFCs operated at low external resistance in previous experiments also resulted in low current transfer (Chapter 5, Table 5.3). This unusual relationship was not the case in this study and low cell potential and moderately sustained currents resulted in moderately higher charge transfer in MFCs operated at low external resistance (200 Ω) and low organic load (50 mg L^{-1}) than those operated at an equivalent organic load but with a higher external resistance (2600 Ω). In this sense, the performance of the MFCs reported in this chapter

appear to be operating more in line with convention than in the study reported Chapter 5.

There is undoubtedly a large overpotential at the anode of the MFCs presented in this chapter and the ones preceding it and this has been the assumption throughout this thesis. The thermodynamic calculations for organic load suggest anode potential of around -450 mV. From the measured mean open circuit E_{AN} value of -10 to 14 mV we can deduce that the anodic overpotential is in the region of 440 – 450 mV and may be explained by oxygen infiltration into the anode chamber. Based on the operational anode potentials, there is a further, operational anodic overpotential of between 230 – 285 mV. It is impossible to overcome all of anodic overpotentials in an MFC as the bacteria that drive anodic electron transfer need also to derive energy from the reaction. Freguia *et al.*, 2007 suggest that operational anode potentials of 200 mV are typical, an assertion that has been confirmed in this chapter and in Chapter 5 (Section 5.7.4). The standard potential of an air cathode is widely calculated as 805 mV (Logan, 2008) but the open circuit cathode overpotential of the MFCs in this study is about 285 mV and we can assume a large cathodic overpotential of 520 mV (805-285 = 520). This is generally attributed to the sluggish kinetics of the ORR and other thermodynamic losses (Harnsich and Schroder, 2010)

There are both large anodic and cathodic limitations in these MFCs. All overpotentials cause a reduction in cell potential but only some also cause a reduction in coulombic efficiency (Harnisch and Schroder, 2010). There is very likely to be large thermodynamic overpotentials (those which cause a potential loss only) at both the anode and cathode whereas the low CE observed in these cells (<16 %) is indicative of overpotential losses caused by processes that compete with electrode reactions. Likely processes include the diffusion of oxygen into the anode chamber and the production of hydrogen peroxide instead of water and the cathode. Operational overpotentials can be ohmic, or at high current densities, caused by transport and biocatalytic limitations but also because bacteria require energy for growth (Torres *et al.*, 2009; Harnsich and Schroder, 2010). The

latter relationship is defined by the difference in the reduction potentials of the electron donor (substrate) and the reduction potential of an organism's terminal reductase. Because there seems to be a definite upper limit in the anode potential in these cells, a large part of the operational anode potential (230–280 mV) may represent the proportion of respiratory energy available to the electrogens reducing the anodes of the MFCs in this study. Future work to characterise the nature of the potential losses and to devise ways to counter them along with investigating the energetic gains by the electrogens would be an interesting research direction.

6.8 SUMMARY

- The influence of each factor (R_{EXT}, OL) on the process outputs (E_{cell}, I and CE) were as follows in decreasing rank order:
    - E_{cell}: R_{EXT}>OL
    - Current: OL>R_{EXT}
    - Coulombic efficiency: OL> R_{EXT}
- A strong positive interaction existed between organic load and external resistance for the process output E_{cell} whereas the interaction between organic load and external resistance exerted a negative effect on coulombic efficiency. Only a moderate interaction between organic load and external resistance was observed in relation to current. The ranked magnitude of effect of the interaction between organic load and external resistance on each of the process output follows the order: E_{cell}>CE>I.
- The statistical significance of each factor varied depending on output. Organic load was the only factor that had a statistically significant effect on all three process outputs ($E_{cell,}$ I and CE). The interaction effect between external resistance and organic load was only significant for the process outputs E_{cell} and CE. The statistically significant factors ($\alpha = 0.05$) for each process output are given below:
    - E_{cell}: OL, R_{EXT}, and Interaction
    - Current: R_{EXT}

- Coulombic efficiency: OL, R_{EXT}, and Interaction

- The modifications to experimental design, informed by the results of the half factorial DoE study presented in chapter 5, represent a significant experimental improvement. The counter intuitive observation of high current at high external resistance, which was also observed in chapter 5, was shown not to be statistically significant for the experiment presented here (Figure 6.2A) and serves to add confidence in the choice of factors and the level at which they were set for this DoE study.
- Bacterial community analysis based on DGGE analysis of 16S rRNA gene fragments, showed that organic load had a greater influence on bacterial anodic community composition than external resistance.
- Organic load was shown to have a significant effect on cell potential but thermodynamic calculations show the effect of solution chemistry in terms of organic load to be negligible. The biology of the anode, which was heavily influenced by the organic load, is likely responsible for the effect of organic load on E_{cell} rather than the effect of organic load on cell potential itself.
- In addition to revealing the effect of interactions between factors, the use of DoE can reveal relationships not possible with OVAT experiments. In this instance, particularly the observation that external resistance exerted the dominant effect on $E_{cell.}$ Conversely, heuristic analysis of the data reveals findings that are not elucidated by DoE analysis, in this case the observation that peak electron transfer occurs at low external resistance was not evident from the factorial plots.
- An upper anode potential of around -230 mV was identified in this experiment. This is thought to represent the upper respiratory limit of the electrogens in the anodic community and is defined by the potential of their terminal redox enzymes.
- Large anodic and cathodic overpotentials exist up to around 500 mV. Whilst some of the overpotentials are thermodynamic in nature some result from competing

anodic and cathodic processes which is evident from the low recovery of electrons in these MFCs.

6.9 CONCLUSIONS

The full factorial DoE study presented in this chapter has yielded useful insights into the MFCs systems under study. The study describes the effect of organic load and external resistance, as well as the effect of interactions between them, on the process outputs cell potential, current and coulombic efficiency. Furthermore, the full factorial experiment was augmented by the findings of the half factorial DoE study presented in Chapter 5 which was intended as a screening study for this experiment. Refining the setting for external resistance and disregarding the use of categorical factors, specifically fuel type, offered improvements in the ability to analyze and interpret the data generated. This information is likely to be of use in developing a full understanding of MFC system under a range of conditions. It will inform operator choice in electing field settings when operational parameters in response to changing conditions such as reactor instability, changes in influent composition or when treatment performance is low. The data also show that the composition of the anodic community is dictated mainly by organic load rather than the external resistance which, in turn, had a substantial influence on MFC performance. Again, this will be of immense importance for MFC start up and biofilm maintenance in full scale. Evidence in this Chapter and in Chapter 5 point to an upper anode potential of 230 mV against SHE compatible with C-type cytochromes and which were the proposed terminal reductases of the electrogenic organisms reducing the anode of the MFCs in the experiments reported in Chapters 5 & 6. Knowledge of the absolute upper limits at which the anode can be reduced is, again, useful to avoid crashes in electrogenic populations inhabiting the mature biofilms of MFCs.

The unusual observation reported in chapter 5 - that the highest current density was observed in MFCs operated at high external resistance - was resolved by careful analysis of the data reported in this chapter and it appears that in instances when maximum peak current is not observed at low external resistances, sustained currents in MFCs operated

at low external resistance relative to MFCs operated at high external resistance result in overall greater current transfer.

7 CONCLUSIONS

7.1 CONCLUSIONS

The results presented in Chapter 4 clearly demonstrated an effect of inoculum on MFC performance and that MFCs operated with return activated sludge inoculum (RAS) performed much better that MFCs inoculated with anaerobic sludge. The experiments were performed with standardised inoculum and the relatively poor performance of anaerobic sludge, which is usually considered as a model inoculum for MFCs, suggests that the relative abundance of electrogens in anaerobic sludge may be low compared with the other inocula used in this study. This has important implications both experimentally and practically in MFC applications and means that inoculum choice is an important consideration when seeding, or perhaps more importantly, reseeding MFCs in field situations in times of biofilm instability because inoculum characteristics will determine the amount of seed material required and the duration of enrichment times. Using standardised inocula in these tests was a useful experimental innovation and has implications in MFC research. Where biomass effects may confound experimental results in MFC studies, standardising biomass according to the methods in Chapter 4 is strongly recommended. The treatment efficiencies of the MFCs presented in Chapter 4 was high (≈80%) and the effluent quality was within guidelines set by the Wastewater Treatment Directive (91/217/EEC), furthermore treatment efficiencies of 80% would mean that MFCs such as the ones used throughout this thesis could be used to treat wastewaters with a strength of up to 600 mg L^{-1} COD in a single step process. Because of the high treatment efficiencies, MFCs still hold promise as WWT treatment technology provided a low cost design can be developed.

The results presented in Chapter 5 represent a screening study to assess the suitability of fuel type (acetate and glucose), external resistance (200, 2600 and 5000 Ω) and organic load (50, 175, 300 mg L^{-1}) for the DoE approach presented in the subsequent chapter. Acetate was associated with poor MFC performance relative to glucose which was surprising given that acetate is usually observed to perform better as a fuel compared with fermentable substrates. The possible reason for the poor performance of acetate

relative to glucose is that glucose can be converted to acetate and hydrogen in anaerobic systems and offers the potential for dual anodic reactions (acetate and hydrogen oxidation) to occur simultaneously thus boosting the current production in MFCs operated with glucose under limiting conditions and in possible competition with oxygen. While it may not be practical to control the composition of waste streams in field situations, insights into the way different fuel types induce different responses in MFCs are important to ensure that MFCs are only used in appropriate field situations and in aiding knowledge based selection of operational parameters such as external load.

Moving on from the screening study presented in Chapter 5, a full factorial DoE study was adopted to look at any interactions between organic load and external resistance and their effects on cell potential, current density and coulombic efficiency. Organic load had a dominant effect on cell potential which was likely an indirect effect caused by the influence of organic load on the anodic microbial community structure rather than a result of a thermodynamic influence of increased fuel concentration. This is of enormous practical importance in field situations as the strength of wastewater is likely to be variable and therefore the potential for organic load to influence the electrogenic microbial community structure in MFCs exists. The long term effects of variable fuel concentration on anodic community structure along with any subsequent effect this may have on MFC performance needs to be thoroughly investigated. Statistically significant interaction effects between organic load and external resistance on coulombic efficiency and cell potential were observed. At low external resistance changes in organic load had less of an effect on cell potential than changes in organic load did at high external resistance and the converse was true for coulombic efficiency. Controlling the organic load of wastewater is not likely to be practical in real world applications, and in this sense, the use of organic load as a factor in MFC experiments is analogous to understanding the dynamic response of MFCs in field situations to changing wastewater strengths. Fully understanding the interactions between factors such as organic load and external resistance and their effect on MFC performance will allow full operational

control of MFCs by allowing optimal selection of operational parameters in response to changing conditions.

Poor performance in all of the systems presented in this thesis was noted and characterised by both large cathodic and anodic overpotentials. The large anodic overpotential at open circuit conditions is likely to be the result of oxygen infiltration into the cathode chamber. MFCs using liquid catholytes (such as ferricyanide) were not used in this study because of a desire for realistic operating conditions. With hindsight, using ferricyanide as a laboratory convenience to describe the fundamental relationships between MFC operational parameters may have been a good starting point for this research as it would have eliminated the problem of oxygen diffusion across the cathode.

The findings presented in this thesis are undoubtedly very useful and, because of their reproducibility, are representative of systems under study. While it was never the aim of this work to optimise MFCs for performance, the question remains as to the general applicability of the findings to a range of MFC systems. The techniques presented here (in particular the inoculum standardisation method and the DoE approach) have proven themselves to be useful research tools and experiments using optimised systems should be carried out. The DoE approach, in particular, holds much promise as tool for describing novel behaviour in MFCs.

8 FUTURE WORK

8.2 FUTURE WORK

The results presented in Chapter 4 clearly illustrate the importance of inoculum type, particularly in relation to start up or enrichment times, on MFC performance, and the practical implications of this have been discussed. The most likely explanation for the observed differences in MFC performance presented in Chapter 4 is the natural abundance of microbes that are capable of reducing the anode in each particular inoculum with the caveat that with the current data it is impossible to rule out that methodological procedures may have influenced the microbial composition of the inoculum nor that natural mediators present in the inocula could have been responsible for the enhanced performance. Even though we suspect that the abundance of electrogens in the inoculum sources used in Chapter 4 were responsible for the differences in MFC performance reported in that Chapter, we still have no away of assessing this directly. Therefore a natural progression from the work presented in Chapter 4 would be, after ruling out any methodological effects or the confounding presence of mediators, to devise an assay for assessing the electrogenic activity of an inoculum. This will allow precise knowledge of how much inoculum to use and when to achieve a particular effect in MFC research and development.

Another interesting observation discussed in Chapter 4 is the evidence for different mechanisms of electron transfer to the anode (direct vs mediated). Whether or not there are different mechanisms of electron transfer to the anode as a function of inoculum could easily be confirmed with microscopic techniques.

One aspect that has overshadowed this work is the poor electrochemical performance of the MFCs which raises the question of the wider applicability of the observations presented in this thesis. For this reason it would be prudent to repeat the experiments presented here in this thesis using a liquid catholyte (such as ferricyanide) to overcome the large cathodic overpotentials that contributed to poor MFC performance. This would be particularly useful for the DoE experiments to add confidence to the findings and ensure their wider applicability.

Whilst there are many challenges to the scale up of MFCs they remain an attractive technology not only because of the high rewards associated with success but simply because they are a deeply fascinating technology. Much of the current advances in MFC technology are diverging from initial clean energy targets to diverse areas such as bioremediation and novel cathodic products into a discipline that would more rightly be called electromicrobiology. It is this area where we can expect the field to blossom over the next decade and where the most exciting discoveries are likely to be made. A burgeoning area in electromicrobiology to watch is the development of transmembrane electron transfer molecules or molecular wires. These are conjugated oligoelectrolyte molecules which can self assemble into microbial membranes and enhance exocellular electron transfer and are likely to stimulate the advances in the MXC field.

REFERENCES

Abrevaya, X. C., Mauas, P. J. D., and Corton, E., 2009, Microbial Fuel Cells Applied to the Metabolically Based Detection of Extraterrestrial Life: Astrobiology, v. 10, no. 10, p. 965-971.

Aelterman, P., Freguia, S., Keller, J., Verstraete, W., and Rabaey, K., 2008, The Anode Potential Regulates Bacterial Activity in Microbial Fuel Cells: Applied Microbiology and Biotechnology, v. 78, no. 3, p. 409-418.

Aelterman, P., Rabaey, K., Pham, H. T., Boon, N., and Verstraete, W., 2006, Continuous Electricity Generation at High Voltages and Currents Using Stacked Microbial Fuel Cells: Environmental Science & Technology, v. 40, no. 10, p. 3388-3394.

Allen, M. R., Bennetto, H. P., 1993, Electricity Production from Carbohydrates: Applied Biochemistry and Biotechnology, v. 39, no. 40, p. 27-40.

Allen, R., and Bennetto, H., 1993, Microbial Fuel-Cells: Applied Biochemistry and Biotechnology, v. 39-40, no. 1, p. 27-40.

Antony, J., 2008, Design of Experiments for Engineers and Scientists, Oxford, Butterworth-Heinemann (Elsevier), 152 p.

Axe, J., Billmyre, R. B., Duty, K. H., Hitz, G., Trager, L., and Weatherford, A., 2009, Harvesting Life's Energy: Increase in the Aerotolerence of the Electrogenic Anaerobe Geobacter Sulfurreducens Due to over-Expression of Superoxide Dismutase and Catalase: Gemstone Team Research.

Bard, A. J., and Faulkner, L. R., 2001, Electrochemical Methods: Fundamentals and Applications, Wiley.

Bennetto, H. P., Stirling, J. L., Tanaka, K., 1985, Reduction of 'Redox' Mediators by NADH and Electron Transduction in Biolelectrochemical Systems: Chemistry and Industry, p. 695-697.

Berk, R. S., and Canfield, J. H., 1964, Bioelectrochemical Energy Conversion: Applied and Environment Microbiology, v. 12, no. 1, p. 10-12.

Berney, M., Hammes, F., Bosshard, F., Weilenmann, H.-U., and Egli, T., 2007, Assessment and Interpretation of Bacterial Viability by Using the Live/Dead Baclight Kit in Combination with Flow Cytometry: Applied and Environment Microbiology, v. 73, no. 10, p. 3283-3290.

Bond, D. R., Holmes, D. E., Tender, L. M., Lovely, D. R., 2002, Electrode-Reducing Microorganisms That Harvest Energy from Marine Sediments: Science, v. 295, p. 483-485.

Bond, D. R., Lovely, D. R., 2003, Electricity Production by *Geobacter sulfurreducens* Attached to Electrodes: Applied and Environmental Microbiology, v. 69, no. 3, p. 1548-1555.

Borole, A. P., Hamilton, C. Y., Aaron, D. S., and Tsouris, C., 2009, Investigating Microbial Fuel Cell Bioanode Performance under Different Cathode Conditions: Biotechnology Progress, v. 25, no. 6, p. 1630-1636.

Bullen, R. A., Arnot, T. C., Lakeman, J.B., Walsh, F.C., 2006, Biofuel Cells and Their Development: Biosensors and Bioelectronics, v. 21, p. 2015-2045.

Caccavo, F., Lonergan, D. J., Lovley, D. R., Davis, M., Stolz, J. F., and McInerney, M. J., 1994, *Geobacter sulfurreducens* Sp-Nov, a Hydrogen-Oxidizing and Acetate-Oxidizing Dissimilatory Metal-Reducing Microorganism: Applied and Environmental Microbiology, v. 60, no. 10, p. 3752-3759.

Catal, T., Li, K., Bermek, H., and Liu, H., 2008, Electricity Production from Twelve Monosaccharides Using Microbial Fuel Cells: Journal of Power Sources, v. 175, no. 1, p. 196-200.

Chang, R., 1981, Physical Chemistry with Applications to Biological Systems, New York, Macmillan

Chaudhuri, S. K., and Lovley, D. R., 2003, Electricity Generation by Direct Oxidation of Glucose in Mediatorless Microbial Fuel Cells: Nat Biotech, v. 21, no. 10, p. 1229-1232.

Chen, Y. P., Zhao, Y., Qiu, K. Q., Chu, J., Lu, R., Sun, M., Liu, X. W., Sheng, G. P., Yu, H. Q., Chen, J., Li, W. J., Liu, G., Tian, Y. C., and Xiong, Y., 2011, An Innovative Miniature Microbial Fuel Cell Fabricated Using Photolithography: Biosensors & Bioelectronics, v. 26, no. 6, p. 2841-2846.

Cheng, K. Y., Ho, G., and Cord-Ruwisch, R., 2011, Novel Methanogenic Rotatable Bioelectrochemical System Operated with Polarity Inversion: Environmental Science & Technology, v. 45, no. 2, p. 796-802.

Cheng, S., Liu, H., Logan, B. E., 2006, Power Densities Using Different Cathode Catalysts (Pt and CoTMPP MFC) and Polymer Binders (Nafion and Ptfe) in Single Chamber Microbial Fuel Cells: Environmental Science & Technology, v. 40, no. 1, p. 364-369.

Cheng, S., Xing, D., and Logan, B. E., 2011, Electricity Generation of Single-Chamber Microbial Fuel Cells at Low Temperatures: Biosensors and Bioelectronics, v. In Press, Corrected Proof.

Christgen, B., 2010, Electricity Generation from Wastewater Using Microbial Fuel Cells: A Study of Electrode and Membrane Materials [PhD Doctorate, UK]: Newcastle University, 175 p.

Clarke, K., R., Green, R, H., 1988, Statistical Design and Analysis for a "Biological Effects" Study.: Marine Ecology Progres Series, v. 46, no. 3, p. 213-226.

Clarke, K. R., Warwick, R.M., 2001, Change in Marine Communities: An Approach to Statistical Analysis and Interpretation, Plymouth, Primer-E.

Clauwaert, P., Aelterman, P., Pham, T., De Schamphelaire, L., Carballa, M., Rabaey, K., and Verstraete, W., 2008, Minimizing Losses in Bio-Electrochemical Systems: The Road to Applications: Applied Microbiology and Biotechnology, v. 79, no. 6, p. 901-913.

Cohen, 1931, The Bacterial Culture as an Electrical Half-Cell: Journal of Bacteriology, v. 21, no. 1, p. 18.

Coskuner, G., Ballinger, S. J., Davenport, R. J., Pickering, R. L., Solera, R., Head, I. M., and Curtis, T. P., 2005, Agreement between Theory and Measurement in Quantification of Ammonia-Oxidizing Bacteria: Applied and Environmental Microbiology, v. 71, no. 10, p. 6325-6334.

Crutzen, P. J., and Goldammer, J. G., 1993, Fire in the Environment: The Ecological, Atmospheric, and Climatic Importance of Vegetation Fires: Report of the Dahlem Workshop, Held in Berlin, 15-20 March 1992, Wiley.

Cusick, R., Bryan, B., Parker, D., Merrill, M., Mehanna, M., Kiely, P., Liu, G., and Logan, B., 2011, Performance of a Pilot-Scale Continuous Flow Microbial Electrolysis Cell Fed Winery Wastewater: Applied Microbiology and Biotechnology, v. 89, no. 6, p. 2053-2063.

Davis, J. B., and Yarbrough, H. F., Jr., 1962, Preliminary Experiments on a Microbial Fuel Cell: Science, v. 137, no. 3530, p. 615-616.

Dekker, A., Ter Heijne, A., Saakes, M., Hamelers, H. V. M., and Buisman, C. J. N., 2009, Analysis and Improvement of a Scaled-up and Stacked Microbial Fuel Cell: Environmental Science & Technology, v. 43, no. 23, p. 9038-9042.

Deng, L., Zhou, M., Liu, C., Liu, L., Liu, C., and Dong, S., 2010, Development of High Performance of Co/Fe/N/Cnt Nanocatalyst for Oxygen Reduction in Microbial Fuel Cells: Talanta, v. 81, no. 1–2, p. 444-448.

Di Lorenzo, M., Curtis, T. P., Head, I. M., and Scott, K., 2009, A Single-Chamber Microbial Fuel Cell as a Biosensor for Wastewaters: Water Research, v. 43, no. 13, p. 3145-3154.

Drake, F., 2000, Global Warming: The Science of Climate Change, Arnold.

Drever, J., 1997, The Geochemistry of Natural Waters, New Jersey, Prentice Hall

Du, Z., Li, H., and Gu, T., 2007, A State of the Art Review on Microbial Fuel Cells: A Promising Technology for Wastewater Treatment and Bioenergy: Biotechnology Advances, v. 25, no. 5, p. 464-482.

Dulon, S., Parot, S., Delia, M.-L., and Bergel, A., 2007, Electroactive Biofilms: New Means for Electrochemistry: Journal of Applied Electrochemistry, v. 37, no. 1, p. 173-179.

El-Naggar, M. Y., Wanger, G., Leung, K. M., Yuzvinsky, T. D., Southam, G., Yang, J., Lau, W. M., Nealson, K. H., and Gorby, Y. A., 2010, Electrical Transport Along Bacterial Nanowires from *Shewanella oneidensis* Mr-1: Proceedings of the National Academy of Sciences of the United States of America, v. 107, no. 42, p. 18127-18131.

Fan, Y., Hu, H., and Liu, H., 2007, Sustainable Power Generation in Microbial Fuel Cells Using Bicarbonate Buffer and Proton Transfer Mechanisms: Environmental Science & Technology, v. 41, no. 23, p. 8154-8158.

Fan, Y., Sharbrough, E., and Liu, H., 2008, Quantification of the Internal Resistance Distribution of Microbial Fuel Cells: Environmental Science & Technology, v. 42, no. 21, p. 8101-8107.

Fan, Y. Z., Hu, H. Q., and Liu, H., 2007, Enhanced Coulombic Efficiency and Power Density of Air-Cathode Microbial Fuel Cells with an Improved Cell Configuration: Journal of Power Sources, v. 171, no. 2, p. 348-354.

Farman, J. C., Gardiner, B. G., and Shanklin, J. D., 1985, Large Losses of Total Ozone in Antarctica Reveal Seasonal Clox/Nox Interaction: Nature, v. 315, no. 6016, p. 207-210.

Fetzer, S., and Conrad, R., 1993, Effect of Redox Potential on Methanogenesis by *Methanosarcina barkeri*: Archives of Microbiology, v. 160, no. 2, p. 108-113.

Finkelstein, D. A., Tender, L. M., and Zeikus, J. G., 2006, Effect of Electrode Potential on Electrode-Reducing Microbiota: Environmental Science & Technology, v. 40, no. 22, p. 6990-6995.

Findlay, R. H., King, G. M., and Watling, L., 1989, Efficacy of Phospholipid Analysis in Determining Microbial Biomass in Sediments: Applied and Environmental Microbiology, v. 55, no. 11, p. 2888-2893.

Frank, P. G., McFadden, C., and Yu, X. O., 2010, Microbial Power House: Design and Optimization of a Single Chamber Microbial Fuel Cell, *in* Tomizuka, M., Yun, C. B., Giurgiutiu, V., and Lynch, J. P., eds., Sensors and Smart Structures Technologies for Civil, Mechanical, and Aerospace Systems 2010, Volume 7647: Bellingham, Spie-Int Soc Optical Engineering.

Franks, A. E., and Nevin, K. P., 2010, Microbial Fuel Cells, a Current Review: Energies, v. 3, no. 5, p. 899-919.

Freguia, S., Rabaey, K., Yuan, Z. G., and Keller, J., 2007, Electron and Carbon Balances in Microbial Fuel Cells Reveal Temporary Bacterial Storage Behavior During Electricity Generation: Environmental Science & Technology, v. 41, no. 8, p. 2915-2921.

-, 2008, Syntrophic Processes Drive the Conversion of Glucose in Microbial Fuel Cell Anodes: Environmental Science & Technology, v. 42, no. 21, p. 7937-7943.

Freguia, S., Teh, E. H., Boon, N., Leung, K. M., Keller, J., and Rabaey, K., 2010, Microbial Fuel Cells Operating on Mixed Fatty Acids: Bioresource Technology, v. 101, no. 4, p. 1233-1238.

Gibson, D. G., Benders, G. A., Andrews-Pfannkoch, C., Denisova, E. A., Baden-Tillson, H., Zaveri, J., Stockwell, T. B., Brownley, A., Thomas, D. W., Algire, M. A., Merryman, C., Young, L., Noskov, V. N., Glass, J. I., Venter, J. C., Hutchison, C. A., and Smith, H. O., 2008, Complete Chemical Synthesis, Assembly, and Cloning of a *Mycoplasma genitalium* Genome: Science, v. 319, no. 5867, p. 1215-1220.

Gil, G.-C., Chang, I.-S., Kim, B. H., Kim, M., Jang, J.-K., Park, H. S., and Kim, H. J., 2003, Operational Parameters Affecting the Performannce of a Mediator-Less Microbial Fuel Cell: Biosensors and Bioelectronics, v. 18, no. 4, p. 327-334.

Goodhead, A. K., 2009, Towards Rational Risk Assessment [pHD Doctorate, UK]: Newcastle University, 221 p.

Gorby, Y., Wanger, G., Yuzvinski, T., Fields, M., and El-Naggar, M., 2010, Electronic and Biogeochemical Properties of Bacterial Nanowires: Geochimica et Cosmochimica Acta, v. 74, no. 12, p. A349-A349.

Gorby, Y. A., Yanina, S., McLean, J. S., Rosso, K. M., Moyles, D., Dohnalkova, A., Beveridge, T. J., Chang, I. S., Kim, B. H., Kim, K. S., Culley, D. E., Reed, S. B., Romine, M. F., Saffarini, D. A., Hill, E. A., Shi, L., Elias , D. A., Kennedy, D. W., Pinchuk, G., Watanabe, K., Ishii, S., Logan, B., Nealson, K. H., Fredrickson, J. K., 2006, Electrically Conductive Bacterial Nanowires Produced by *Shewanella oneidensis* Strain Mr-1 and Other Microorganisms: PNAS, v. 103, no. 30, p. 11358-11363.

Gribbin, J. R., 1978, Climate Change: Proceedings of the Second World Climate Conference, Cambridge University Press.

Harnisch, F., and Schroder, U., 2010, From MFC to MXC: Chemical and Biological Cathodes and Their Potential for Microbial Bioelectrochemical Systems: Chem Soc Rev, v. 39, no. 11, p. 4433-4448.

He, Z., Wagner, N., Minteer, S. D., and Angenent, L. T., 2006, An Upflow Microbial Fuel Cell with an Interior Cathode: Assessment of the Internal Resistance

by Impedance Spectroscopy: Environmental Science & Technology, v. 40, no. 17, p. 5212-5217.
Higuchi, E., Adachi, K., Nohara, S., and Inoue, H., 2009, Oxygen Reduction Reaction Activity of Monodispersed Pt Nanoparticles-Loaded Carbon Black Catalyst Prepared with a Pt Carbonyl Cluster Anion: Research on Chemical Intermediates, v. 35, no. 8, p. 985-995.
Holmes, D. E., Chaudhuri, S. K., Nevin, K. P., Mehta, T., Methe, B. A., Liu, A., Ward, J. E., Woodard, T. L., Webster, J., and Lovley, D. R., 2006, Microarray and Genetic Analysis of Electron Transfer to Electrodes in *Geobacter sulfurreducens*: Environmental Microbiology, v. 8, no. 10, p. 1805-1815.
Horneck, G., 2000, Special Issue: Exobiology in the Solar System - Preface: Planetary and Space Science, v. 48, no. 11, p. 1021-1021.
Houghton, J. T., 2004, Global Warming: The Complete Briefing, Cambridge University.
Hu, Z. Q., 2008, Electricity Generation by a Baffle-Chamber Membraneless Microbial Fuel Cell: Journal of Power Sources, v. 179, no. 1, p. 27-33.
Huang, L. P., Regan, J. M., and Quan, X., 2011, Electron Transfer Mechanisms, New Applications, and Performance of Biocathode Microbial Fuel Cells: Bioresource Technology, v. 102, no. 1, p. 316-323.
Humphrey-Smith, I., Hecker, M., 2006, Microbial Proteomics, Hobocken, John Wiley & Sons, 512 p.:
Hunter, W. J., and Manter, D. K., 2011, Increased Electrical Output When a Bacterial ABTS Oxidizer Is Used in a Microbial Fuel Cell: Current Microbiology, v. 62, no. 2, p. 633-638.
Ieropoulos, I., Greenman, J., and Melhuish, C., 2010, Improved Energy Output Levels from Small-Scale Microbial Fuel Cells: Bioelectrochemistry, v. 78, no. 1, p. 44-50.
Ieropoulous, I. A., Greenman, J., Melhuish, C., Hart, J., 2005, Comparative Study of Three Types of Microbial Fuel Cell: Enzyme and Microbial Technolgy.
Ishii, S. i., Shimoyama, T., Hotta, Y., and Watanabe, K., 2008, Characterization of a Filamentous Biofilm Community Established in a Cellulose-Fed Microbial Fuel Cell: BMC Microbiology, v. 8, no. 1, p. 6.
Jadhav, G. S., and Ghangrekar, M. M., 2009, Performance of Microbial Fuel Cell Subjected to Variation in Ph, Temperature, External Load and Substrate Concentration: Bioresource Technology, v. 100, no. 2, p. 717-723.
Jaouen, F., Proietti, E., Lefevre, M., Chenitz, R., Dodelet, J.-P., Wu, G., Chung, H. T., Johnston, C. M., and Zelenay, P., 2010, Recent Advances in Non-Precious Metal Catalysis for Oxygen-Reduction Reaction in Polymer Electrolyte Fuel Cells: Energy & Environmental Science, v. 4, no. 1, p. 114-130.
Jiang, D., Curtis, M., Troop, E., Scheible, K., McGrath, J., Hu, B., Suib, S., Raymond, D., and Li, B., 2010, A Pilot-Scale Study on Utilizing Multi-Anode/Cathode Microbial Fuel Cells (MAC MFCs) to Enhance the Power Production in Wastewater Treatment: International Journal of Hydrogen Energy, v. 36, no. 1, p. 876-884.

Jiang, J., Zhao, Q., Wei, L., Wang, K., and Lee, D.-J., 2010, Degradation and Characteristic Changes of Organic Matter in Sewage Sludge Using Microbial Fuel Cell with Ultrasound Pretreatment: Bioresource Technology, v. 102, no. 1, p. 272-277.

Jones, J. G., 1979, A Guide to Methods for Estimating Microbial Numbers and Biomass in Freshwater, Ambleside, Freshwater Biological Association.

Jouzel, J., Lorius, C., Petit, J. R., Genthon, C., Barkov, N. I., Kotlyakov, V. M., and Petrov, V. M., 1987, Vostok Ice Core: A Continuous Isotope Temperature Record over the Last Climatic Cycle (160,000 Years): Nature, v. 329, no. 6138, p. 403-408.

Jung, S., and Regan, J. M., 2011, Influence of External Resistance on Electrogenesis, Methanogenesis, and Anode Prokaryotic Communities in Microbial Fuel Cells: Applied and Environment Microbiology, v. 77, no. 2, p. 564-571.

Karube, I., Matsunaga, T., Mitsuda, S., and Suzuki, S., 1977, Microbial Electrode BOD Sensors: Biotechnology and Bioengineering, v. 19, no. 10, p. 1535-1547.

Karube, I., Matsunaga, T., Tsuru, S., and Suzuki, S., 1977, Biochemical Fuel-Cell Utilizing Immobilized Cells of *Clostridium-butyricum*: Biotechnology and Bioengineering, v. 19, no. 11, p. 1727-1733.

Katuri, K. P., Scott, K., Head, I. M., Picioreanu, C., Curtis, T. P., 2010, Microbial Fuel Cells Meet with External Resistance: Bioresource Technology.

Katuri, K. P., and Scott, K., 2011, On the Dynamic Response of the Anode in Microbial Fuel Cells: Enzyme and Microbial Technology, v. 48, no. 4-5, p. 351-358.

Katz, E., Shipway, A. N., Willner, I., 2003, Biochemical Fuel Cells, *in* Vielstich, W., Gasteiger, H. A., Lamm, A., ed., Handbook of Fuel Cells- Fundamentals, Technology and Applications, Volume 1: Fundamentals and Survey of Systems, John Wiley & Sons, Ltd., p. 355-379.

Ke, G.-R., Lai, C.-M., Liu, Y.-Y., and Yang, S.-S., 2010, Inoculation of Food Waste with the Thermo-Tolerant Lipolytic Actinomycete *Thermoactinomyces vulgaris* A31 and Maturity Evaluation of the Compost: Bioresour Technol, v. 101, no. 19, p. 7424-7431.

Khan, A. M., Ali, M. M., Naz, S., and Sohail, M., 2010, Generation of Bioenergy by the Aerobic Fermentation of Domestic Wastewater: Journal of the Chemical Society of Pakistan, v. 32, no. 2, p. 209-214.

Khanal, S. K., 2009, Anaerobic Biotechnology for Bioenergy Production: Principles and Applications, Hoboken, Wiley-Blackwell.

Kim, B., Chang, I., and Gadd, G., 2007, Challenges in Microbial Fuel Cell Development and Operation: Applied Microbiology and Biotechnology, v. 76, no. 3, p. 485-494.

Kim, B. H., Ikeda, T., Park, H. S., Kim, H. J., Hyun, M. S., Kano, K., Takagi, K., and Tatsumi, H., 1999, Electrochemical Activity of an Fe(Iii)-Reducing Bacterium, *Shewanella putrefaciens* Ir-1, in the Presence of Alternative Electron Acceptors: Biotechnology Techniques, v. 13, no. 7, p. 475-478.

Kim, G. T., Webster, G., Wimpenny, J.W.T., Kim, B.H., Kim, H.J., Weightman, A.J., 2006, Bacterial Community Structure, Comparmentalization and Activity in a Microbial Fuel Cell: Journal of Applied Microbiology, v. 101, p. 698-710.

Kim, H. J., Hyun, M. S., Chang, I. S., and Kim, B. H., 1999, A Microbial Fuel Cell Type Lactate Biosensor Using a Metal-Reducing Bacterium, *Shewanella putrefaciens*: Journal of Microbiology and Biotechnology, v. 9, no. 3, p. 365-367.

Kim, J. R., Min, B., Logan, B. E., 2005, Evaluation of Procedures to Acclimate a Microbial Fuel Cell for Electricity Production: Applied Microbiology and Biotechnology, v. 68, p. 23-30.

Kim, J. R., Jung, S. H., Regan, J. M., and Logan, B. E., 2007, Electricity Generation and Microbial Community Analysis of Alcohol Powered Microbial Fuel Cells: Bioresource Technology, v. 98, no. 13, p. 2568-2577.

Kim, M.-S., and Lee, Y.-j., 2010, Optimization of Culture Conditions and Electricity Generation Using *Geobacter sulfurreducens* in a Dual-Chambered Microbial Fuel-Cell: International Journal of Hydrogen Energy, v. 35, no. 23, p. 13028-13034.

Kim, N., Choi, Y., Jung, S., Kim, S., 2000, Effect of Initial Carbon Sources on the Performance of Microbial Fuel Cells Containing *Proteus vulgaris*: Biotechnology and Bioengineering, v. 70, no. 1, p. 109-114.

Larrosa-Guerrero, A., Scott, K., Katuri, K. P., Godinez, C., Head, I. M., and Curtis, T., 2010, Open Circuit Versus Closed Circuit Enrichment of Anodic Biofilms in MFC: Effect on Performance and Anodic Communities: Appl Microbiol Biotechnol, v. 87, no. 5, p. 1699-1713.

Lee, C. Y., and Lee, Y. P., 2007, Degradation of 4-Chlorophenol by Enriched Mixed Cultures Utilizing Phenol and Glucose as Added Growth Substrate: World Journal of Microbiology and Biotechnology, v. 23, no. 3, p. 383-391.

Lefebvre, O., Uzabiaga, A., Ng, H, Y., Energy Considerations for Self-Sustainable Microbial Fuel Cells, *in* Proceedings 2nd Microbial Fuel Cell Conference, Gwangju, Korea, 2009, Volume 1, Gwangju Institure of Science and Technology, p. 153.

Lefebvre, O., Uzabiaga, A., Chang, I. S., Kim, B. H., and Ng, H. Y., 2011, Microbial Fuel Cells for Energy Self-Sufficient Domestic Wastewater Treatment-a Review and Discussion from Energetic Consideration: Applied Microbiology and Biotechnology, v. 89, no. 2, p. 259-270.

Li, H. R., Feng, Y. L., Tang, X. H., Zhang, J. J., and Lian, J., 2010, The Factors Affecting Biofilm Formation in the Mediatorless Microbial Fuel Cell: Chemical and Biochemical Engineering Quarterly, v. 24, no. 3, p. 341-346.

Li, W. W., Sheng, G. P., Liu, X. W., and Yu, H. Q., 2011, Recent Advances in the Separators for Microbial Fuel Cells: Bioresource Technology, v. 102, no. 1, p. 244-252.

Li, Z. J., Zhang, X. W., Zeng, Y. X., and Lei, L. C., 2009, Electricity Production by an Overflow-Type Wetted-Wall Microbial Fuel Cell: Bioresource Technology, v. 100, no. 9, p. 2551-2555.

Liu, H., Grot, S., Logan, B. E., 2005, Electrochemically Assisted Microbial Production of Hydrogen from Acetate: Environmental Science &Technology, v. 39, no. 2 p. 4317.

Liu, H., Cheng, S., Logan, B. E., 2005, Power Generation in Fed-Batch Microbial Fuel Cells as a Function of Ionic Strength, Temperature, and Reactor Configuration: Environmental Science & Technology, v. 39, no. 14, p. 5488-5493.

Liu, H., and Logan, B. E., 2004, Electricity Generation Using an Air-Cathode Single Chamber Microbial Fuel Cell in the Presence and Absence of a Proton Exchange Membrane: Environmental Science & Technology, v. 38, no. 14, p. 4040-4046.

Liu, H., Ramnarayanan, R., and Logan, B. E., 2004, Production of Electricity During Wastewater Treatment Using a Single Chamber Microbial Fuel Cell: Environmental Science & Technology, v. 38, no. 7, p. 2281-2285.

Liu, Z. D., Liu, J., Zhang, S. P., and Su, Z. G., 2008, A Novel Configuration of Microbial Fuel Cell Stack Bridged Internally through an Extra Cation Exchange Membrane: Biotechnology Letters, v. 30, no. 6, p. 1017-1023.

Logan, B. E., Murano, C., Scott, K., Gray, N. D., Head, I. M., 2005, Electricity Generation from Cysteine in a Microbial Fuel Cell: Water Research, v. 39, p. 942-952.

Logan, B. E., Hamelers, B., Rozendal, R., Schroeder, U., Keller, J., Freguia, S., Aelterman, P., Verstraete, W., Rabaey, K., 2006, Microbial Fuel Cells: Methodology and Technology: ENVIRON SCI & TECHNOL, v. 39, no. 2, 5174.

Logan, B. E., 2008, Microbial Fuel Cells, Hoboken, John Wiley and Sons, 200 p.:

Logan, B. E., 2009, Exoelectrogenic Bacteria That Power Microbial Fuel Cells: Nat Rev Micro, v. 7, no. 5, p. 375-381.

Logan, B. E., Call, D., Cheng, S., Hamelers, H. V. M., Sleutels, T., Jeremiasse, A. W., and Rozendal, R. A., 2008, Microbial Electrolysis Cells for High Yield Hydrogen Gas Production from Organic Matter: Environmental Science & Technology, v. 42, no. 23, p. 8630-8640.

Logan, B., Cheng, S., Watson, V., and Estadt, G., 2007, Graphite Fiber Brush Anodes for Increased Power Production in Air-Cathode Microbial Fuel Cells: Environmental Science & Technology, v. 41, no. 9, p. 3341-3346.

Logan, B. E., Hamelers, B., Rozendal, R., Schröder, U., Keller, J. r., Freguia, S., Aelterman, P., Verstraete, W., and Rabaey, K., 2006, Microbial Fuel Cells: Methodology and Technology: Environmental Science & Technology, v. 40, no. 17, p. 5181-5192.

Lovely, D. R., 2006, Microbial Fuel Cells: Novel Microbial Physiologies and Enginerring Approaches: Current Opinion in Biotechnology.

Lovley, D. R., 1991, Dissimilatory Fe(iii) and Mn(iv) Reduction: Microbiological Reviews, v. 55, no. 2, p. 259-287.

Lovley, D. R., 1993, Anaerobes into Heavy Metal: Dissimilatory Metal Reduction in Anoxic Environments: Trends in Ecology & Evolution, v. 8, no. 6, p. 213-217.

Lovley, D. R., 2006, Bug Juice: Harvesting Electricity with Microorganisms (Vol 4, Pg 497, 2006): Nature Reviews Microbiology, v. 4, no. 10, p. 797-797.
Lovley, D. R., and Phillips, E. J. P., 1988, Novel Mode of Microbial Energy Metabolism: Organic Carbon Oxidation Coupled to Dissimilatory Reduction of Iron or Manganese: Applied and Environment Microbiology, v. 54, no. 6, p. 1472-1480.
Lyon, D. Y., Buret, F., Vogel, T. M., and Monier, J. M., 2009, Is Resistance Futile? Changing External Resistance Does Not Improve Microbial Fuel Cell Performance: Bioelectrochemistry, v. 78, no. 1, p. 2-7.
Madigan, M. T., 2011, Brock Biology of Microorganisms, Pearson Education, Limited.
Mara, D., 2003, Domestic Wastewater Treatment in Developing Countries, London, Earthscan.
McLean, J. S., Wanger, G., Gorby, Y. A., Wainstein, M., McQuaid, J., Ishii, S. I., Bretschger, O., Beyenal, H., and Nealson, K. H., 2010, Quantification of Electron Transfer Rates to a Solid Phase Electron Acceptor through the Stages of Biofilm Formation from Single Cells to Multicellular Communities: Environmental Science & Technology, v. 44, no. 7, p. 2721-2727.
Mehta, P., Hussain, A., Tartakovsky, B., Neburchilov, V., Raghavan, V., Wang, H., and Guiot, S. R., 2010, Electricity Generation from Carbon Monoxide in a Single Chamber Microbial Fuel Cell: Enzyme and Microbial Technology, v. 46, no. 6, p. 450-455.
Min, B., Logan., B.E., 2004, Continuous Electricity Generation from Domestic Wastewater and Organic Substrates in a Flat Plate Microbial Fuel Cell: Environmental Science & Technology, v. 38, p. 5809-5814.
Min, B., Cheng, S., Logan, B.E., 2005, Electricity Generation Using Membrane and Salt Bridge Microbial Fuel Cells: Water Research, v. 39, p. 1675-1686.
Mu, Y., Rabaey, K., Rozendal, R. A., Yuan, Z. G., and Keller, J., 2009, Decolorization of Azo Dyes in Bioelectrochemical Systems: Environmental Science & Technology, v. 43, no. 13, p. 5137-5143.
Mu, Y., Rozendal, R. A., Rabaey, K., and Keller, J., 2009, Nitrobenzene Removal in Bioelectrochemical Systems: Environmental Science & Technology, v. 43, no. 22, p. 8690-8695.
Muyzer, G., de Waal, E. C., and Uitterlinden, A. G., 1993, Profiling of Complex Microbial Populations by Denaturing Gradient Gel Electrophoresis Analysis of Polymerase Chain Reaction-Amplified Genes Coding for 16s rRNA: Applied and Environment Microbiology, v. 59, no. 3, p. 695-700.
Myers, C. R., and Nealson, K. H., 1988, Bacterial Manganese Reduction and Growth with Manganese Oxide as the Sole Electron-Acceptor: Science, v. 240, no. 4857, p. 1319-1321.
Nealson, K. H., and Myers, C., 1992, Acetate Oxidation by Dissimilatory Fe(Iii) Reducers - Reply: Applied and Environmental Microbiology, v. 58, no. 9, p. 3206-3208.
Nevin, K. P., Richter, H., Covalla, S. F., Johnson, J. P., Woodard, T. L., Orloff, A. L., Jia, H., Zhang, M., and Lovley, D. R., 2008, Power Output and Columbic Efficiencies from Biofilms of Geobacter Sulfurreducens Comparable to

Mixed Community Microbial Fuel Cells: Environmental Microbiology, v. 10, no. 10, p. 2505-2514.
Nielsen, L. P., Risgaard-Petersen, N., Fossing, H., Christensen, P. B., and Sayama, M., 2010, Electric Currents Couple Spatially Separated Biogeochemical Processes in Marine Sediment: Nature, v. 463, no. 7284, p. 1071-1074.
Nielsen, M. E., Reimers, C. E., White, H. K., Sharma, S., and Girguis, P. R., 2008, Sustainable Energy from Deep Ocean Cold Seeps: Energy & Environmental Science, v. 1, no. 5, p. 584-593.
Oh, S., Booki, M., Logan, B.E., 2004, Cathode Performance as a Factor in Electricity Generation in Microbial Fuel Cells: Environmental Science & Technology, v. 38, p. 4900-4904.
Oh, S., Min, B., and Logan, B. E., 2004, Cathode Performance as a Factor in Electricity Generation in Microbial Fuel Cells: Environmental Science & Technology, v. 38, no. 18, p. 4900-4904.
Oh, S. E., and Logan, B. E., 2007, Voltage Reversal During Microbial Fuel Cell Stack Operation: Journal of Power Sources, v. 167, no. 1, p. 11-17.
Oreskes, N., 2004, The Scientific Consensus on Climate Change: Science, v. 306, no. 5702, p. 1686.
Park, D. H., Zeikus, J. G., 2002, Impact of Electrode Composition on Electricity Generation in a Single-Compartment Fuel Cell Using *Schewenella putrifaciens*: Applied Microbiology and Biotechnology, v. 59, p. 58-61.
-, 2003, Improved Fuel Cell and Electrode Designs for Producing Electricity from Microbial Degradation: Biotechnology and Bioengineering, v. 81, no. 3, p. 348-355.
Parry, M. L., and Intergovernmental Panel on Climate Change. Working, G., II, 2007, Climate Change 2007: Impacts, Adaptation and Vulnerability: Contribution of Working Group Ii to the Fourth Assessment Report of the Intergovernmental Panel on Climate Change, Cambridge University Press.
Phung, N. T., Lee, J., Kang, K. H., Chang, I. S., Gadd, G. M., and Kim, B. H., 2004, Analysis of Microbial Diversity in Oligotrophic Microbial Fuel Cells Using 16s Rdna Sequences: FEMS Microbiology Letters, v. 233, no. 1, p. 77-82.
Piccolino, M., 1998, Animal Electricity and the Birth of Electrophysiology: The Legacy of Luigi Galvani: Brain Research Bulletin, v. 46, no. 5, p. 381-407.
Picioreanu, C., Head, I. M., Katuri, K. P., van Loosdrecht, M. C. M., and Scott, K., 2007, A Computational Model for Biofilm-Based Microbial Fuel Cells: Water Research, v. 41, no. 13, p. 2921-2940.
Picioreanu, C., van Loosdrecht, M. C. M., Curtis, T. P., and Scott, K., 2010, Model Based Evaluation of the Effect of Ph and Electrode Geometry on Microbial Fuel Cell Performance: Bioelectrochemistry, v. 78, no. 1, p. 8-24.
Pitter, P. C., J, 1990, Biodegradability of Organic Substances in the Aquatic Environment, Boca Raton, CRC press, 306 p.:
Potter, M. C., 1911, Electrical Effects Accompanying the Decomposition of Organic Compounds: Proceedings of the Royal Society of London Series B, Containing Papers of a Biological Character, v. 84, no. 571, p. 260-276.

Premier, G. C., Kim, J. R., Michie, I., Dinsdale, R. M., and Guwy, A. J., 2011, Automatic Control of Load Increases Power and Efficiency in a Microbial Fuel Cell: Journal of Power Sources, v. 196, no. 4, p. 2013-2019.

Prescott, C., 2009, Carbon Accounting in the United Kingdom Water Sector: A Review: Water Science and Technology, v. 60, no. 10, p. 2721-2727.

Rabaey, K., Boon, N., Siciliano, S. D., Verhaege, M., Verstraete, W., 2004, Biofuel Cells Select for Microbial Consortia That Self-Mediate Electron Transfer: Applied and Environmental Microbiology, v. 70, no. 9, p. 5373-5382.

Rabaey, K., Verstraete, W., 2005, Microbial Fuel Cells: Novel Biotechnology for Energy Generation: Trends in Biotechnology, v. 23, no. 6, p. 291-298.

Rabaey, K., Angenent, L., Schroder, U., Keller., J, 2010, Bioelectrochemical Systems, London, IWA, Lens, I P.

Rabaey, K., Bu tzer, S., Brown, S., Keller, J. R., and Rozendal, R. A., 2010, High Current Generation Coupled to Caustic Production Using a Lamellar Bioelectrochemical System: Environmental Science & Technology, v. 44, no. 11, p. 4315-4321.

Ramasamy, R. P., Ren, Z., Mench, M. M., and Regan, J. M., 2008, Impact of Initial Biofilm Growth on the Anode Impedance of Microbial Fuel Cells: Biotechnology and Bioengineering, v. 101, no. 1, p. 101-108.

Reguera, G., McCarthy, K. D., Mehta, T., Nicoll, J. S., Tuominen, M. T., and Lovley, D. R., 2005, Extracellular Electron Transfer Via Microbial Nanowires: Nature, v. 435, no. 7045, p. 1098-1101.

Reguera, G., Nevin, K. P., Nicoll, J. S., Covalla, S. F., Woodard, T. L., and Lovley, D. R., 2006, Biofilm and Nanowire Production Leads to Increased Current in *Geobacter sulfurreducens* Fuel Cells: Applied and Environmental Microbiology, v. 72, no. 11, p. 7345-7348.

Reguera, G., Pollina, R. B., Nicoll, J. S., and Lovley, D. R., 2006, Possible Non-Conductive Role of *Geobacter sulfurreducens* Pili Nanowires in Biofilm Formation: Journal of Bacteriology, p. JB.01284-01206.

Reguera, G., Pollina, R. B., Nicoll, J. S., and Lovley, D. R., 2007, Possible Nonconductive Role of *Geobacter sulfurreducens* Pilus Nanowires in Biofilm Formation: Journal of Bacteriology, v. 189, no. 5, p. 2125-2127.

Reimers, C. E., Tender, L. M., Fertig, S., and Wang, W., 2001, Harvesting Energy from the Marine Sediment−Water Interface: Environmental Science & Technology, v. 35, no. 1, p. 192-195.

Ren, Z., Ward, T. E., and Regan, J. M., 2007, Electricity Production from Cellulose in a Microbial Fuel Cell Using a Defined Binary Culture: Environmental Science & Technology, v. 41, no. 13, p. 4781-4786.

Rodrigo, M. A., Cañizares, P., García, H., Linares, J. J., and Lobato, J., 2009, Study of the Acclimation Stage and of the Effect of the Biodegradability on the Performance of a Microbial Fuel Cell: Bioresource Technology, v. 100, no. 20, p. 4704-4710.

Rohrback, G. H., Scott, W. R., Canfield, J. H., 1962, Proceedings of the 16th Annual Power Sources Conference.

Rozendal, R. A., Hamelers, H. V. M., Rabaey, K., Keller, J., and Buisman, C. J. N., 2008, Towards Practical Implementation of Bioelectrochemical Wastewater Treatment: Trends in Biotechnology, v. 26, no. 8, p. 450-459.
Scholey, J. M., and Harrison, J. E., 2003, Publication Bias: Raising Awareness of a Potential Problem in Dental Research: Br Dent J, v. 194, no. 5, p. 235-237.
Schroeder, U., Niessen, J., Scolz, F., 2003, A Generation of Microbial Fuel Cells with Current Outputs Boosted by More Than One Order of Magnitude: Angewandte Chemie International Editition, v. 42, p. 2880-2883.
Schubert, C., 2006, Microbiology: Batteries Not Includedcircuits of Slime: Nature, v. 441, no. 7091, p. 277-279.
Scott, K., and Murano, C., 2007, Microbial Fuel Cells Utilising Carbohydrates: Journal of Chemical Technology and Biotechnology, v. 82, no. 1, p. 92-100.
Sharma, V., and Kundu, P. P., 2010, Biocatalysts in Microbial Fuel Cells: Enzyme and Microbial Technology, v. 47, no. 5, p. 179-188.
Shimoyama, T., Komukai, S., Yamazawa, A., Ueno, Y., Logan, B. E., and Watanabe, K., 2008, Electricity Generation from Model Organic Wastewater in a Cassette-Electrode Microbial Fuel Cell: Applied Microbiology and Biotechnology, v. 80, no. 2, p. 325-330.
Shukla, A. K., Suresh, P., Berchmans, S., Rajendran, A., 2004, Biological Fuel Cells and Their Applications: Current Science, v. 87, no. 4, p. 455-468.
Stams, A. J. M., de Bo, F.A.M., Plugge, C.A., van Eekert, M.H.A., Dolfing, J., Schraa, G., 2006, Exocellular Electron Transfer in Anaerobic Microbial Communities: Environmental Microbiology, v. 8, no. 3, p. 37-.
Stern, N. H., and Great Britain, T., 2007, The Economics of Climate Change: The Stern Review, Cambridge University Press.
Stirling, J. l., Bennetto, H.P., Delaney, G.M., Mason, J.R., Roller, S.D., Tanaka, K., Thurston, C.F., 1983, Microbial Fuel Cells: Biochemical Society Transactions.
Swiderska-Broz, M., and Wolska, M., 2011, Removal of Total Organic Carbon Fractions from Surface Water by Coagulation: Ochrona Srodowiska, v. 33, no. 1, p. 9-12.
Tchobanoglous, G., Burton, F. L., Stensel, H. D., Metcalf, and Eddy, 2003, Wastewater Engineering: Treatment and Reuse, McGraw-Hill.
Tender, L. M., Reimers, C. E., Stecher III, H. A., Holmes, D. E., Bond, D. R., Lowy, D. A., Pilobello, K., Fertig, S. J., Lovely, D. R., 2002, Harnessing Microbially Generated Power on the Seafloor: Nature Biotechnology, v. 20, p. 821-825.
Thauer, R. K., and Shima, S., 2008, Methane as Fuel for Anaerobic Microorganisms: Annals of the New York Academy of Sciences, v. 1125, no. 1, p. 158-170.
Torres, C. I., Marcus, A. K., Lee, H.-S., Parameswaran, P., Krajmalnik-Brown, R., and Rittmann, B. E., 2009, A Kinetic Perspective on Extracellular Electron Transfer by Anode-Respiring Bacteria: FEMS Microbiology Reviews, v. 34, no. 1, p. 3-17.
Velasquez-Orta, S. B., Head, I. M., Curtis, T. P., and Scott, K., 2011, Factors Affecting Current Production in Microbial Fuel Cells Using Different

Industrial Wastewaters: Bioresource Technology, v. 102, no. 8, p. 5105-5112.

Venkata Mohan, S., Saravanan, R., Raghavulu, S. V., Mohanakrishna, G., and Sarma, P. N., 2008, Bioelectricity Production from Wastewater Treatment in Dual Chambered Microbial Fuel Cell (Mfc) Using Selectively Enriched Mixed Microflora: Effect of Catholyte: Bioresource Technology, v. 99, no. 3, p. 596-603.

Wang, B., and Han, J. I., 2009, A Single Chamber Stackable Microbial Fuel Cell with Air Cathode: Biotechnology Letters, v. 31, no. 3, p. 387-393.

Wang, H.-Y., Bernarda, A., Huang, C.-Y., Lee, D.-J., and Chang, J.-S., 2010, Micro-Sized Microbial Fuel Cell: A Mini-Review: Bioresource Technology, v. 102, no. 1, p. 235-243.

Watson, V. J., and Logan, B. E., 2010, Analysis of Polarization Methods for Elimination of Power Overshoot in Microbial Fuel Cells: Electrochemistry Communications, v. 13, no. 1, p. 54-56.

Weber, K. A., Achenbach, L. A., and Coates, J. D., 2006, Microorganisms Pumping Iron: Anaerobic Microbial Iron Oxidation and Reduction: Nature Reviews Microbiolgy, v. 4, no. 10, p. 752-764.

Wei, J. C., Liang, P., Cao, X. X., and Huang, X., 2010, A New Insight into Potential Regulation on Growth and Power Generation of *Geobacter sulfurreducens* in Microbial Fuel Cells Based on Energy Viewpoint: Environmental Science & Technology, v. 44, no. 8, p. 3187-3191.

Woodcock, S., van der Gast, C. J., Bell, T., Lunn, M., Curtis, T. P., Head, I. M., and Sloan, W. T., 2007, Neutral Assembly of Bacterial Communities: FEMS Microbiology Ecology, v. 62, no. 2, p. 171-180.

Woodward, L., Perrier, M., Srinivasan, B., Pinto, R. P., and Tartakovsky, B., 2010, Comparison of Real-Time Methods for Maximizing Power Output in Microbial Fuel Cells: AIChE Journal, v. 56, no. 10, p. 2742-2750.

Woodward, L., Perrier, M., Srinivasan, B., and Tartakovsky, B., 2009, Maximizing Power Production in a Stack of Microbial Fuel Cells Using Multiunit Optimization Method: Biotechnology Progress, v. 25, no. 3, p. 676-682.

www.alita.com, 2011, Alita N3 Pump Specifications.

www.isiknowlege.com, 2011, Web of Knowledge Database.

www.kitco.com, 2011, Platinum Spot Prices.

www.mathwork.com, 2011, Polarisation Curve (Figure 2.3).

www.microbialfuelcell.org, 2011, Jurg Keller Presentation.

www.wrap.com, 2011, Electricity Prices.

www.co2now.org, 2012, Current global CO_2 concentrations

You, S. J., Wang, X. H., Zhang, J. N., Wang, J. Y., Ren, N. Q., and Gong, X. B., 2011, Fabrication of Stainless Steel Mesh Gas Diffusion Electrode for Power Generation in Microbial Fuel Cell: Biosensors & Bioelectronics, v. 26, no. 5, p. 2142-2146.

You, S.-J., Ren, N.-Q., Zhao, Q.-L., Kiely, P. D., Wang, J.-Y., Yang, F.-L., Fu, L., and Peng, L., 2009, Improving Phosphate Buffer-Free Cathode Performance of Microbial Fuel Cell Based on Biological Nitrification: Biosensors and Bioelectronics, v. 24, no. 12, p. 3698-3701.

Yuan, Y., Zhou, S., Xu, N., and Zhuang, L., 2010, Electrochemical Characterization of Anodic Biofilms Enriched with Glucose and Acetate in Single-Chamber Microbial Fuel Cells: Colloids and Surfaces B: Biointerfaces, v. 82, no. 2, p. 641-646.

Zehnder, A. J. B., 1988, Biology of Anaerobic Microorganisms, New York, John Wiley & Sons.

Zhuang, L., and Zhou, S. G., 2009, Substrate Cross-Conduction Effect on the Performance of Serially Connected Microbial Fuel Cell Stack: Electrochemistry Communications, v. 11, no. 5, p. 937-940.

Zuo, Y., Maness, P.-C., and Logan, B. E., 2006, Electricity Production from Steam-Exploded Corn Stover Biomass: Energy & Fuels, v. 20, no. 4, p. 1716-1721.